



**THE UNIVERSITY OF CALGARY**

**The Effects of Climate Change and Urbanization**

**on Flood Frequencies**

**by**

**Ernst Nicolas Kerkhoven**

**A THESIS**

**SUBMITTED TO THE FACULTY OF GRADUATE STUDIES**

**IN PARTIAL FULFILMENT OF THE REQUIREMENTS FOR THE**

**DEGREE OF MASTER OF SCIENCE IN CIVIL ENGINEERING**

**DEPARTMENT OF CIVIL ENGINEERING**

**CALGARY, ALBERTA**

**APRIL, 1998**

**© Ernst Nicolas Kerkhoven 1998**



**National Library  
of Canada**

**Acquisitions and  
Bibliographic Services**

**395 Wellington Street  
Ottawa ON K1A 0N4  
Canada**

**Bibliothèque nationale  
du Canada**

**Acquisitions et  
services bibliographiques**

**395, rue Wellington  
Ottawa ON K1A 0N4  
Canada**

*Your file Votre référence*

*Our file Notre référence*

**The author has granted a non-exclusive licence allowing the National Library of Canada to reproduce, loan, distribute or sell copies of this thesis in microform, paper or electronic formats.**

**The author retains ownership of the copyright in this thesis. Neither the thesis nor substantial extracts from it may be printed or otherwise reproduced without the author's permission.**

**L'auteur a accordé une licence non exclusive permettant à la Bibliothèque nationale du Canada de reproduire, prêter, distribuer ou vendre des copies de cette thèse sous la forme de microfiche/film, de reproduction sur papier ou sur format électronique.**

**L'auteur conserve la propriété du droit d'auteur qui protège cette thèse. Ni la thèse ni des extraits substantiels de celle-ci ne doivent être imprimés ou autrement reproduits sans son autorisation.**

**0-612-31391-3**

**Canada**

## **ABSTRACT**

Two computer models for the Little Red Deer River near Water Valley watershed in the Alberta foothills were developed to simulate the rainfall-runoff relationship using the S.C.S. curve number and unit hydrograph methods. One model simulated the watershed as a single system while the other modeled the watershed as the sum of twelve sub-basins. Extreme rainfall statistics were used to produce synthetic flood frequency curves. Model parameters were then varied to simulate the effects of climate change and urbanization.

The results were analyzed in terms of flood return period, statistical parameters, and logarithmic statistical parameters. The relationship between skewness and kurtosis was found to consistently follow a linear trend very similar to that of the generalized extreme value distribution. The most significant effect of both climate change and urbanization was found to be a large increase in the frequency of large floods.

## **ACKNOWLEDGMENTS**

I would like to acknowledge Dr. Ivan Muzik for providing me with the opportunity to complete my Master of Science Degree. I would also like to thank the University of Calgary and Dr. Muzik for suppling funds for my research without which I could never have even started my work.

I should also mention my fellow students in the department of Civil Engineering, both graduate and undergraduate, for generating such a pleasant and entertaining atmosphere over the past two years.

Finally, I wish to thank Eden Koster for all her support and encouragement when I needed a lift, and for keeping me grounded when I started to get carried away.

**Dedicated to my  
grandparents:**

**Rudolf Kerkhoven  
Charlotte Reuhl  
&  
Herman Benschop  
Clara Rueter**

## **TABLE OF CONTENTS**

<b>APPROVAL PAGE</b>	<b>ii</b>
<b>ABSTRACT</b>	<b>iii</b>
<b>ACKNOWLEDGMENTS</b>	<b>iv</b>
<b>DEDICATION</b>	<b>v</b>
<b>TABLE OF CONTENTS</b>	<b>vi</b>
<b>LIST OF TABLES</b>	<b>viii</b>
<b>LIST OF FIGURES</b>	<b>x</b>
<b>LIST OF ABBREVIATIONS AND SYMBOLS</b>	<b>xii</b>
<b>CHAPTER 1 INTRODUCTION</b>	<b>1</b>
1.1 General	1
1.2 Objectives of the study	3
1.3 Scope of the study	3
1.4 Thesis organization	5
<b>CHAPTER 2 LITERATURE REVIEW</b>	<b>7</b>
2.1 Temperature and climate change	7
2.2 Vegetation and climate change	8
2.3 Seasonal cycles and climate change	9
2.4 Rainfall - runoff and climate change	9
2.5 Mean runoff and climate change	11
2.6 Extreme events and climate change	17
2.7 Urbanization and flooding	19
2.8 Synthetic flood-frequency curves in Alberta	22
<b>CHAPTER 3 METHOD OF ANALYSIS</b>	<b>24</b>
3.1 Study region	24
3.2 Model summaries	27
3.2.1 Lumped model	27
3.2.2 Sub-basin model	27
3.3 Rainfall	30
3.3.1 Storm duration	30
3.3.2 Total rainfall depth	33
3.3.3 Time distribution of rainfall	35
3.4 Abstractions and excess rainfall	35
3.4.1 S.C.S. curve number method	38
3.4.2 Application of the curve number method	39
3.4.3 Antecedent moisture condition	46
3.5 From excess rainfall to runoff - the unit hydrograph	48
3.5.1 Lumped model and the unit hydrograph	51
3.5.2 Sub-basin model and the unit hydrograph	57

3.6	Control Variables	64
3.6.1	Climate change	64
3.6.2	Urbanization	66
3.6.3	Choice of storms	66
3.7	Computer hardware and software	69
3.8	Statistical analysis	69
3.8.1	N-year floods	69
3.8.2	Statistical parameters	70
3.8.3	Logarithmic statistical parameters	72
3.8.4	Chi-square tests	73
3.8.5	Extreme value distributions	74
<b>CHAPTER 4</b>	<b>RESULTS AND DISCUSSION</b>	<b>76</b>
4.1	Comparison of models with observed data	76
4.2	Changes in rainfall - mean and standard deviation	80
4.2.1	N-year floods	80
4.2.2	Statistical parameters	84
4.3	Changes in rainfall - standard deviation	88
4.3.1	N-year floods	88
4.3.2	Statistical parameters	93
4.4	Rainfall climate scenarios	96
4.5	Urbanization	100
4.5.1	N-year floods	100
4.5.2	Statistical parameters	105
4.6	Summary of data results	108
<b>CHAPTER 5</b>	<b>CONCLUSIONS AND RECOMMENDATIONS</b>	<b>115</b>
5.1	Conclusions	115
5.2	Recommendations	118
<b>REFERENCES</b>		<b>121</b>
<b>APPENDIX A</b>	<b>Summary of results</b>	<b>126</b>



## **LIST OF TABLES**

<b>Table 2.1</b>	<b>Percent change in mean annual flow</b>	<b>14</b>
<b>Table 3.1</b>	<b>Extreme rainfall statistics</b>	<b>31</b>
<b>Table 3.2</b>	<b>Quartile probabilities (after Huff(1967))</b>	<b>37</b>
<b>Table 3.3</b>	<b>Conversion of Canadian soil classification to SCS classification</b>	<b>42</b>
<b>Table 3.4</b>	<b>Land use / soil type to curve number</b>	<b>44</b>
<b>Table 3.5</b>	<b>Sub-basin curve numbers</b>	<b>45</b>
<b>Table 3.6</b>	<b>Antecedent moisture condition probabilities</b>	<b>49</b>
<b>Table 3.7</b>	<b>Excess rainfall depths</b>	<b>54</b>
<b>Table 3.8</b>	<b>7 June 1984 optimum unit hydrograph</b>	<b>58</b>
<b>Table 3.9</b>	<b>Optimum unit hydrograph parameters</b>	<b>59</b>
<b>Table 3.10</b>	<b>Sub-basin unit hydrograph parameters</b>	<b>61</b>
<b>Table 3.11</b>	<b>Comparison of HEC-1 and sub-basin models</b>	<b>65</b>
<b>Table 3.12</b>	<b>Urbanized curve numbers</b>	<b>68</b>
<b>Table 4.1</b>	<b>Chi-square test</b>	<b>79</b>
<b>Table 4.2</b>	<b>Climate scenario statistics</b>	<b>97</b>
<b>Table A.1</b>	<b>N-year floods - rainfall - Lumped model</b>	<b>127</b>
<b>Table A.2</b>	<b>N-year floods - rainfall - Sub-basin model</b>	<b>128</b>
<b>Table A.3</b>	<b>N-year floods - rainfall standard deviation - Lumped model</b>	<b>129</b>
<b>Table A.4</b>	<b>N-year floods - rainfall standard deviation - Sub-basin model</b>	<b>130</b>
<b>Table A.5</b>	<b>N-year floods - climate scenarios</b>	<b>131</b>
<b>Table A.6</b>	<b>N-year floods - urbanization - Lumped model</b>	<b>132</b>

<b>Table A.7</b>	<b>N-year floods - urbanization - Sub-basin model</b>	<b>133</b>
<b>Table A.8</b>	<b>Statistics - rainfall - Lumped model</b>	<b>134</b>
<b>Table A.9</b>	<b>Statistics - rainfall - Sub-basin model</b>	<b>135</b>
<b>Table A.10</b>	<b>Statistics - rainfall standard deviation - Lumped model</b>	<b>136</b>
<b>Table A.11</b>	<b>Statistics - rainfall standard deviation - Sub-basin model</b>	<b>137</b>
<b>Table A.12</b>	<b>Statistics - climate scenarios</b>	<b>138</b>
<b>Table A.13</b>	<b>Statistics - urbanization - Lumped model</b>	<b>139</b>
<b>Table A.14</b>	<b>Statistics - urbanization - Sub-basin model</b>	<b>140</b>

## **LIST OF FIGURES**

<b>Figure 3.1</b>	<b>Location of study area</b>	<b>25</b>
<b>Figure 3.2</b>	<b>Little Red Deer River near Water Valley</b>	<b>26</b>
<b>Figure 3.3</b>	<b>Modeling procedure flow chart</b>	<b>28</b>
<b>Figure 3.4</b>	<b>Lumped model flow chart</b>	<b>29</b>
<b>Figure 3.5</b>	<b>Sub-basin model flow chart</b>	<b>31</b>
<b>Figure 3.6</b>	<b>Rainfall distribution curves (after Huff (1967))</b>	<b>36</b>
<b>Figure 3.7</b>	<b>Land use map of Little Red Deer River near Water Valley watershed</b>	<b>41</b>
<b>Figure 3.8</b>	<b>Soil type map of Little Red Deer River near Water Valley watershed</b>	<b>43</b>
<b>Figure 3.9</b>	<b>CN vs. Baseflow</b>	<b>47</b>
<b>Figure 3.10</b>	<b>Baseflow separation</b>	<b>53</b>
<b>Figure 3.11</b>	<b>Triangular unit hydrograph</b>	<b>55</b>
<b>Figure 3.12</b>	<b>Progression of urbanization for sub-basin model</b>	<b>67</b>
<b>Figure 4.1</b>	<b>Flood frequency curves</b>	<b>77</b>
<b>Figure 4.2</b>	<b>N-year floods and rainfall</b>	<b>81</b>
<b>Figure 4.3</b>	<b>% change in flood level</b>	<b>82</b>
<b>Figure 4.4</b>	<b>Changes in flood frequency due to a 25% increase in extreme rainfall</b>	<b>83</b>
<b>Figure 4.5</b>	<b>Skewness vs Kurtosis - Rainfall</b>	<b>85</b>
<b>Figure 4.6</b>	<b>Ln Skewness vs Ln kurtosis - Rainfall</b>	<b>86</b>

Figure 4.7	Flood standard deviation - rainfall standard deviation	89
Figure 4.8	N-year floods - Rainfall standard deviation	90
Figure 4.9	% change in flood level - Rainfall standard deviation	91
Figure 4.10	Changes in flood frequency - Rainfall standard deviation +50%	92
Figure 4.11	Skewness vs Kurtosis - Rainfall standard deviation	94
Figure 4.12	Ln skewness vs Ln kurtosis - Rainfall standard deviation	95
Figure 4.13	Climate change scenarios	98
Figure 4.14	Changes in flood frequency - Climate scenarios	99
Figure 4.15	N-year floods - Urbanization	101
Figure 4.16	% change in flood levels - Urbanization	103
Figure 4.17	Changes in flood frequency - 30% urbanization	104
Figure 4.18	Skewness vs kurtosis - Urbanization	106
Figure 4.19	Ln skewness vs Ln kurtosis - urbanization	107
Figure 4.20	Summary of skewness and kurtosis results - Sub-basin model	109
Figure 4.21	Summary of Ln skewness and Ln kurtosis results - Sub-basin model	111
Figure 4.22	Summary of Ln skewness and Ln kurtosis results - Lumped model	113

## **LIST OF ABBREVIATIONS AND SYMBOLS**

<b>A</b>	Distribution parameter for Log-Pearson III distribution, Equation 3.1  Watershed area, Equation 3.12  Cross-sectional area of flow, Equation 3.16
<b>AMC I</b>	Antecedent moisture condition (dry conditions)
<b>AMC II</b>	Antecedent moisture condition (normal conditions)
<b>AMC III</b>	Antecedent moisture condition (wet conditions)
<b>B</b>	Distribution parameter for Log-Pearson III distribution, Equation 3.1  Area under normal distribution, Equation 3.2  Channel width, Equations 3.15, 3.17, 3.19
<b>Br</b>	Brush
<b><math>c_k</math></b>	Kinematic wave celerity
<b><math>C_k</math></b>	Coefficient of kurtosis
<b>CN</b>	Soil Conservation Service curve number
<b><math>CN_0</math></b>	Curve number for 0% urbanization
<b><math>CN_{100}</math></b>	Curve number for 100% urbanization
<b><math>CN_I</math></b>	Curve number under dry conditions
<b><math>CN_{II}</math></b>	Curve number under normal moisture conditions
<b><math>CN_{III}</math></b>	Curve number under wet conditions
<b><math>CN_u</math></b>	Urbanized curve number
<b><math>C_s</math></b>	Coefficient of skewness
<b><math>C_v</math></b>	Coefficient of variation

<b>DUH</b>	<b>Discrete unit hydrograph</b>
<b>EBM</b>	<b>Energy-balance model</b>
<b>EV1</b>	<b>Extreme value I, or Gumbel, distribution</b>
<b>GCM</b>	<b>Global-circulation model</b>
<b>GEV</b>	<b>General extreme value distribution</b>
<b>Gr</b>	<b>Grassland</b>
<b>I</b>	<b>Immature Forest</b>
<b>I(t)</b>	<b>Excess rainfall intensity at time 't'</b>
<b>I<sub>a</sub></b>	<b>Initial Abstractions (mm)</b>
<b>IUH</b>	<b>Instantaneous unit hydrograph</b>
<b>L</b>	<b>Length of main channel</b>
<b>LAGc</b>	<b>Time lag from centroid of excess rainfall to centroid of unit hydrograph</b>
<b>L<sub>ca</sub></b>	<b>Distance along main channel to point nearest the watershed centroid</b>
<b>LRD</b>	<b>Little Red Deer River</b>
<b>m</b>	<b>Distribution parameter for Log-Pearson III distribution</b>
<b>M</b>	<b>Mature Forest</b>
<b>Mk</b>	<b>Muskeg</b>
<b>n</b>	<b>Manning's roughness coefficient</b>
<b>p</b>	<b>Number of parameters used to fit a distribution</b>
<b>P</b>	<b>Old annual precipitation, Equation 2.1</b>
	<b>Total rainfall depth, Equations 3.3, 3.4</b>
	<b>Wetted perimeter, Equation 3.16</b>

<b>P2/P1%</b>	<b>Ratio of new annual precipitation to old</b>
<b>P<sub>e</sub></b>	<b>Excess rainfall depth (mm)</b>
<b>PF</b>	<b>Protected forest</b>
<b>P<sub>m</sub></b>	<b>Excess rainfall depth in m<sup>th</sup> time interval</b>
<b>PP</b>	<b>Potentially productive</b>
<b>Q(t)</b>	<b>Runoff at time 't'</b>
<b>Q<sub>n</sub></b>	<b>Instantaneous flow rate at the end of n<sup>th</sup> time interval</b>
<b>R<sub>1</sub>, R<sub>2</sub></b>	<b>Random numbers from a uniform distribution between 0 and 1</b>
<b>R2/R1%</b>	<b>Ratio of new annual runoff to old (%)</b>
<b>RCM</b>	<b>Radiative-convective model</b>
<b>s</b>	<b>Sample standard deviation</b>
<b>S</b>	<b>Potential maximum retention (mm)</b>
<b>S.C.S.</b>	<b>Soil Conservation Service</b>
<b>S<sub>o</sub></b>	<b>Average slope of main channel</b>
<b>t</b>	<b>Time</b>
<b>T</b>	<b>Mean annual temperature, Equation 2.1</b>
	<b>Return period, Equation 3.30</b>
<b>t<sub>f</sub></b>	<b>Final time of triangular unit hydrograph</b>
<b>T<sub>w</sub></b>	<b>Weighted temperature</b>
<b>u(t)</b>	<b>Ordinate of instantaneous unit hydrograph at time 't'</b>
<b>UH</b>	<b>Unit hydrograph</b>
<b>U<sub>n</sub></b>	<b>Value of discrete unit hydrograph at the end of the n<sup>th</sup> time interval</b>

$U_p$	Peak of triangular unit hydrograph
$\bar{x}$	Sample arithmetic mean
$x_i$	Value of $i^{\text{th}}$ data point
$X_T$	Magnitude of a T-year event
$y$	Depth of flow
$y_i$	Natural logarithm of $x_i$
$z$	Standard normal deviate
$z_g$	Gumbel reduced variate

#### Greek Symbols

$\alpha$	Significance level
$\nu$	Number of degrees of freedom
$\tau$	Time
$\chi_c^2$	Chi-square test statistic



## **CHAPTER 1**

### **INTRODUCTION**

#### **1.1 General**

The word hydrology literally means "the study of water", and in general it refers to "the scientific study of water and its properties, distribution, and effects on the earth's surface, in the soil, and in the atmosphere" (McCuen, 1989). Fire, iron, gold, and oil may have been more glamorous, but throughout the history of man water has been our most important resource. Over the centuries countless civilizations have arisen, prospered and fallen because of their abilities to supply water in times of want and protect themselves from water in times of abundance. As we approach a new millennium, water is still the single most important factor influencing our quality of life, either directly via drinking water and sewage or indirectly via the environment. Long after fire, iron, gold, and oil cease to have any relevance in our daily lives, water will still maintain its current position.

As important as it is to us as a resource, during a flood, water can have devastating consequences. To properly plan for such events we need to know the probability that a flood of any given size has of occurring. One of the most common tasks asked of hydrologists is to determine flood probabilities using historical data. Over the decades a great many statistical techniques have been developed to estimate these probabilities. Unfortunately, all these methods are essentially very sophisticated ways of extrapolating a line beyond the range of the available data. Since these methods have no physical reality underlying them,

extrapolation is unlikely to give reliable answers. This has long been recognized as a fundamental flaw of such analyses, but the great complexity of the rainfall-runoff process combined with a lack of computation power left early hydrologists little choice. With today's ever increasingly powerful computers, new models have been employed that use geographic, geologic, and atmospheric data to simulate floods. While such methods should improve the reliability of extrapolations, a new problem is starting to be recognized. As our technological might continues to grow, we humans are starting to realize that we are having a growing influence on our environment.

By definition, historical data is based on conditions that existed in the past. If we change our environmental conditions either directly by urbanization or indirectly by atmospheric emissions that can lead to climate change, then this data is no longer relevant and therefore any conclusions drawn from the data will also be irrelevant. To help alleviate this problem it is important to determine what effect such environmental changes have on flood probabilities.

Unfortunately, very little is known about how individual aspects of the hydrologic cycle will be affected by climate change, especially at the storm event scale. Nobody knows how rainfall patterns, vegetation, and soil might react to climate change. This study was an attempt to take what little is known and try to estimate the range of potential impact using established engineering hydrology methods.

## **1.2 Objectives of the study**

The objective of this study was to determine what effects environmental change has on flood probabilities. Two aspects of environmental change were to be looked at, land use change via urbanization, and climate change via rainfall change.

To do this, a watershed in the Alberta foothills was chosen for which the rainfall-runoff process was simulated using two models, a lumped model where all the parameters were constant for the entire watershed, and a distributed model where the watershed was broken up into several sub-basins which were each lump modelled.

Both models then simulated 10 000 random rainstorms from which flood probabilities could be determined. This process was then repeated for various:

- 1) urbanization levels;
- 2) rainfall intensity levels;
- 3) rainfall standard deviations;
- 4) rainfall climate change scenarios.

Finally, all this was accomplished using standard hydrological engineering methods along with minimal data requirements.

## **1.3 Scope of the study**

For this study the watershed that contributes to the streamflow station 05CB002 - Little Red Deer River near Water Valley was selected. This site was chosen for the following reasons:

- 1) appropriate size, 449 km<sup>2</sup>;
- 2) complete soil type and land cover data are available;
- 3) streamflow records going back 32 years;
- 4) availability of hourly rainfall and streamflow data.

Climate change is one of the most complex fields in modern research with entire institutes committed to full time study of all its subtle causes, effects, and implications (Kacholia and Reck, 1997). To this day there have been no reliable estimates of whether event scale rainfall will increase or decrease as a result of increases in atmospheric greenhouse gases (Knox and Kundzewicz, 1997). What research has been done has been limited to changes in mean annual precipitation and total annual streamflow. There has been almost no study of how climate change will affect individual storm events. For these reasons, no attempt was made in this study to determine how extreme rainfall events in the study area will change as the result of a 1 °C increase in average annual surface air temperature. As stated by Boorman and Sefton (1997):

*"While recognizing the limitations and uncertainties of this type of approach, the conclusion drawn in this, and other studies, is that they are not so severe that they invalidate it. Firstly, to incorporate all ... second order effects would require a great many assumptions about future conditions. ... Secondly, it is important to attempt to quantify change as soon as possible so that resulting problems can be addressed in advance. In the context of river flows, the extreme conditions of flood and drought are of particular concern since it is possible that, although there is only a small shift in*

*average conditions, there may be larger, more significant, changes in the extremes. Coping with increased flood magnitudes or reduced flows may require long-term planning and be very costly."*

The principal focus of this study was to determine how flood probabilities change in response to changes in environmental conditions, and was limited to determining the effects of a change in the intensity of extreme rainfall events, assuming all other factors don't change. The main hope is that this study will help increase insight into the extent that flood levels may change so that we can answer questions such as: how much might flood damage increase?, will new control structures need to be built?, could we just improve existing structures?, and is current government policy adequate to deal with any possible changes? None of these questions can be answered with the rather obvious observation that increased rainfall and urbanization will increase flood levels.

Relative to the issue of climate change, urbanization is a simple problem. The effect of urbanization is a decrease in the volume of infiltration of rain water into the soil, resulting in increased surface runoff and streamflow.

#### **1.4 Thesis Organization**

Following this introduction, Chapter 2 is a literature review of past research pertinent to this study. It is a review of recent research into climate change and urbanization and how these relate to the rainfall-runoff process.

Chapter 3 describes the procedure used in this study. It begins with a description of the Little Red Deer River near Water Valley watershed. Every step of the methodology used

to set up the models is described, followed by a summary of the statistical methods used for the analysis.

Chapter 4 deals with the results of the simulations and their analysis.

Chapter 5 is the conclusion of the study and includes a number of recommendations to improve and expand on this work.

The main body of the thesis is followed by an appendix which is a summary of the computer simulation output.

## **CHAPTER 2**

### **LITERATURE REVIEW**

#### **2.1 Temperature and climate change**

Kacholia and Reck (1997) compiled 108 climate change studies from 1980 to 1995, each of which projected the impact on global surface-air temperature due to a doubling of atmospheric CO<sub>2</sub>. The climate models were based on mathematical equations that simulate the behaviour of components of the earth's climate including the atmosphere, oceans, snow and ice, vegetation, and land surfaces. Most of the models surveyed were one of three types: "energy-balance models (EBMs) based upon thermodynamics, radiative-convective models (RCMs) also based upon thermodynamics but including a convective contribution, and general circulation models (GCMs) which introduce hydrodynamics as well" (Kacholia and Reck, 1997). The models were also either steady-state or transient simulations. In steady-state simulations, CO<sub>2</sub> concentrations were doubled instantaneously and the models were then run until an equilibrium was reached. In transient models CO<sub>2</sub> concentrations were slowly increased over a period of time. Both model types could predict long term global temperature increases, but only transient models could predict temperatures at a given date like 2050 or 2100.

Of the 108 studies, 93 included both a global simulation and the authors' best simulation. From these studies a global mean warming projection was calculated to be 2.62 °C, with 80% of the models falling in the range of 1.5 to 4.5 °C. The average EBM projection

was 2.54 °C, with a low of 0.7 °C and a high of 8.7 °C. The average RCM projection was 1.98 °C, with a low of 0.3 °C and a high of 4.2 °C. The average GCM projection was 2.98 °C, with a low of 0.16 °C and a high of 6.3 °C.

These results are consistent with other climate model reviews. In Reck (1981) models from the 1960s to 1981 were around 2 to 3 °C. The National Research Council (1982) determined a mean estimate of  $3.0 \pm 1.5$  °C. The Intergovernmental Panel on Climate Change (1990) chose 2.5 °C as its best estimate.

## **2.2 Vegetation and climate change**

Recent research suggests that CO<sub>2</sub> may affect water availability by changing how vegetation uses water. Experiments have shown that higher CO<sub>2</sub> concentrations increase stomatal resistance to water vapour transport. This would result in lower transpiration rates for each unit of plant leaf area. However, this effect is offset by the tendency of CO<sub>2</sub> to increase plant growth, increase leaf temperatures, and change vegetation species (Friederick and Major, 1997). In a computer simulation of the effects of a doubling in atmospheric CO<sub>2</sub>, Loukas and Quick (1996) found that increased biomass compensated for stomata closure by enough to produce no change in evapotranspiration in one watershed. Aston (1984) estimated that streamflow may increase 40 to 90% due to the effect of a doubling of CO<sub>2</sub> on stomatal closure. However, studies have reported that the effects of rainfall change dominate over other factors in runoff production (Skiles and Hanson, 1994; Frederick and Major, 1997).

These studies have focussed on the effects of climate change on the seasonal and



annual cycles of vegetation. At present, no one knows how vegetation might react to climate change in the form of changing species, or how these changes will effect event scale processes.

### **2.3 Seasonal cycles and climate change**

One of the most likely results of greenhouse warming will be a change in regional hydrologic cycles (Frederick and Major, 1997). Even if warming has little effect on annual precipitation and the frequency of large storms, warming would reduce winter snowfall in favour of rainfall and an earlier onset of spring runoff. This could result in large shifts in seasonal runoff patterns away from the spring and summer towards the winter. Gleick (1986, 1987) used several future climate scenarios and a water-balance model for the Sacramento River basin to show that annual runoff is determined by precipitation changes more than temperature changes, and that seasonal runoff distribution depends on changes in monthly temperature. Even when precipitation decreased Gleick found that winter runoff increased due to a higher rain/snow ratio.

### **2.4 Rainfall - runoff and climate change**

How climate change will be reflected in precipitation changes is far from clear. Karl and Riebsame (1989) cite work by Schlesinger and Mitchell which found that predictions of precipitation change were not consistent from model to model, although models tended to predict a stronger, more extreme, hydrologic cycle. McCabe and Wollock (1992) analyzed the moisture conditions in the Delaware River basin using different GCM simulations. One

GCM predicted a drop in annual precipitation of 46 mm, while another GCM predicted a rise in annual precipitation of 144 mm. In a study of 18 major United States watersheds, Knox (1990) found that three commonly used GCMs indicated both agreement and disagreement. With higher mean temperatures and modest increases in precipitation, the three models predicted an average decrease in annual runoff of 0.4 mm, but with a standard deviation of 32 mm. Schneider, Gleick, and Mearns (1990) concluded that a doubling of atmospheric CO<sub>2</sub> would result in a range of likely changes of  $\pm 20\%$  in annual precipitation and  $\pm 50\%$  in runoff and soil moisture for any given region of the United States. Since this study, advances in climate modelling have done little to decrease the uncertainty in the effects of greenhouse warming on regional water supplies (Frederick and Major, 1997).

In their study of 82 basins across the United States, Karl and Riebsame (1989) found that changes in annual precipitation can be amplified by as much as six times in annual runoff changes. However, temperature changes of 2 °C had little effect on annual runoff. Schaake (1990) estimated that for some basins in the United States a one percent change in precipitation and temperature could result in a ten percent change in annual runoff (i.e. the elasticity of runoff with respect to precipitation and temperature could be as high as ten). Also, runoff elasticities were found to be higher for dry climates and that the elasticity with respect to precipitation was higher than that for evapotranspiration.

## **2.5 Mean runoff and climate change**

Several studies that examine the effects of climate change on flow rates have focussed on changes in annual or seasonal mean flow rates (Nemec and Schaake, 1982; Gleick, 1986, 1987; Flaschka et al., 1987; Karl and Riebsame, 1989; Nash and Gleick, 1991; Rao and Al-Wagdany, 1995; Loukas and Quick, 1996; Dvorak et al., 1997; Boorman and Sefton, 1997).

Nemec and Schaake (1982) used a water-balance model to simulate the effects of climate change on the Pease River in Texas. Temperature change was simulated by assuming that evapotranspiration increased by 4% for each 1 °C increase in temperature. Gleick (1986, 1987) studied the Sacramento River Basin in northern California using a water-balance model. Flaschka et al. (1987) used another water-balance model in their study of several rivers in the Great Basin in Nevada and Utah.

Nash and Gleick (1993) also used a water-balance model in their study of the White, East, and Animas Rivers and the inflow into Lake Powell in the Colorado Basin in the southwest United States. They used two temperature increments (+2 and +4 °C) and five precipitation increments (-20%, -10%, 0, +10%, and +20%) as well as five GCM scenarios.

Rao and Al-Wagdany (1995) used a monthly water-balance model to study the Wabush River in northern Indiana. After calibrating the model using observed climatic and runoff data, eight simulations were conducted for two temperature increments (+1 and +3 °C) and four precipitation increments (-20%, -10%, +10%, and +20%). They found that in general temperature changes had less effect on mean annual runoff than precipitation changes.

Loukas and Quick (1996) studied the effects of climate change on two watersheds in British Columbia, the Upper Campbell River on Vancouver Island, and the Illecillewaet near

Revelstoke in the eastern British Columbia mountains. The Canadian Climate Centre GCM predicted a doubling of atmospheric CO<sub>2</sub> would cause an increase in mean annual temperature of more than 3 °C for both watersheds and an increase in mean annual precipitation of 7.5% for the Campbell watershed and 17% for the Illecillewaet watershed. They calibrated the UBC watershed model with 7 years of daily streamflow data from the Upper Campbell and 10 years of data from the Illecillewaet. The model was then verified using another 10 years of data from the Illecillewaet. The model was not verified for the Upper Campbell because there was no further data available. The GCM predictions were then applied to the available data and simulations of the same years, but with double the CO<sub>2</sub> and increased temperature and precipitation, were conducted. They found that mean annual streamflow increased by 21% in the Illecillewaet watershed, and by 7.5% in the Upper Campbell.

Dvorak et al. (1997) studied the Elbe, Zelivka, Upa, and Metuje Rivers in the Czech Republic. Two water-balance models and a conceptual model were used to simulate eight incremental scenarios (+2 and +4 °C, and -5%, 0%, +5%, +10% precipitation) and three GCM scenarios. These models were used to predict changes in mean annual runoff, the 90th percentile flow rate (flow with an exceedance probability of 90%), and the storage capacity of a reservoir. These results were then compared to predictions of future water demands to determine the vulnerability of the water supply to climate change.

Boorman and Sefton (1997) studied the Greta, Coln, and Fal in England. Two conceptual models were used to simulate eight incremental scenarios (0, +2, and +4 °C, and -10%, 0%, +10% precipitation) and two GCM scenarios. Predictions were made for changes in the mean annual runoff, the 95th percentile flow, and the mean annual flood. Although

both models reproduced current conditions equally well, they gave very different results under changed climate conditions. In the case of the Coln with a temperature increase of 4°C and a precipitation increase of 10%, one model predicted a drop in the mean annual flood of 33% while the other predicted an increase of 14%. Upon review it was found that one of the models (the one that predicted a 33% drop in the example) had a poor algorithm for the rainfall-runoff relationship. As a result the authors suggested that its results could not be trusted. Table 2.1 summarizes the results of the other model as well as the results of the other studies mentioned above. The table includes the results of all the incremental climate change scenarios used in the studies for a given change in annual temperature and precipitation, as well as the predictions for specific GCM predictions, if applicable.

Langbein (1949) used data from 22 basins across the United States to determine a relationship between mean annual runoff, mean annual temperature, and weighted temperature. The weighted temperature is the average of mean monthly temperatures weighted by the mean precipitation in each month. This results in a heavier weighting for wet months and a lighter weighting for dry months. Karl and Reibsame (1989) found that although Langbein's relationship characterized runoff differences between different regions of the United States, it was inadequate for predicting runoff changes due to climate change. In their study of 82 basins across the United States, Karl and Reibsame used methods similar to Langbein to determine a relationship between change in annual runoff, change in annual precipitation, initial mean annual precipitation, mean annual temperature, and weighted temperature. They developed the following equation:

Annual temp. increase (°C)	Annual precip. change (%)	White River 1993 (SW US)	Animas River 1993 (SW US)	East River 1993 (SW US)	Lake Powell 1993 (SW US)	Pease River 1982 (Texas)	Great Basin 1987 (Utah)
+1	-10					-50	
	0					-10	
	+10					+50	
+2	-20	-23	-26	-28			
	-10	-14	-17	-19	-23		-28 to -17
	0	-4	-7	-9	-12		
	+10	+7	+3	+1	+1		
	+20	+19	+14	+12			
+3	-10					-50	
	0					-12	
	+10					+35	
+4	-20	-26	-32	-33	-41		
	-10	-18	-23	-26	-32		
	0	-9	-14	-17	-21		
	+10	+1	-5	-3	-10		
	+20	+12	+5	+7	+2		
GCM Simulations		-8 to +12	-18 to -8	-11 to -9	-24 to 0		

**Table 2.1**  
**Percent change in mean annual flow**

Annual temp. increase (°C)	Annual precip. change (%)	Sacram. River 1987 (Calif.)	Wabash River 1995 (Ind.)	Czech Republic Rivers 1997	Greta 1997 (Eng)	Coln 1997 (Eng)	Fal 1997 (Eng)
+1	-20		-41				
	-10		-24				
	+10		+15				
	+20		+37				
+2	-10	-18			-15	-18	-17
	-5			-33 to -15			
	0	-3		-23 to -6	-2	-3	-3
	+5			-13 to +5			
	+10	+12		-2 to +15	+11	+12	+12
+3	-20		-48				
	-10		-32				
	+10		+3				
	+20		+25				
+4	-10	-21			-17	-20	-20
	-5			-45 to -25			
	0	-7		-36 to -16	-4	-6	-6
	+5			-26 to -7			
	+10	+7		-16 to +3	+10	+9	+9
GCM Simulations				-10 to +3	+11 to +26	+11 to +26	+10 to +32

**Table 2.1 (Cont.)**  
**Percent change in mean annual flow**

$$\log(R_2/R_1\%) = a \cdot \log(P_2/P_1\%) + b(T_w - T) + c \cdot T_w + d \cdot P + e \quad (2.1)$$

where:	$R_2/R_1\%$	= ratio of new annual runoff to old (%)
	$P_2/P_1\%$	= ratio of new annual precipitation to old (%)
	$T_w$	= weighted temperature (°C)
	$T$	= mean annual temperature (°C)
	$P$	= old annual precipitation (mm)
	$a$	= 1.77
	$b$	= $5.65 \times 10^{-3}$ for $P_2/P_1\% > 100\%$ = $-5.65 \times 10^{-3}$ for $P_2/P_1\% < 100\%$
	$c$	= $3.01 \times 10^{-3}$ for $P_2/P_1\% > 100\%$ = $-3.01 \times 10^{-3}$ for $P_2/P_1\% < 100\%$
	$d$	= $-1.79 \times 10^{-5}$ for $P_2/P_1\% > 100\%$ = $1.79 \times 10^{-5}$ for $P_2/P_1\% < 100\%$
	$e$	= -1.525

From this equation, Karl and Riebsame concluded that runoff is more sensitive to precipitation change in regions where the bulk of precipitation falls in the warmer months (i.e. where  $T_w > T$ ) and where  $T_w$  is high. To illustrate this they cited an example where if  $P = 1000$  mm,  $T_w = 25$  °C, and  $T_w - T = 10$  °C, then a 10% increase in precipitation would result in a 60% increase in runoff. Conversely, if  $P = 1000$  mm,  $T_w = -10$  °C, and  $T_w - T = 0$  °C, then a 10% increase in precipitation would result in only a 10% increase in runoff.



## **2.6 Extreme events and climate change**

So far, examinations of the hydrologic response to global warming have emphasized changes in average conditions such as mean annual runoff. Research has been conducted into the effects of greenhouse warming on extreme hydrologic events by analyzing observed hydrological records. However, no meaningful evidence of a changed flood regime has been found yet. Despite this it is widely believed that climate change will have a stronger effect on the extremes than on the means (Knox and Kundzewicz, 1997).

Generalizations drawn from global-scale relationships between floods and droughts and atmospheric circulation tend to underestimate the impact of climate change because extreme hydrologic events vary regionally. Much of Europe experienced great floods between 1150 and 1500 AD, while southern Europe saw very little flooding. Chinese flood records going back 1000 years show that large floods were rare in northern China during the warm Middle Ages (1100 to 1250 AD) but became more frequent afterwards into the Little Ice Age of 1650 to 1750 (Knox, 1993).

In an attempt to estimate the effects of modest changes in climate, Knox (1993) used paleologic data from the upper Mississippi River tributaries. By sampling cobble and boulder gravels transported by ancient overbank floods and relating the size of the largest particles to the minimum flow rate required to transport them, he was able to construct a 7000-year record of flooding. During a warm, dry period between 3300 and 5000 years ago, the largest floods were equivalent to what are now considered 50-year floods. 3300 years ago the climate became cooler and wetter and floods that would now occur every 500 years or more became frequent. Even larger floods occurred from 1250 to 1450 AD during the interval

between the warm Middle Ages and the Little Ice Age. All of these changes were associated with mean annual temperature changes of less than 2 °C, and mean annual precipitation changes of less than 15%.

Using a GCM, Whetton et al. (1993) determined the frequency of daily rainfall depths across all of Australia assuming a doubling of atmospheric CO<sub>2</sub>. They found that rainfall events of less than 6 mm/day became 5-10% less frequent while events of over 13 mm/day increased 50% in frequency. They also found that the larger the rainfall event the bigger the shift. For example, a one-year event became a 6-month event while a 10-year event became a 3-year event. No attempt was made in the study to translate rainfall frequency into flood frequency.

Karl et al. (1995) pointed to recent research that a warmer climate could result in a decrease in temperature variability (in a manner analogous to the tendency for tropical climates to experience less temperature variation than polar and sub-polar climates), and an increase in the proportion of precipitation occurring in extreme events. In an attempt to detect such trends, the data from more than 600 stations across the United States, China, the former Soviet Union, and Australia were analyzed. Results from the former Soviet Union, China, and Australia were found to be mostly inconclusive. The United States data, which had by far the longest period of record, showed a clear reduction in day-to-day temperature variability, and a strong increase in the proportion of precipitation from extreme events, especially during the summer months. This increase in summer precipitation since 1911 translates into an average of about one additional extreme event (>50 mm/day) every two years. The proportion of total rainfall contributed by small and medium sized events either

stayed the same or dropped significantly.

In their study of the Upper Campbell and Illecillewaet watersheds in British Columbia, Loukas and Quick (1996) found that a doubling of atmospheric CO<sub>2</sub> would increase the annual maximum flow in the Upper Campbell by 20%, but would decrease the annual maximum flow in the Illecillewaet by 13% despite the fact that the latter would experience a greater increase in mean annual flow. They also found that despite large changes in snowpack, glacier runoff, and the winter snowfall-rainfall ratio, the timing of the annual flood did not change.

As mentioned above, Boorman and Sefton (1997) used a conceptual model in their analysis of the Grea, Coln, and Fal in England to determine their sensitivities to climate change. They found that the mean annual flood increases 12 to 19% for a 10% increase in mean precipitation, and decreases 12 to 19% for a 10% decrease in mean precipitation. The mean annual flood was found to decrease 1 to 3% for a 2 °C increase in mean annual temperature, and decrease 1 to 6% for a 4 °C increase in mean annual temperature. When the scenarios predicted by two GCMs were simulated the mean annual flood was found to increase by 13 to 50%.

## **2.7 Urbanization**

In an unurbanized, natural watershed, a portion of any rainfall is intercepted by vegetation. The remainder falls on the ground where it is held in depressions and infiltrates into the soil. Once the surface is saturated, excess rainfall becomes surface runoff. The soil and vegetation thus act as reservoirs, reducing and delaying flood peaks. In an urbanized

watershed, there is almost no vegetation or infiltration, and so rainfall quickly fills any depressions and all further rainfall is available to become excess rainfall and runoff. This results in a much higher and earlier flood peak (Lazaro, 1979).

Standard flood frequency analysis assumes that historical data comes from a homogenous system. Changes in a watershed's land use would result in a nonhomogeneous record, making analysis problematic (McCuen, 1989).

McCuen and Thomas (1991) used three methods to analyze the Pond Creek watershed near Louisville, Kentucky. This watershed underwent considerable urbanization between 1945 and 1965, especially after 1955. The data for 1945 to 1965 were adjusted using residual analysis, index adjustment, and a watershed model. For the residual analysis, the trend of flood peaks was detected and quantified into an equation. Floods occurring before 1965 were then adjusted by subtracting the value of the trend in their year of occurrence and adding the trend value in 1965. For the index adjustment method, a theoretical relationship between return period, urbanization, and flood level derived by McCuen (1989) from the results of several urbanization studies was used. All recorded floods were ranked, and then adjusted based on their past urbanization level to the current level. The floods were then re-ranked and the process repeated until the order no longer changed. For the watershed model method, a computer model was used to simulate the storms that produced the annual peak flows from 1945 to 1965 under current land use conditions. The predictions for these three methods for the 2-, 10-, and 100-year floods were compared to the observed record between 1964 and 1988. They found that predictions for the 100-year flood agreed much better than predictions for the 2-year flood, but made no

attempt to explain why.

Leopold (1968) combined the results of seven studies between 1961 and 1968 which related the change in the mean annual flood to the implementation of storm sewers and impervious land. The results of these studies were then interpolated and extrapolated to a common scale of 1 square mile. Leopold found that for unsewered areas increasing impervious area from 0% to 100% would increase peak discharge by 2.5 times. For fully sewerred areas with no impervious land, peak flows would increase 1.7 times over unsewered areas. In the case where a watershed was made fully impervious and fully sewerred the mean annual peak flow was found to increase by a factor of about eight. Using these results, Leopold attempted to estimate the effect of urbanization on the frequency of overbank flows in the Brandywine Creek basin in Pennsylvania. After making a number of assumptions about the size of an overbank flood and the effect of urbanization on floods below the mean annual flood, the study estimated that a 50% sewerred and 50% impervious watershed could expect to see roughly four times the number of overbank floods that an unurbanized watershed would.

Urbanization also changes the geomorphology of a watershed's terrain, which can change the speed at which excess rainfall becomes streamflow. Espey et al. (1969) cites research by VanSickle (1962) on the effect of urbanization on the shape of a watershed's unit hydrograph (for a detailed discussion of the unit hydrograph concept, see Chapter 3.5). VanSickle determined the unit hydrographs for six similar storms in the Brays Bayou in Houston, Texas between 1939 and 1960 during a period of extensive urbanization. He found that after urbanization the peak of the unit hydrograph had more than doubled and the time

to the peak had been cut by more than 50%. VanSickle concluded that urbanization in the study region could increase peak flow rates two to five times over peak flow rates under rural conditions.

## **2.8 Synthetic flood-frequency curves in Alberta**

Pomeroy (1987) studied 8 watersheds in the Alberta foothills to develop a procedure for estimating flood flows at ungauged sites. Two methods were used to produce synthetic flood-frequency curves. The first was to select 100 storm events at random and then fit an extreme-value-one (EV1 or Gumbel) distribution. The second was to assume a one-to-one relationship between storm frequency and flood frequency (ie. that a 100-year storm will produce a 100-year flood).

Chang (1992) continued Pomeroy's work with a more in-depth study of 23 watersheds also within the Alberta foothills. Chang modified Pomeroy's techniques in order to more accurately simulate the transition of rainfall into runoff. The basic method employed was:

- 1) randomly select a storm duration;
- 2) randomly select a total rainfall depth;
- 3) randomly select a rainfall distribution in time;
- 4) randomly select an antecedent moisture condition;
- 5) determine excess rainfall;
- 6) determine flood hydrograph;
- 7) select maximum flow rate;

8) repeat procedure several hundred times.

Chang developed synthetic flood-frequency curves for several gauged sites in the study area that were not used in the model calibration procedure. The resulting curves matched the observed flood data within tolerable limits defined by a level of significance above 5 % for a chi-square test.

## **CHAPTER 3**

### **METHOD OF ANALYSIS**

#### **3.1 Study region**

The streamflow station selected for this study was station 05CB002 - Little Red Deer River near Water Valley located at 51° 30' 41" N, 114° 40' 19" W in the foothills of Alberta's Rocky Mountains approximately 70 km northwest of the City of Calgary. This station defines the surface water outlet of a 449 km<sup>2</sup> drainage basin. Figure 3.1 shows the location of the watershed relative to the rest of the Province of Alberta. Figure 3.2 is a map of the watershed showing the major tributaries and sub-basins used in this study.

Elevations in the watershed vary from a high of 1860 m on the western boundary to a low of 1190 m at the streamflow station. The vegetation in the far western region of the watershed is dominated by immature pine forest. Moving towards the east, the vegetation becomes more mature and the pine forests become mixed with spruce. In the northwest there is a significant area covered in muskeg, and in the central region some grasslands. The area surrounding the recording station is mostly clear pasture land. Most of the soils in the watershed are classified as moderately well to well draining, and there are no significant areas of bare rock in the watershed.



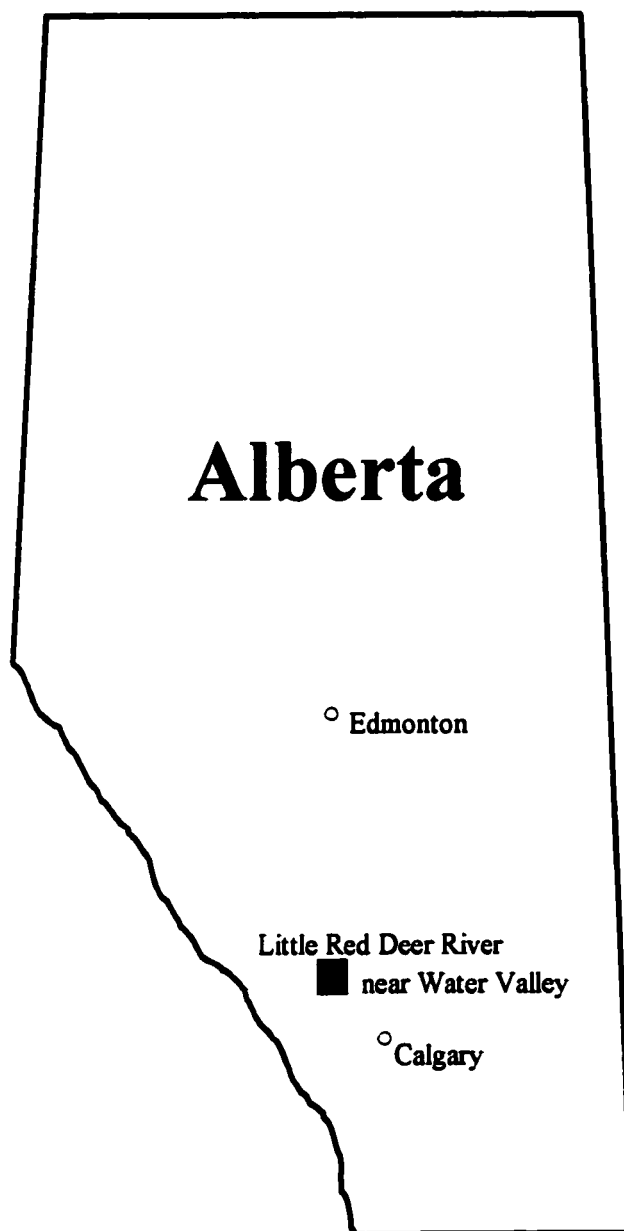


**Figure 3.1**

**Location of study area**

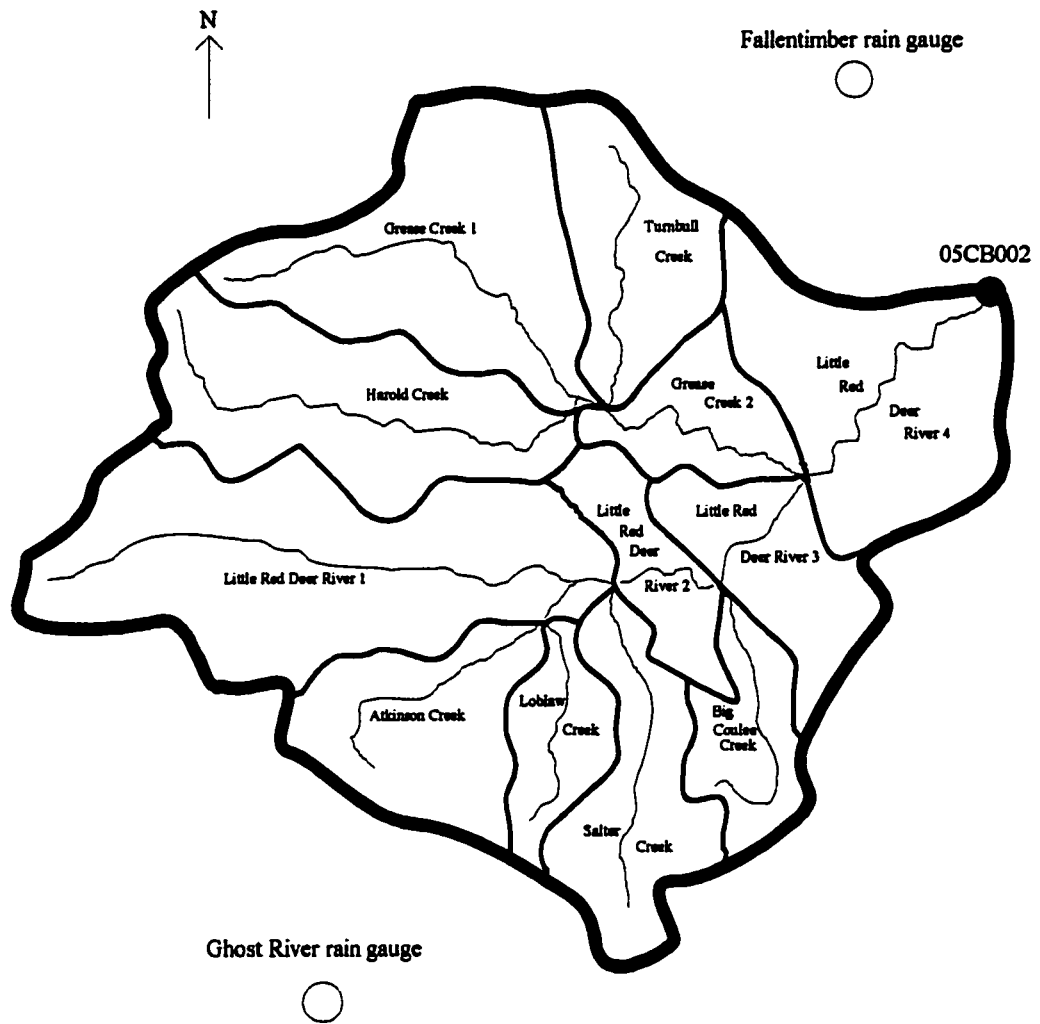


**Figure 3.2**

**Little Red Deer River near Water Valley watershed**

### **3.2 Model summaries**

To simulate the rainfall-runoff process two types of models were used: a lumped model and a sub-basin model. The principal difference between the two models is that in the lumped model the entire watershed was modelled as a single system, while in the sub-basin model the watershed was subdivided into 12 sub-basins and was modelled as the sum of these 12 smaller systems. This was done in order to determine the effect of model scale and the difference between lumped and distributed modelling. Figure 3.3 is a flow-chart of the general modelling procedure used in both models.

#### **3.2.1 Lumped model**

For the lumped model, all parameters are assumed to apply to the entire watershed. The advantage of modelling this way is that there is a streamflow station at the outlet and so the model can be calibrated to match historical data. Unfortunately, this also means that any subtleties resulting from the spatial distribution of these parameters will be lost. Figure 3.4 is a flow-chart of the lumped rainfall-runoff model. As can be seen, there is only one step.

#### **3.2.2 Sub-basin model**

For this model the watershed was divided into the 12 sub-basins ranging in size from 12.5 to 76.5 km<sup>2</sup> as shown in Figure 3.2. For each sub-basin all parameters are assumed to be the same throughout, in much the same manner as in the lumped model. None of these sub-basins has a streamflow station at their outlets and so no calibration procedure was used. Instead, empirical relationships derived by previous studies of other watersheds were used.

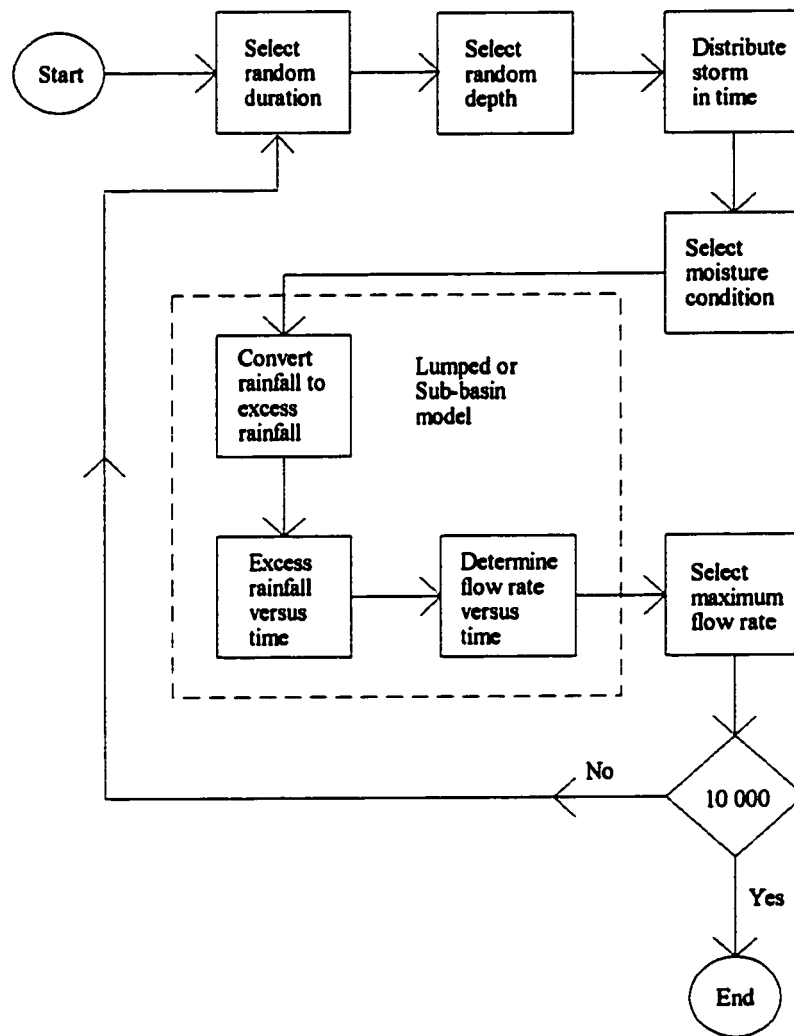


**Figure 3.3**

**Modeling procedure flow chart**

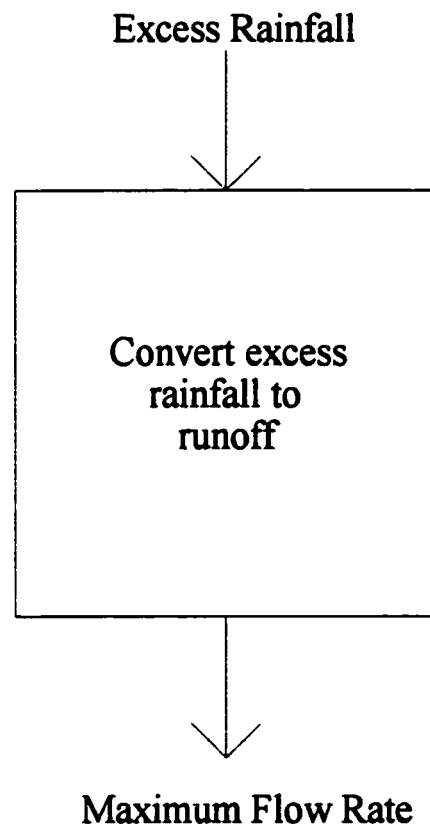


**Figure 3.4**  
**Lumped model flow chart**

Figure 3.5 is a flow-chart of the sub-basin rainfall-runoff model.

### 3.3 Rainfall

The first step in modelling a flooding event is the selection of the storm. For both models this was done using the same three steps:

- 1) select a storm duration;
- 2) select a total rainfall depth;
- 3) distribute the rainfall in time.

All storms were assumed to be evenly distributed in space throughout the watershed.

#### 3.3.1 Storm duration

Chang (1992) analyzed 61 storm events in Alberta's Rocky Mountain foothills to derive an equation for annual extreme storm duration. The storms selected were the most extreme non-snowfall events on record and were mostly, but not all, annual maximum storms. Chang found that storm durations seemed to follow a Log Pearson III distribution. Pilon et al. (1985) proposed the following equation for approximating the Log Pearson III distribution:

$$\ln X_T = m + A \left( \frac{z}{3B^{1/6}} - \frac{1}{9B^{2/3}} + B^{1/3} \right)^3 \quad (3.1)$$

Where:      m, A, B      =   distribution parameters;  
                  z                =   standard normal deviate;

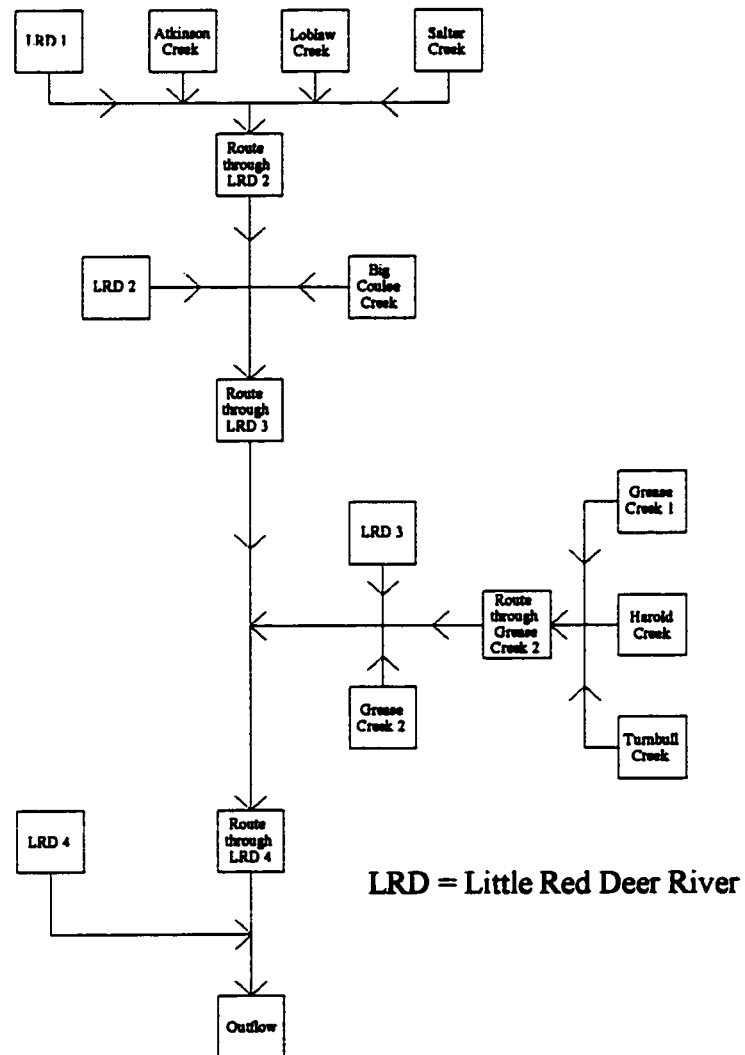


**Figure 3.5**

**Sub-basin model flow chart**

$$X_T = \text{magnitude of a T-year event.}$$

Using this equation, Chang determined that the best data fit was when  $m = 4.715$ ,  $A = -0.159$ , and  $B = 12.11$ . Here,  $X_T$  is the duration of the storm event in hours. This produces a distribution with a mean of 18.7 hours and a standard deviation of 9.5 hours.

To select a random storm duration from this distribution a random number,  $R_1$ , is first generated from a uniform distribution with range between 0 and 1, for example 0.2. The standard normal deviate, also called a z-score, can then be estimated using the following equation derived by Abramowitz and Stegun (1965):

$$B = \frac{1}{2} (1 + 0.196854|z| + 0.115194|z|^2 + 0.000344|z|^3 + 0.019527|z|^4)^{-4} \quad (3.2)$$

$$\begin{aligned} \text{Where: } |z| &= \text{absolute value of } z; \\ B &= R_1 \text{ for } R_1 < 0.5 \\ &= 1 - R_1 \text{ for } R_1 \geq 0.5 \end{aligned}$$

When  $R_1 < 0.5$ ,  $z < 0$  and when  $R_1 > 0.5$ ,  $z > 0$ . Because Equation 3.2 is non-linear in  $z$ , an iterative technique must be used to solve it. In this study, Newton's method was used. When  $R_1 = 0.2$ ,  $z = -0.842$ . This value can now be substituted into Equation 3.1 to determine  $X_T$ . For the example given the storm duration would be 26 hours. In other words, for the distribution Chang derived, 20% of annual extreme storms in the foothills of Alberta last longer than 26 hours.



### 3.3.2 Total rainfall depth

Total rainfall depth was determined from the maps in the "Rainfall Frequency Atlas of Canada" (Environment Canada, 1985) which display extreme rainfall statistics for storms ranging from 5 minutes to 24 hours. These maps give the mean and standard deviation for each duration assuming they follow a Gumbel, or EV1, distribution. The "Hydrological Atlas of Canada" (Fisheries and Environment Canada, 1978) includes isolines for 48/24 hour and 72/24 hour rainfall ratios. In southwestern Alberta these are 1.35 and 1.5 respectively. Table 3.1 shows a summary of the means and standard deviations for durations ranging from 6 to 72 hours.

To select a rainfall depth another random number must be generated,  $R_2$ , and the values for the mean and standard deviation are interpolated from the data in Table 3.1 for the storm duration selected. To continue the previous example, let  $R_2 = 0.4$ . Interpolating Table 3.1 for a 26 hour storm gives a mean of 48.8 mm and a standard deviation of 15.8 mm. The total rainfall depth can be calculated using the equation derived by Chow et al. (1988):

$$P = \bar{x} - s \frac{\sqrt{6}}{\pi} \left\{ 0.5772 + \ln \left[ \ln \left( \frac{1}{R_2} \right) \right] \right\} \quad (3.3)$$

Where:       $P$       = total rainfall depth, mm;  
                   $\bar{x}$       = mean, mm;  
                   $s$       = standard deviation, mm.

For the example total rainfall depth would be 46.6 mm.

Duration (hours)	Mean (mm)	Standard Deviation (mm)
6	26.0	7.0
12	36.5	14.0
24	47.0	15.2
48	63.5	20.5
72	70.5	22.8

**Table 3.1****Extreme rainfall statistics**

### **3.3.3 Time distribution of rainfall**

Huff (1967) derived a series of curves describing the relationship between cumulative time and cumulative rainfall for heavy storms in the U.S. Midwest. These curves were split into four quartiles which each had nine curves corresponding to probabilities of 10 to 90%. An  $n^{\text{th}}$  quartile storm is one in which the maximum rainfall intensity occurs in the  $n^{\text{th}}$  quarter of the storm. Figure 3.6 shows graphs of the four quartiles. Huff found that not all quartiles had an equal probability of occurring, second quartile storms were the most common and fourth quartile storms were the least common. Table 3.2 lists the probabilities of occurrence of each quartile. Because these curves only refer to cumulative duration and rainfall, they assume that there is no correlation between total duration and the time distribution of rainfall.

To select a time distribution curve, two random numbers must be generated. The first number determines which quartile the storm is in and the second number determines which curve is to be selected.

### **3.4 Abstractions and excess rainfall**

Chow et al. (1988) defines abstractions as "interception of precipitation on vegetation above ground, depression storage on the ground surface as water accumulates in hollows over the surface, and infiltration of water into the soil". Excess rainfall is the portion of rainfall that becomes short-term runoff. In general, excess rainfall is equal to the difference between total rainfall and total abstractions.

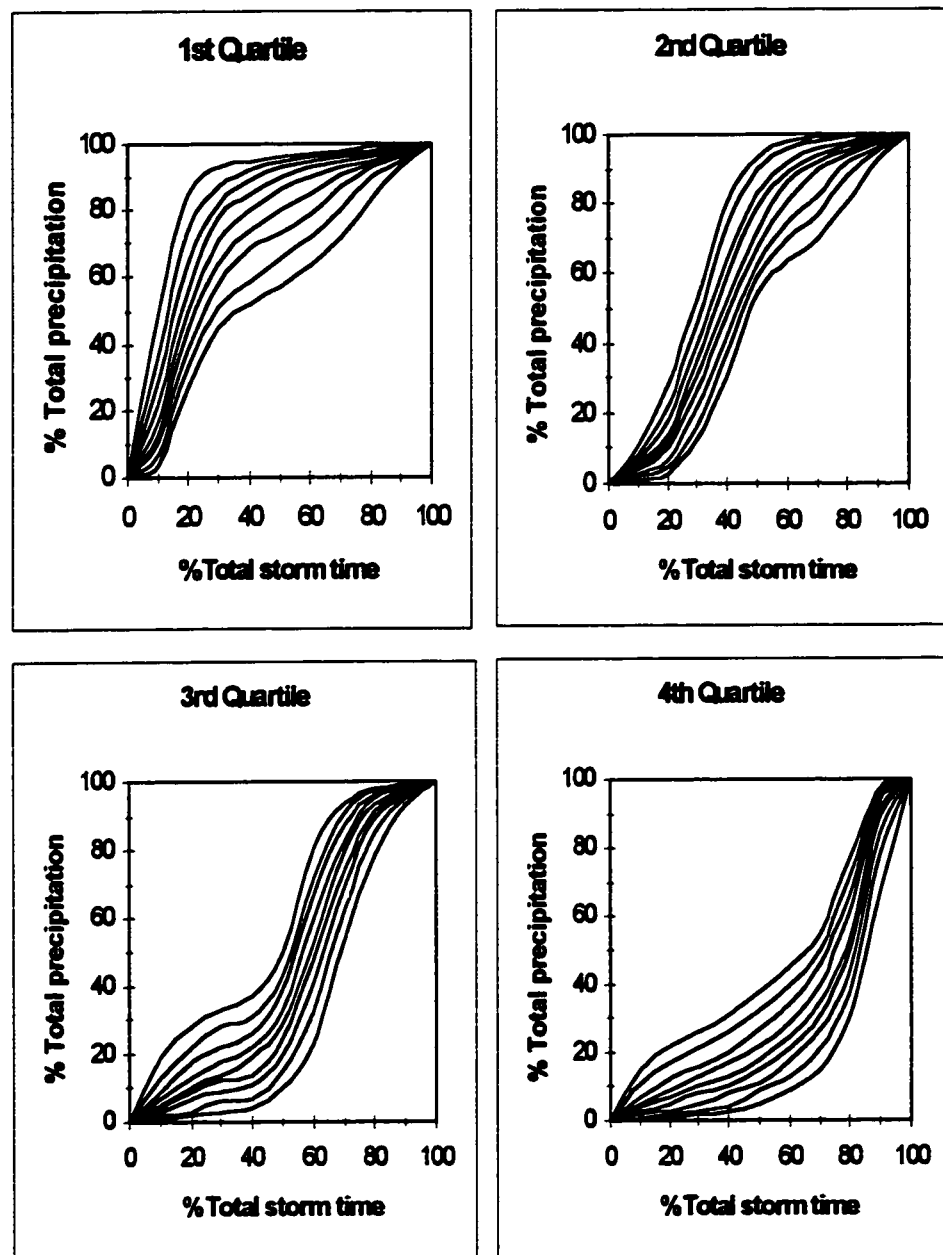


**Figure 3.6**

**Rainfall distribution curves (after Huff (1967))**

Quartile	Probability (%)
1st	30
2nd	36
3rd	19
4th	15

**Table 3.2**

**Quartile probabilities (after Huff(1967))**

### 3.4.1 S.C.S. curve number method

The U.S. Soil Conservation Service (1972) developed a method for computing abstractions from a rainfall event called the S.C.S. curve number method. In their method there is a minimum amount of rainfall,  $I_a$ , called initial abstractions which is defined as the minimum amount of rainfall required before any runoff can occur. Rainfall beyond this amount can either become runoff or be further abstracted. The S.C.S. derived the following equation:

$$P_e = \frac{(P - I_a)^2}{P - I_a + S} \quad (3.4)$$

Where:

- $P$  = total rainfall, mm;
- $P_e$  = excess rainfall, mm;
- $I_a$  = initial abstractions, mm;
- $S$  = potential maximum retention, mm.

By studying many watersheds, the S.C.S. developed the following relationship:

$$I_a = 0.2 S \quad (3.5)$$

The S.C.S. also developed the concept of a dimensionless curve number, CN, such that  $0 \leq CN \leq 100$ . For impervious and water surfaces  $CN = 100$ . A curve number of zero refers to a surface with an infinite capacity to absorb water. The curve number is related to potential maximum retention by:

$$CN = \frac{25400}{S + 254} \quad (3.6)$$

The S.C.S. published tables relating curve number to land use and hydrologic soil type. They used four soil types:

- A      deep, well to excessively drained, sands and gravels (minimum runoff);
- B      moderately deep, moderately well drained, moderate to coarse texture;
- C      slow infiltration when wetted, impeding layer of or moderately fine soil;
- D      very slow infiltration, very fine soil such as clays (maximum runoff).

The numbers published were for normal antecedent moisture conditions (AMC II). Chow et al. (1988) published the following equations for dry conditions (AMC I) and wet conditions (AMC III):

$$CN_I = \frac{4.2CN_{II}}{10 - 0.058CN_{II}} \quad (3.7)$$

$$CN_{III} = \frac{23CN_{II}}{10 + 0.13CN_{II}} \quad (3.8)$$

### 3.4.2 Application of the curve number method

To use the curve number method, one must first estimate the AMC II curve number for the watershed. Land use in the watershed was taken from a series of maps called the "Composite Forest Cover Series" (Alberta Energy and Natural Resources, 1975) and soil

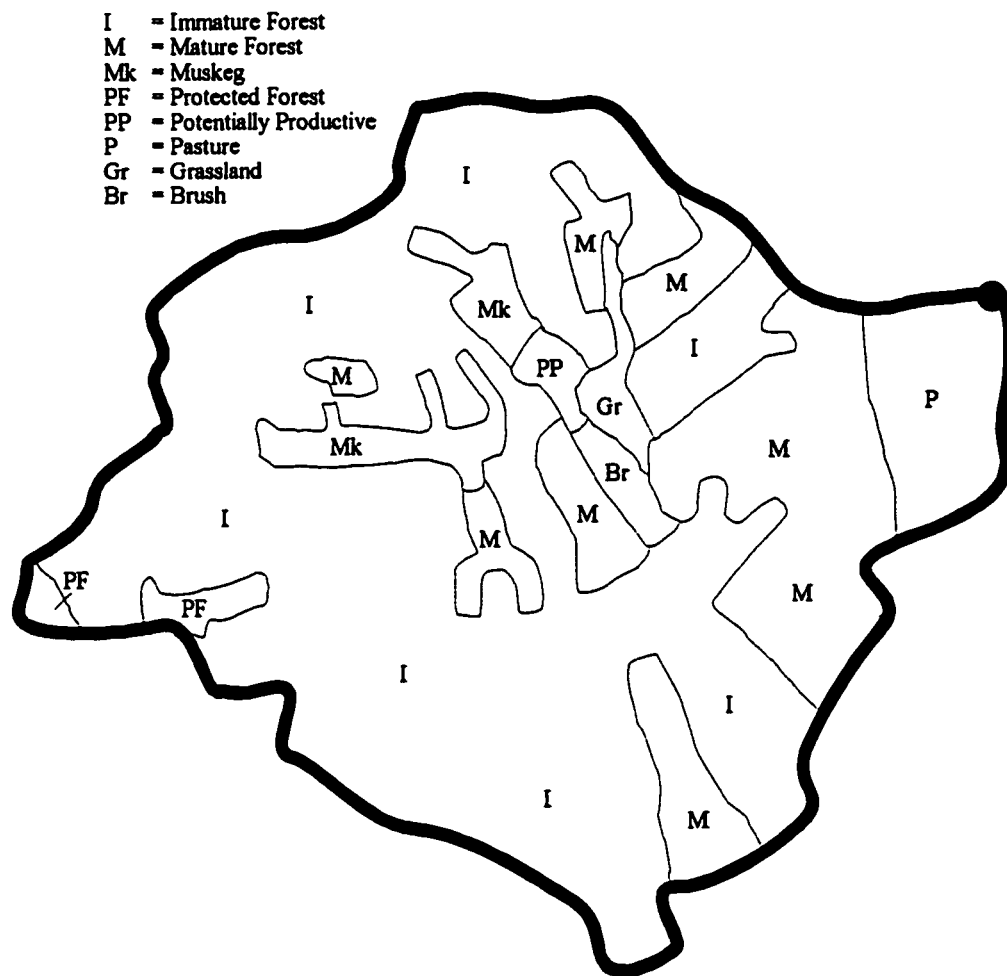
type was determined from the "Ecological Land Classification and Evaluation" (Alberta Energy and Natural Resources, 1978) series of maps.

Figure 3.7 is a map of the land use in the Little Red Deer River near Water Valley watershed showing the distribution of eight land use classes. The vast majority of the watershed is covered by mature and immature forests, with the rest split between muskeg, pasture, potentially productive land, grassland, and brush.

The Ecological Land Classification and Evaluation series of maps uses the Canadian soil classification system established by the Canadian National Soil Survey Committee (1974). This system divides soils into six classes ranging from the rapidly draining class 1, to the very poorly draining class 6. Pomeroy (1987) derived an empirical relationship between the Canadian and S.C.S. classifications. The modified version of this relationship used in this study is shown in Table 3.3. A map of the soil types in the Little Red Deer River near water Valley watershed is shown in Figure 3.8.

To determine the curve number of the watershed and its sub-basins, the two maps shown in Figures 3.7 and 3.8 were overlayed on top of a grid. For each sub-basin, the area of every combination of land use and soil type was measured. Table 3.4 shows the relationship of curve number to land use and soil type used in this study. Curve number values for classes A+, B+, C-, and C+ were linearly interpolated between classes A, B, C, and D. Curve numbers were then assigned to each sub-basin, and the entire watershed, based on an area weighted average. A summary of the curve numbers of the entire watershed and its sub-basins is shown in Table 3.5.





**Figure 3.7**

**Land use map of Little Red Deer River near Water Valley watershed**

Canadian	SCS (Pomeroy, 1987)	SCS (Kerkhoven, 1998)
1	A	A
1-2	---	A+
2	B	B
2-3	---	B+
3	C	C-
4	C	C
5	C	C+
6	D	D

**Table 3.3**

**Conversion of Canadian soil classification to SCS classification**

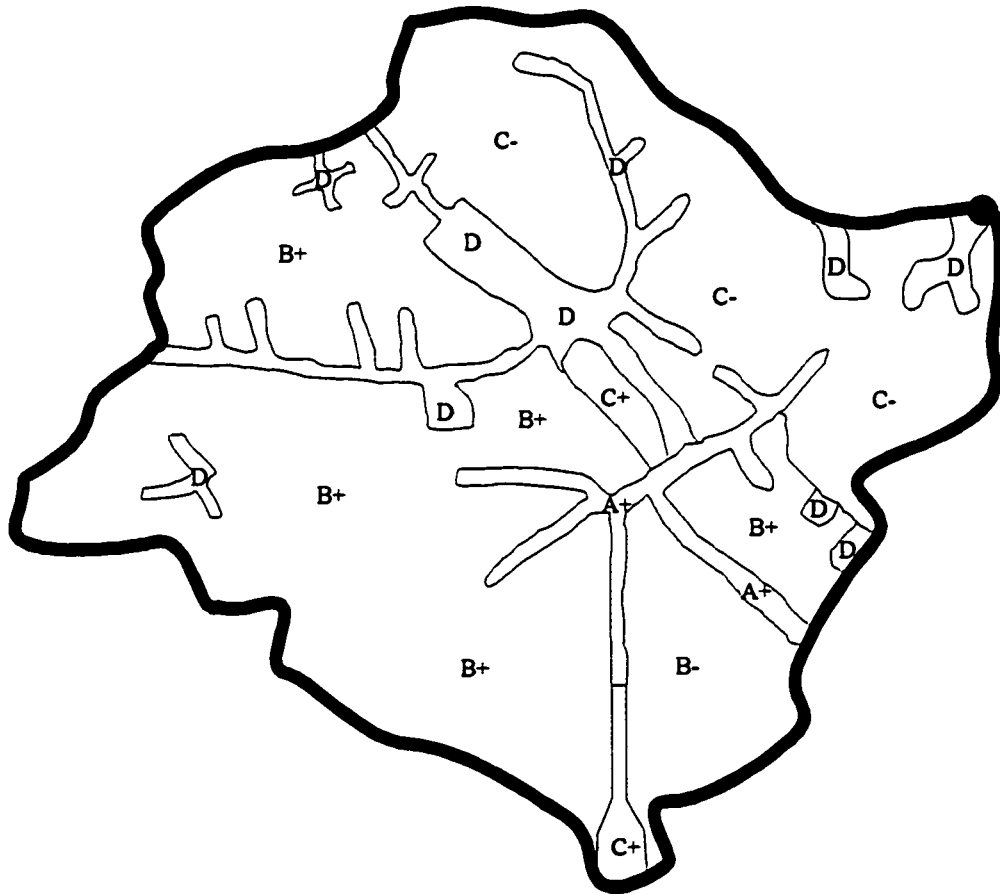


**Figure 3.8**

**Soil type map of Little Red Deer River near Water Valley watershed**

Land use	A	A+	B	B+	C-	C	C+	D
Pasture	54	62	70	73	77	80	83	85
Grassland	49	59	69	72	76	79	82	84
Pot. Productive	36	48	60	63	67	70	73	76
Prot. Forest	36	48	60	63	67	70	73	76
Mature Forest	26	39	52	55	59	62	66	69
Immature Forest	46	57	68	71	75	78	81	84
Brush	49	59	69	72	76	79	82	84
Muskeg	55	59	69	78	76	79	82	84
Urban, 50% imp.	69	76	80	82	84	86	88	89

**Table 3.4**

**Land use / soil type to curve number**

Sub-basin	Area (km <sup>2</sup> )	Curve Number
Little Red Deer River 1	76.5	68.2
Little Red Deer River 2	20.5	64.7
Little Red Deer River 3	16.5	59.4
Little Red Deer River 4	54.0	68.1
Atkinson Creek	30.5	70.2
Loblaw Creek	12.5	71.0
Salter Creek	28.0	69.0
Big Coulee Creek	19.5	65.5
Harold Creek	73.5	73.0
Grease Creek 1	54.5	75.6
Grease Creek 2	21.5	69.0
Turnbull Creek	41.5	68.7
<b>Little Red Deer River watershed</b>	<b>449.0</b>	<b>69.6</b>

**Table 3.5****Sub-basin Curve Numbers**

### 3.4.3 Antecedent moisture condition

With the AMC II values determined it was then necessary to determine the relative frequency of conditions I, II, and III. Normally this is done using five day antecedent rainfall data, but such data was not available for this study. Instead it was decided to use the daily flow data from the HYDAT database (Environment Canada, 1995). Although baseflow is probably a better measure of moisture condition than five day rainfall, it is also specific to an individual watershed and there were no existing methods for relating baseflow to any kind of moisture condition. For this reason, a method for relating baseflow to curve number had to be developed.

Four storm events, recorded at the Ghost River and Fallentimber rainfall gauges starting on 2 July 1983, 8 July 1983, 7 June 1984, and 12 September 1985, for which hourly rainfall and streamflow data were available were selected. Baseflow was subtracted from the streamflow hydrograph to produce the direct runoff hydrograph. By definition, the area under the direct runoff hydrograph equals the depth of excess rainfall multiplied by the area of the watershed. With total rainfall and excess rainfall both known it is possible to combine Equations 3.4, 3.5, and 3.6 to calculate the curve number for each storm. Figure 3.9 is a plot of curve number vs. baseflow for the four storms. The points show a close to linear relationship and so a least squares linear fit was performed to derive the equation:

$$CN = 54.06 + 4.572 \text{ Baseflow} \quad (3.9)$$

where baseflow is measured in m<sup>3</sup>/s.

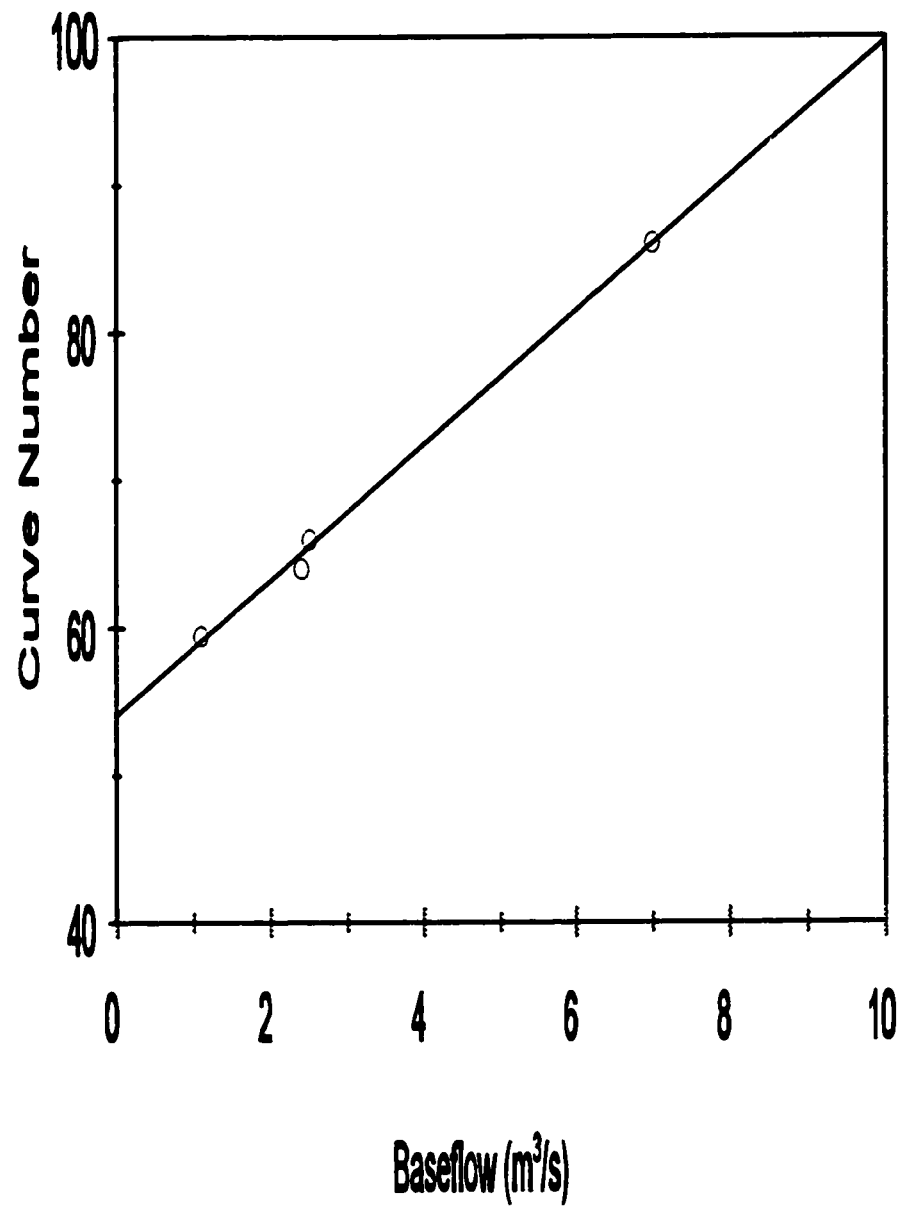


**Figure 3.9**

**CN vs. Baseflow**

It cannot be stressed enough that this equation is based on only four data points and so extreme caution should be used when applying it. The CN-baseflow relationship may be fairly linear in the range shown, but there is no reason to believe that it should remain so outside of it, especially for baseflows over  $10 \text{ m}^3/\text{s}$  where the predicted CN value becomes greater than 100, which has no physical meaning.

As shown in Table 3.5, the AMC II CN value for the watershed is 69.6. From Equations 3.7 and 3.8, the AMC I and III curve numbers are 49.0 and 84.0 respectively. It was assumed that the cutoff between each condition related to a CN value halfway between these CN values (ie. 59.3 for the I-II cutoff and 76.7 for the II to III cutoff). Fortunately, these cutoff values are either well inside the range of Equation 3.9 or right beside a real data point, and so the equation can be used without too much fear.

From Equation 3.9 the baseflow associated with the AMC I-II cutoff is  $1.15 \text{ m}^3/\text{s}$ . Any baseflow below this suggests that the conditions in the watershed are dry. The AMC II-III cutoff is  $4.97 \text{ m}^3/\text{s}$  and any flow greater than this suggests wet conditions. The antecedent baseflows for each annual peak flow were retrieved from the HYDAT database. Seven of the 31 baseflows were less than  $1.15 \text{ m}^3/\text{s}$ , and 9 were greater than  $4.97 \text{ m}^3/\text{s}$ . Table 3.6 shows a summary of the relative frequencies of each AMC condition for the watershed. These probabilities were used to randomly select an AMC condition in both models.

### **3.5 From excess rainfall to runoff - the unit hydrograph**

For this study, excess rainfall was transformed into runoff using the unit hydrograph (UH) method first used by Sherman (1932). A unit hydrograph is the runoff response of a



Antecedent Moisture Condition	Probability (%)
I	0.2258
II	0.4839
III	0.2903

**Table 3.6**

**Antecedent moisture condition probabilities**

given watershed to a unit depth of excess rainfall. This unit depth of rainfall can be considered to have fallen instantaneously (resulting in an instantaneous unit hydrograph, IUH) or over a discrete time period usually equal to the time interval of the available data (a one hour period of rainfall would give a one hour discrete unit hydrograph, 1hr-DUH). For simplicity, the depth of excess rainfall is usually taken to be a convenient depth such as one millimetre, centimetre, or inch. The units of a UH are volumetric flow rate ( $L^3/T$ ) over depth ( $L$ ), or  $L^2/T$ . Plotted against time, the area under the UH is equivalent to the area of the watershed, a feature often used to help define the shape of a UH.

Given an IUH,  $u(t)$ , and a distribution of excess rainfall,  $I(\tau)$ , the resulting runoff,  $Q(t)$ , is given by:

$$Q(t) = \int_0^t I(\tau)u(t-\tau)d\tau \quad (3.10)$$

Although mathematically less precise than the continuous IUH, a DUH is more common in practice due to the discrete nature of hydrologic data collection and the fact that it can be manipulated without the use of calculus. If  $P_m$  is the depth of excess rainfall in the  $m^{\text{th}}$  time interval and  $Q_n$  is the instantaneous flow rate at the end of the  $n^{\text{th}}$  time interval then:

$$Q_n = \sum_{m=1}^n P_m U_{n-m+1} \quad (3.11)$$

Where  $U_{n-m+1}$  is the value of the DUH at the end of the  $n-m+1^{\text{th}}$  time interval.

Chow et al. (1988) describes the five basic assumptions inherent in the unit

**hydrograph method:**

- 1) excess rainfall has a constant duration throughout each time interval;
- 2) excess rainfall is uniformly distributed within the watershed;
- 3) the time base of direct runoff is independent of rainfall intensity;
- 4) the direct runoff hydrograph for a given excess rainfall reflects the unchanging characteristics of the watershed;
- 5) the ordinates of the direct runoff hydrograph for a storm of a given duration are directly proportional to the total excess rainfall.

Unit hydrograph theory basically assumes that the rainfall-runoff process is a linear system, and this assumption has been the source of much criticism. It has been pointed out that hydraulic theory for overland and channel flow states that water flows faster at greater depths than at lesser depths. From this fact alone it is clear that a real watershed will not respond to excess rainfall in a linear fashion. Despite this, the unit hydrograph method has been used extensively by hydrologists and engineers throughout the world because the method is simple, well developed, and generally acceptable for most engineering problems (Ajward, 1996).

### **3.5.1 Lumped model and the unit hydrograph**

In this model, excess rainfall was converted to direct runoff using a single unit hydrograph for all simulated storms. This unit hydrograph was derived from the same four storm events used to derive the baseflow-curve number relationship in Section 3.4.3. The procedure used was:

- 1) separate baseflow from streamflow hydrographs recorded at the Little Red

Deer River near Water Valley station;

- 2) calculate the total volume of excess rainfall depth;
- 3) determine time at which runoff starts to increase rapidly (assumed to indicate onset of excess rainfall);
- 4) make an initial guess of excess rainfall duration;
- 5) find the best fitting triangular unit hydrograph;
- 6) note absolute error between the observed hydrograph and best fitting hydrograph;
- 7) repeat steps (4)-(6) until optimum excess rainfall duration is found.

Baseflow separation was performed using the variable slope method as described by Chow et al. (1988), see Figure 3.10. Total excess rainfall depth was determined by calculating the area under the excess rainfall hydrograph and dividing the result by the area of the watershed, and then converting from  $\text{m}^3\text{hr/skm}^2$  to mm. Table 3.7 gives a summary of these values.

Triangular unit hydrographs were used in this study because of their simplicity. As can be seen in Figure 3.11, triangular unit hydrographs are defined by three points. The first of these points is always at the origin, the second defines the peak, and the third defines the end. Because the area under the unit hydrograph must equal the area of the watershed, the time of the final point can be calculated from:

$$t_f = \frac{A}{1.8U_p} \quad (3.12)$$

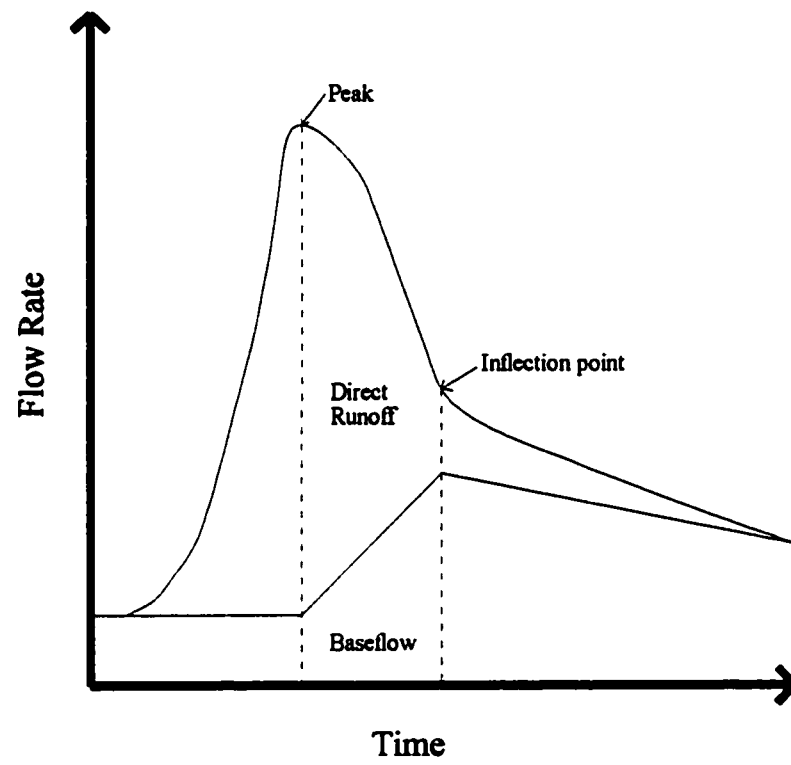


**Figure 3.10**

**Baseflow separation**

Date	Excess Rainfall Depth (mm)
2 July 1983	4.38
8 July 1983	1.05
7 June 1984	2.00
12 September 1985	3.50

**Table 3.7****Excess rainfall depths**

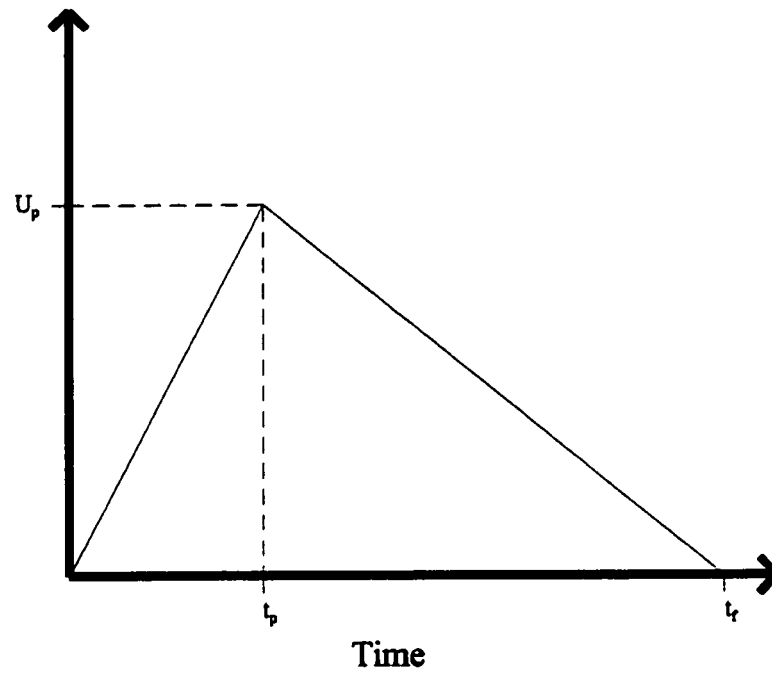


**Figure 3.11**

**Triangular unit hydrograph**

Where:  $t_f$  = final time, hours  
 $U_p$  = peak flow rate,  $m^3/s/mm$   
 $A$  = watershed area,  $km^2$

Therefore, the shape of the entire triangular unit hydrograph can be determined if watershed area, peak flow, and time to peak are known.

When excess rainfall and runoff are known, Equation 3.11 can be solved for the ordinates of the unit-hydrograph,  $U$ . Unfortunately this involves a system of equations with more equations than unknowns and a unique solution rarely exists. A least-squares algorithm can be employed to find the best fitting unit hydrograph but this tends to result in undulating curves with negative ordinates. One way to prevent this is to assume the basic shape of the unit hydrograph (such as a triangle) and find the shape parameters that allow for the best fit with the data. Triangular unit hydrographs make least-squares approximations very difficult because they are defined by two distinct curves whose ranges change as the parameters change. In this study, the best fitting unit hydrograph was determined using iterative techniques. First, initial guesses of peak flow and time to peak were made. Equation 3.11 was then solved for  $Q$  and the results were compared with the observed runoff hydrograph by calculating the absolute error. The same procedure was conducted for small deviations from the initial guess. For example, if the initial guess was  $t_p = 9.5$  hours and  $U_p = 8.3$   $m^3/s/mm$ , then the other values would be:



$t_p = 9.5$ hours	$U_p = 8.4 \text{ m}^3/\text{s}/\text{mm};$
$t_p = 9.5$ hours	$U_p = 8.2 \text{ m}^3/\text{s}/\text{mm};$
$t_p = 9.4$ hours	$U_p = 8.3 \text{ m}^3/\text{s}/\text{mm};$
$t_p = 9.6$ hours	$U_p = 8.3 \text{ m}^3/\text{s}/\text{mm}.$

From these five points and their absolute errors an estimate was made of the optimum values of peak flow and time to peak (those associated with the minimum absolute error). This procedure was repeated until the optimum values were found.

Because no excess rainfall data was available, the duration of excess rainfall was unknown. To compensate for this a duration was estimated with an initial guess and, using the procedure described above, the best fitting unit hydrograph was found. Excess rainfall was assumed to commence at the time that the streamflow hydrograph started to increase rapidly. Excess rainfall was assumed to have a constant intensity for the entire duration. New guesses were made until the optimum storm duration was found. Table 3.8 is a summary of this procedure for the 7 June 1984 storm event. A summary of the optimum unit hydrograph parameters for each storm and the average values used in the lumped model is in Table 3.9.

### **3.5.2 Sub-basin model and the unit hydrograph**

None of the sub-basins shown in Figure 3.2 have streamflow gages on them and so the procedure described in the previous section could not be used for this model. Instead, synthetic unit hydrographs were used for each sub-basin. The Soil Conservation Service (1972) derived a triangular synthetic unit hydrograph with only one parameter, the time to the

Duration (hr)	$U_p$ (m <sup>3</sup> /s/mm)	$t_p$ (hr)	Absolute Error
20	6.26	15.97	46.31
25	6.56	11.31	40.09
30	7.13	8.28	44.13
15	3.96	11.76	72.13
27	6.89	10.51	39.67
26	6.63	10.74	39.61
28	7.01	9.94	40.59
26.5	6.71	10.63	39.57
<b>** 26.6 **</b>	6.72	10.60	39.558
26.7	6.73	10.56	39.563

**Table 3.8**

**7 June 1984 optimum unit hydrograph**

**\*\* \*\* = optimum**

Date	$U_p$ (m <sup>3</sup> /s/mm)	$t_p$ (hr)
2 July 1983	7.46	10.60
8 July 1983	8.60	8.37
7 June 1984	6.72	10.60
12 September 1985	6.12	11.57
<b>Average</b>	<b>7.23</b>	<b>10.29</b>

**Table 3.9**

**Optimum unit hydrograph parameters**

peak of the unit hydrograph. In the S.C.S. method, the ratio  $t_r/t_p$  is assumed to be 2.67. This was derived from as an average for many watersheds of all sizes. The ratio  $t_r/t_p$  for the best fitting unit hydrograph derived for the lumped model (see Table 3.9) is 3.35. For this model it was decided that the S.C.S. method would be followed with no adjustments and so the 2.67 value was used.

Pomeroy (1987) derived the following relationship using 1:50 000 maps for watersheds in the southwestern Alberta Foothills:

$$LAG_c = 8.35 \left( \frac{L L_{ca}}{\sqrt{S_o}} \right)^{0.181} \quad (3.13)$$

Where:  $LAG_c$  = time lag from the centroid of excess rainfall to the centroid of the unit hydrograph, hours;

$L$  = length of the main channel, km;

$L_{ca}$  = distance along the main channel to the point nearest the watershed centroid, km;

$S_o$  = average slope of the main channel, m/km.

Pomeroy's time lag is not the same as time to peak. To convert the two the following equation was used:

$$t_p = \frac{3(LAG_c + 0.5)}{3.67} \quad (3.14)$$

This equation is only valid for the S.C.S. triangular unit hydrograph. Table 3.10 is a summary

Sub-basin	Area (km <sup>2</sup> )	L (km)	L <sub>ca</sub> (km)	S <sub>o</sub> (m/km)	LAG <sub>c</sub> (hr)	t <sub>p</sub> (hr)
Little Red Deer River 1	76.5	21.6	12.1	25.6	17.1	14.3
Little Red Deer River 2	20.5	7.2	3.4	23.2	11.2	9.6
Little Red Deer River 3	16.5	6.6	4.6	25.4	11.6	9.9
Little Red Deer River 4	54.0	12.0	7.3	22.9	14.1	12.0
Atkinson Creek	30.5	11.4	5.8	28.1	13.2	11.2
Loblaw Creek	12.5	10.6	7.0	28.8	13.4	11.4
Salter Creek	28.0	11.7	6.3	21.2	13.8	11.7
Big Coulee Creek	19.5	10.5	5.5	29.0	12.8	10.9
Harold Creek	73.5	21.6	11.5	16.9	17.5	14.7
Grease Creek 1	54.5	19.4	9.2	18.9	16.4	13.8
Grease Creek 2	21.5	9.5	5.9	22.5	13.1	11.1
Turnbull Creek	41.5	13.7	7.9	11.1	15.7	13.2

**Table 3.10**

**Sub-basin unit hydrograph parameters**

of the  $L$ ,  $L_{ca}$ ,  $S_o$ ,  $LAG_c$ , and  $t_p$  values for each sub-basin. The single most important parameter effecting the peak of the flood hydrograph is the value of the peak of the unit hydrograph. Analysis of the values in Figure 3.10 would show that if a  $t_r/t_p$  ratio of 3.35 were used instead of 2.67, the values of  $U_p$  would for the sub-basins would only decrease about 5%.

Because the 12 sub-basins don't all meet at the watershed outlet, it was necessary to route the flow from the upstream basins through the downstream basins. This was done using the kinematic wave equation:

$$c_k = \frac{1}{B} \frac{dQ}{dy} \quad (3.15)$$

and the Manning equation:

$$Q = \frac{1}{n} \frac{A^{5/3}}{P^{2/3}} \sqrt{S_o} \quad (3.16)$$

where:

- $c_k$  = kinematic wave celerity, m/s;
- $B$  = channel width at water surface, m;
- $Q$  = volumetric flow rate, m<sup>3</sup>/s;
- $y$  = depth of flow, m;
- $A$  = cross-sectional area of flow, m<sup>2</sup>;
- $P$  = wetted perimeter, m;
- $S_o$  = channel slope, m/m;
- $n$  = Manning roughness coefficient.

If the channel is assumed to have a rectangular cross-section then Equation (3.16) can be approximated as:

$$Q = \frac{B\sqrt{S_o}}{n} y^{5/3} \quad (3.17)$$

Substituting Equation 3.17 into Equation 3.15 and rearranging gives:

$$y = \left( \frac{3}{5} \frac{n}{\sqrt{S_o}} c_k \right)^{3/2} \quad (3.18)$$

Finally, substituting Equation 3.18 back into Equation 3.17 and rearranging gives the following equation for kinematic wave celerity as a function of volumetric flow:

$$c_k = \frac{5 S_o^{0.3} Q^{0.4}}{3 B^{0.4} n^{0.6}} \quad (3.19)$$

In this study all channels were assumed to be rectangular in cross-section, with a width of 5 m, and a Manning's roughness of 0.04. These values were rough estimates based on typical values for natural streams (Chow et al., 1988). The kinematic wave model is valid in channels with narrow widths and where gravity dominates the momentum equation. The assumption of a 5 m wide rectangular section, and the fact that the channels considered are rather steep means that the kinematic wave model is suitable for this watershed.

To simplify the programming code, and speed up the running time, for a given routing operation the travel time of the peak inflow was calculated and this value was applied to the

entire inflow hydrograph. As a result, the rising and falling limbs were routed through too quickly, but the peaks were routed at the appropriate rate. Since the peak flows were the only values this study was interested in, this discrepancy was not considered a problem. As a test, the outflow hydrographs of three hypothetical storms of 12, 24, and 48 hour durations, and rainfall depths of 50, 70, and 90 mm were generated using this study's model and using the HEC-1 Flood Hydrograph Package (US Army Corps of Engineers, 1987). HEC-1 was setup to use the same unit hydrographs, curve numbers, and stream network as the sub-basin model. The only difference was that HEC-1 used a more rigorous algorithm for the kinematic wave. A summary of the results can be found in Table 3.11. A comparison of the outflow hydrographs showed that although the rising and falling limbs were off by as much as 3 hours, the peak flows came at the same time. Although HEC-1 can easily simulate watershed response to a single rainfall event quite well, it is totally inadequate for dealing with simulating several thousand events.

### **3.6 Control Variables**

#### **3.6.1 Climate change**

The effects of climate change were modelled in three ways. The first was to adjust both the mean and standard deviation values given in Table 3.1 by -25% to +25%. The second was to change only the standard deviations by -50% to +50%. The third was to pick locations in southern Alberta, Montana, and Colorado. The extreme rainfall statistics at these locations were then used to simulate the effect of a southern climate 'moving' north. Both the lumped and sub-basin models were treated identically.



Storm	Peak flow	Peak flow	Time to peak	Time to peak
	HEC-1	Sub-basin	HEC-1	Sub-basin
	(m <sup>3</sup> /s)	(m <sup>3</sup> /s)	(hours)	(hours)
12 hr, 50 mm	35.82	34.98	21	21
24 hr, 70 mm	74.54	74.34	25	25
48 hr, 90 mm	102.62	103.39	31	31

**Table 3.11**

**Comparison of HEC-1 and Sub-basin models**

### 3.6.2 Urbanization

To simulate urbanization, the curve number for each sub-basin was calculated assuming the entire basin was urbanized with 50% of the area impervious. In the lumped model, the new curve number was calculated by linear interpolation:

$$CN_u = \frac{CN_0(100\% - U_{\%}) + CN_{100}U_{\%}}{100\%} \quad (3.20)$$

where:  $CN_u$  = urbanized curve number;  
 $U_{\%}$  = % urbanization;  
 $CN_{100}$  = curve number for 100% urbanization;  
 $CN_0$  = curve number for 0% urbanization.

For the lumped model, urbanization was varied from 1% to 100%. For the sub-basin model urbanization was assumed to start at the eastern edge of the watershed and move progressively westward as it expanded. Figure 3.12 is a map of the assumed progression. In the sub-basin model, urbanization varied from 5% to 100%. Table 3.12 summarizes the urbanized curve numbers of each sub-basin as well as the average urbanized curve number for the entire watershed.

### 3.6.3 Choice of storms

All storms were selected randomly. Despite the fact that 10 000 storms were simulated in each model run, early analysis found that this was not enough to capture the entire probability distribution. For example, increasing rainfall by 2% would often result in

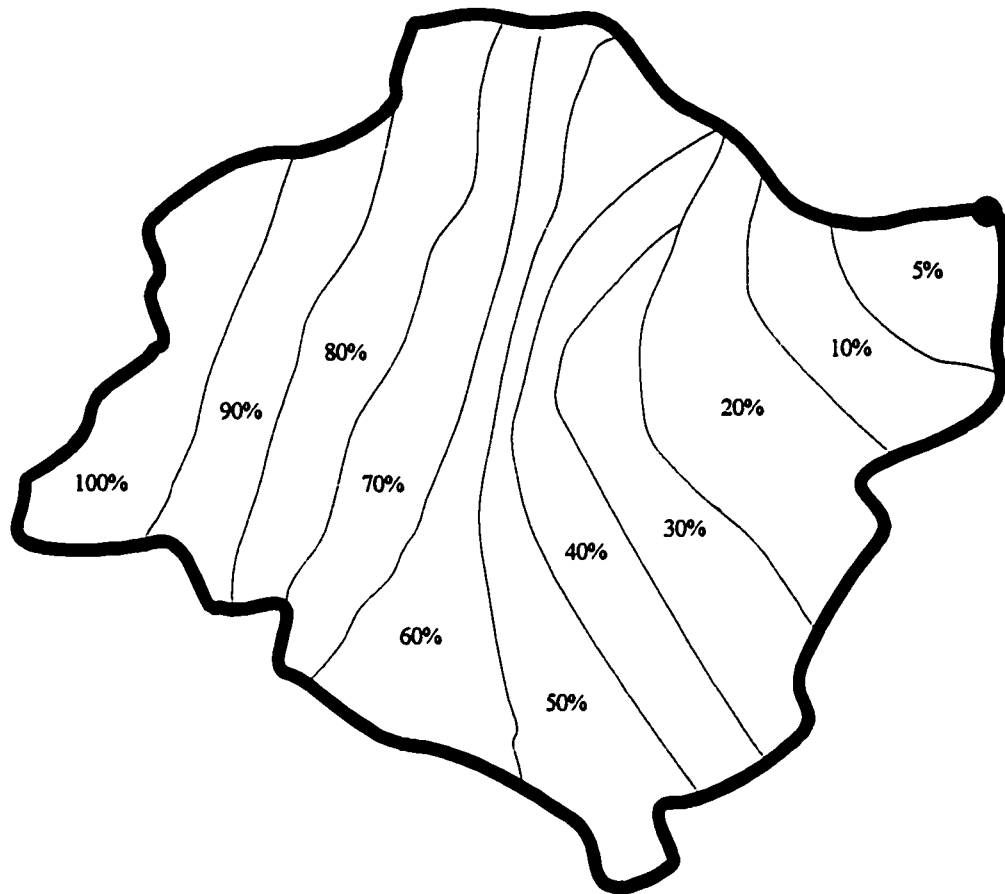


**Figure 3.12**

**Progression of urbanization for sub-basin model**

Sub-basin	Area (km2)	Urbanized Curve Number
Little Red Deer River 1	76.5	84.4
Little Red Deer River 2	20.5	82.2
Little Red Deer River 3	16.5	84.8
Little Red Deer River 4	54.0	83.6
Atkinson Creek	30.5	82.6
Loblaw Creek	12.5	82.1
Salter Creek	28.0	82.2
Big Coulee Creek	19.5	81.8
Harold Creek	73.5	82.9
Grease Creek 1	54.5	81.1
Grease Creek 2	21.5	85.2
Turnbull Creek	41.5	84.6
<b>Little Red Deer River watershed</b>	<b>449.0</b>	<b>83.2</b>

**Table 3.12**

**Urbanized curve numbers**

a smaller average flood. For each model, simulations of 10 000 storms each were run 15 times with the model parameters set to match current conditions in the watershed. The mean flood was found to vary  $\pm 2\%$ , other statistical parameters were found to vary by as much as  $\pm 50\%$ . To alleviate this, a set of 50 000 random numbers was selected (5 random numbers for each storm defining rainfall duration, total storm depth, storm quartile, time distribution curve, and moisture condition) and this was used as the random number source for all other simulations.

### **3.7 Computer hardware and software**

All analysis was carried out on a Latech 100 MHz Intel Pentium computer with 16 MB of random access memory (RAM), 120 MB hard disk, 3.5" high-density 1.44 MB floppy disk drive and in a Microsoft Windows 95 environment. All original programs were written in BASIC and executed in compiled form using FirstBasic (PowerBASIC, 1996). Microsoft Excell version 7.0 (Microsoft, 1995) was used for all statistical analysis.

### **3.8 Statistical analysis**

#### **3.8.1 *N*-year floods**

An *n*-year flood is a flood level that can be expected to be exceeded an average of once every *n* years. *N*-year floods are common measures of flood probability because they are ideal measures for construction design purposes. Design criteria for projects subject to flood damage frequently include the requirement that a structure be able to withstand a 10-year flood in the case of a highway culvert, or a 200-year flood in the case of a levee around

a city. This study looked at 2, 10, and 100 year floods and how they change due to climate change and urbanization. The level of an  $n$ -year flood is defined as the flood exceeded by  $1/n$  of the simulated flood peaks. For example, the 50-year flood is equal to the peak flow exceeded by  $1/50$ th of the simulated floods, or the 200<sup>th</sup> highest value.

### 3.8.2 Statistical parameters

Chow et al. (1988) defines statistics as “numbers calculated from a sample which summarize its important characteristics” and defines statistical parameters as “characteristics of a population”. Population statistical parameters are those that are calculated using the entire population, usually by means of integration calculus. In this study sample estimates of statistical parameters calculated from the generated data for mean, coefficient of variation, coefficient of skewness, and coefficient of kurtosis.

The parameter mean is the expected value of a random function and is a measure of the midpoint of a distribution. The sample estimate for the mean of a distribution is the average,  $\bar{x}$ , of the sample data:

$$\bar{x} = \frac{1}{n} \sum_{i=1}^n x_i \quad (3.21)$$

Where:  $n$  = number of data points;

$x_i$  = value of the  $i$ th data point.

Coefficient of variation is a unitless measure of the variance or ‘spread’ of a distribution and is calculated from the second moment about the mean. The sample estimate

for the coefficient of variation,  $C_v$ , is calculated from:

$$C_v = \frac{s}{\bar{x}} \quad (3.22)$$

where,  $s$  = sample estimate for standard deviation.

The sample estimate for standard deviation is given by:

$$s = \frac{1}{n-1} \sum_{i=1}^n (x_i - \bar{x})^2 \quad (3.23)$$

The coefficient of skewness is a unitless measure of the symmetry of a distribution and is calculated from the third moment about the mean. The sample estimate for the coefficient of skewness,  $C_s$ , is calculated from:

$$C_s = \frac{n}{s^3(n-1)(n-2)} \sum_{i=1}^n (x_i - \bar{x})^3 \quad (3.24)$$

When  $C_s < 0$  the distribution is said to be 'negatively skewed' or skewed to the left meaning the mean is being moved to the left due to the influence of a few very small values. Distributions where  $C_s > 0$  are said to be 'positively skewed' or skewed to the right.

The coefficient of kurtosis is a unitless measure of peakedness, or the tendency of a distribution to exist in the tails, and is calculated from the fourth moment about the mean. The sample estimate for the coefficient of skewness,  $C_k$ , can be calculated from:

$$C_k = \frac{n(n+1)}{s^4(n-1)(n-2)(n-3)} \sum_{i=1}^n (x_i - \bar{x})^4 - \frac{3(n-1)^2}{(n-2)(n-3)} \quad (3.25)$$

Using Equation 3.25, the coefficient of kurtosis of the normal distribution would be zero. When  $C_k < 0$ , the distribution is said to be 'leptokurtotic' with a lesser proportion of the data lying in the tails than for the normal distribution. Distributions for which  $C_k > 0$  are 'platykurtotic' with a greater proportion of the data lying in the tails than for the normal distribution.

### 3.8.3 Logarithmic statistical parameters

Logarithmic statistical parameters are identical to those discussed in the previous section except the sample data are first converted using the equation:

$$y_i = \ln x_i \quad (3.26)$$

All statistical parameters are calculated in the same manner as those in Section 3.8.2. The advantage of logarithmic statistics is that they reduce the large positive skewness and kurtosis commonly found in hydrologic data because logarithms reduce large numbers more than they reduce small numbers (Chow et al., 1988). Log statistics are also bounded by zero, and so negative flow rates are never an issue.



### 3.8.4 Chi-square tests

The goodness of fit of a theoretical probability distribution to observed data can be evaluated by comparing the two with a chi-square test. The range of the data is first split into  $m$  intervals, and the chi-square test statistic,  $\chi_c^2$ , is calculated by:

$$\chi_c^2 = \sum_{i=1}^m \frac{(n_i - n_{pi})^2}{n_{pi}} \quad (3.27)$$

where,  $n_i$  = number of observed data points in interval  $i$ ;

$n_{pi}$  = number of predicted data points in interval  $i$ .

The chi-square distribution with  $v$  degrees of freedom is defined as “the distribution for the sum of  $v$  independent standard normal random variables  $z_i$ ; this sum is the random variable” (Chow et al., 1988) calculated by:

$$\chi_v^2 = \sum_{i=1}^v z_i^2 \quad (3.28)$$

The chi-square distribution is tabulated in Abramowitz and Stegun (1965). In the chi-square test:

$$v = m - p - 1 \quad (3.29)$$

where,  $p$  = number of parameters used to fit the distribution.

The chi-square test statistic calculated from Equation 3.27 is then compared to tabulated chi-

square values with  $v$  degrees of freedom and a significance level,  $\alpha$ . The significance level is a measure of how well the two distributions match. The higher the significance level, the better the match. A common minimal required significance level is 5%, meaning that 95% of all sets of  $n$  numbers randomly selected from the theoretical distribution would fit better than the observed data.

### **3.8.5 Extreme value distributions**

Chow et al. (1988) defines extreme values as the “selected maximum or minimum values of sets of data”. The annual maximum flow rate at a given location is the largest flow rate recorded during a year, and the set of annual maximum flow rates make up a set of extreme values. Fisher and Tippett (1928) showed that distributions of extreme values selected from sets of samples of any probability distribution converge to one of three forms of extreme value distributions, called I, II, and III, when the number of selected values approaches infinity. Type I is frequently called the Gumbel distribution and is used for the extreme rainfall statistics described in Section 3.3.2. Type III, also called the Weibull distribution, is constrained by an upper limit and type II, also called the Frechet distribution, is constrained by a lower limit. These three distributions were found by Jenkinson (1955) to be special cases of a single distribution called the Generalized Extreme Value (GEV) distribution, which is now commonly used in flood frequency analysis.

Flood frequency curves in this study are plotted against the gumbel reduced variate. The gumbel reduced variate is defined by:

$$z_g = -\ln\left(\ln\left(\frac{T}{T-1}\right)\right) \quad (3.30)$$

where,  $z_g$  = Gumbel reduced variate;

$T$  = return period (years).

## **CHAPTER 4**

### **RESULTS AND DISCUSSION**

#### **4.1 Comparison of models with observed data**

The historical record of observed maximum annual floods at the Little Red Deer near Water Valley station was not used in any stage of the modeling process. Because of this, comparing the models' predictions under current climate conditions with the observed flood data is a legitimate method of testing the validity of the models.

Figure 4.1 compares the flood frequency predictions of the two models used in this study based on simulations under current climactic and land use conditions, with the observed flood data from 1964-1994. The figure is a plot of peak flow rate against probability of exceedence, represented by the Gumbel reduced variate and return period. The data shown are for rain floods only. Annual maximum floods that had significant contributions from spring runoff were not included. In their place, the maximum rainfall floods in those same years were used. Seven of the recorded maximum annual floods were snowmelt generated floods, but none of these floods were among the ten largest recorded floods. The figure also shows the predictions of two previous studies (Pomeroy, 1987; Chang, 1992) of the same watershed which both used the standard S.C.S. curve number method. As can be seen, both models yield almost identical predictions for medium and large floods.

The main difference between the two models is their predictions of small floods. This is primarily due to how each model treats abstractions. In the lumped model, either the entire

# Little Red Deer River near Water Valley

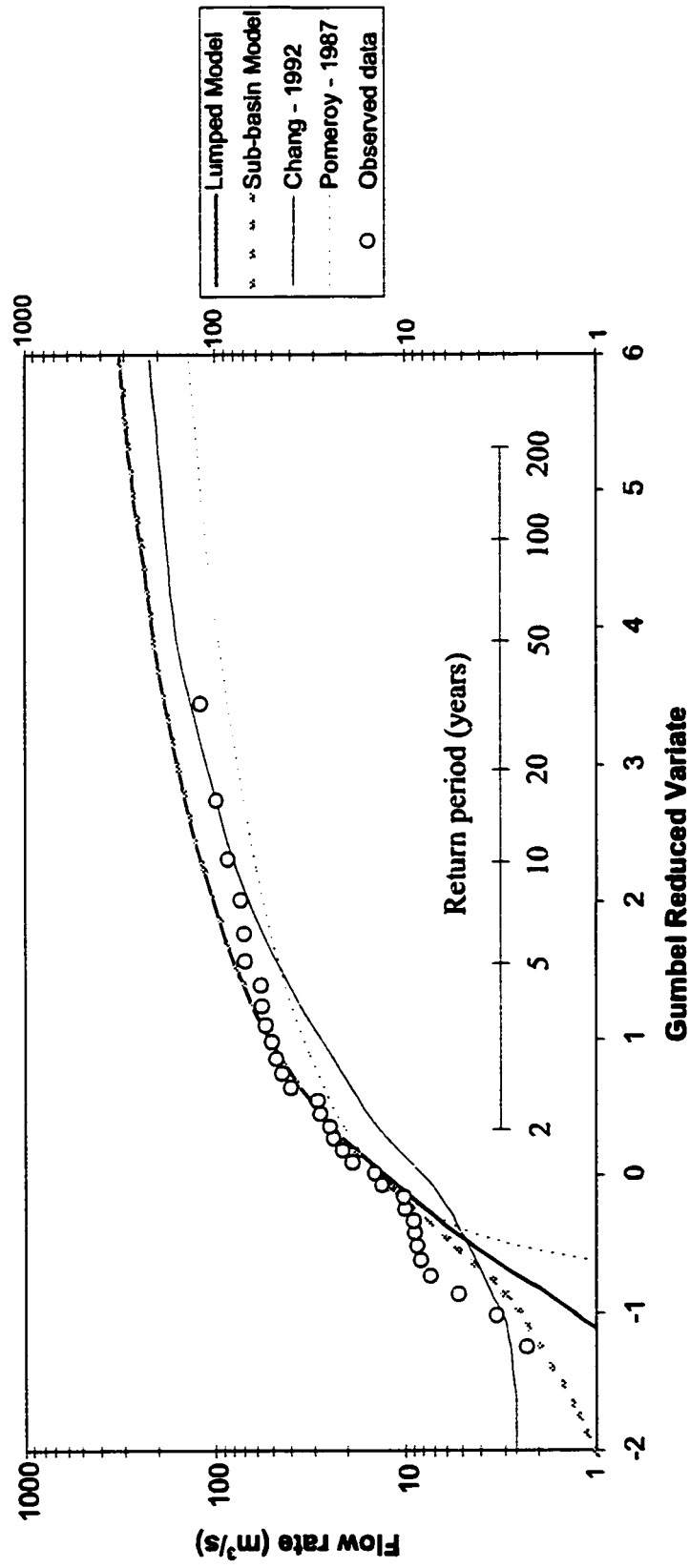


Figure 4.1 - Flood Frequency Curves

watershed contributes to runoff or none of it does, but in the sub-basin model, sub-basins with high curve numbers such as Grease Creek 1, and Harold Creek will begin contributing runoff before the rest of the watershed does. The effect of this is negligible during very large rainfalls, but during smaller storms this effect becomes very important. A common measure of how well a theoretical model's predictions compare to observed data is the chi-square test. Table 4.1 summarizes the chi-square tests conducted for both models. The chi-square test statistics for the lumped and sub-basin models are 11.58 and 8.68 respectively. To put these numbers in perspective, they correspond to a significance level for 11 degrees of freedom (12 intervals and no fitted parameters, therefore  $v = 12 - 0 - 1 = 11$ ) of 40% and 65% respectively (Zar, 1984). As mentioned in Chapter 3, the greater the significance level the better the fit, with a significance level below 5% generally considered grounds to reject the theoretical distribution (Chow et al., 1988). From Zar (1984), this means the 11 degrees of freedom chi-square test statistic would have to be greater than 19.7 for rejection. The fact that the significance levels are much greater than 5% implies that both models fit the data well. However, it should be noted that the 30-year flood predicted by both models is almost 50% larger than the largest observed flood in the 30 year record. This difference may be due to random variability. For instance, there is no reason why the long term 30-year flood should arrive every 30 years, and a single 200 m<sup>3</sup>/s flood would make the data fit almost perfectly. The chi-square tests show that this discrepancy is not statistically significant, however the possibility that the model predictions may be off by 50% is physically significant. Because this study was primarily concerned with changes in flood levels, this difference is not as important as it would be in a study concerned with actual flood levels.

Sub-basin Model				Lumped Model			
Range (m <sup>3</sup> /s)	Model	Data	Chi-sqr statistic	Range (m <sup>3</sup> /s)	Model	Data	Chi-sqr statistic
0 - 2.08	1.55	0	1.55	0 - 1.01	1.55	0	1.55
2.09 - 3.14	1.55	1	0.20	1.02 - 2.00	1.55	0	1.55
3.15 - 5.76	3.1	2	0.39	2.01 - 4.75	3.1	2	0.39
5.77 - 9.71	3.1	5	1.16	4.76 - 8.67	3.1	4	0.26
9.72 - 15.9	3.1	4	0.26	8.68 - 15.0	3.1	6	2.71
16.0 - 24.9	3.1	3	0.00	15.1 - 24.4	3.1	3	0.00
25.0 - 36.3	3.1	3	0.00	24.5 - 36.1	3.1	3	0.00
36.4 - 53.0	3.1	4	0.26	36.2 - 53.5	3.1	4	0.26
53.1 - 75.7	3.1	6	2.71	53.6 - 76.3	3.1	6	2.71
75.8 - 114	3.1	2	0.39	76.4 - 116	3.1	2	0.39
115 - 153	1.55	1	0.20	117 - 156	1.55	1	0.20
154+	1.55	0	1.55	156+	1.55	0	1.55
<b>SUM =</b>	<b>31</b>	<b>31</b>	<b>8.68</b>	<b>SUM =</b>	<b>31</b>	<b>31</b>	<b>11.58</b>

Table 4.1

Chi-square test

## **4.2 Changes in rainfall - mean and standard deviation**

The first series of simulations involved adjusting both the rainfall means and standard deviations by -25% to +25% for both models.

### **4.2.1 N-year floods**

Figure 4.2 is a plot of the lumped and sub-basin model predictions for the mean, 2-year, 10-year, and 100-year floods. As can be seen, there is almost no difference between the two model predictions. Figure 4.3 is a plot of these same flood levels but they are plotted in terms of percent change from current flood levels. As can be seen, the smaller the flood the greater the effect of climate change. A 25% increase in extreme rainfall results in a 40% increase in the 100-year flood, a 50% increase in the 10-year flood, a 60% increase in the mean annual (approximately 3-year) flood, and a 90% increase in the 2-year flood.

Another way of analyzing the data is to compare how the frequency of current floods changes with the climate. Figure 4.4 is a plot of current flood frequencies versus their equivalent frequencies in a +25% extreme rainfall climate. Under such conditions, what would now be considered a 500-year flood, becomes an 80-year flood. The current 100-year flood becomes a 25-year flood, and a 20-year flood becomes an 8-year flood.

Figures 4.3 and 4.4 suggest that although the size of large floods doesn't increase as much as with smaller floods, their frequency increases greatly. This means that strengthening larger structures such as bridges and dams could prevent premature failure at a low cost, at least relative to the costs of replacing such structures and repairing any other damage resulting from their failure.



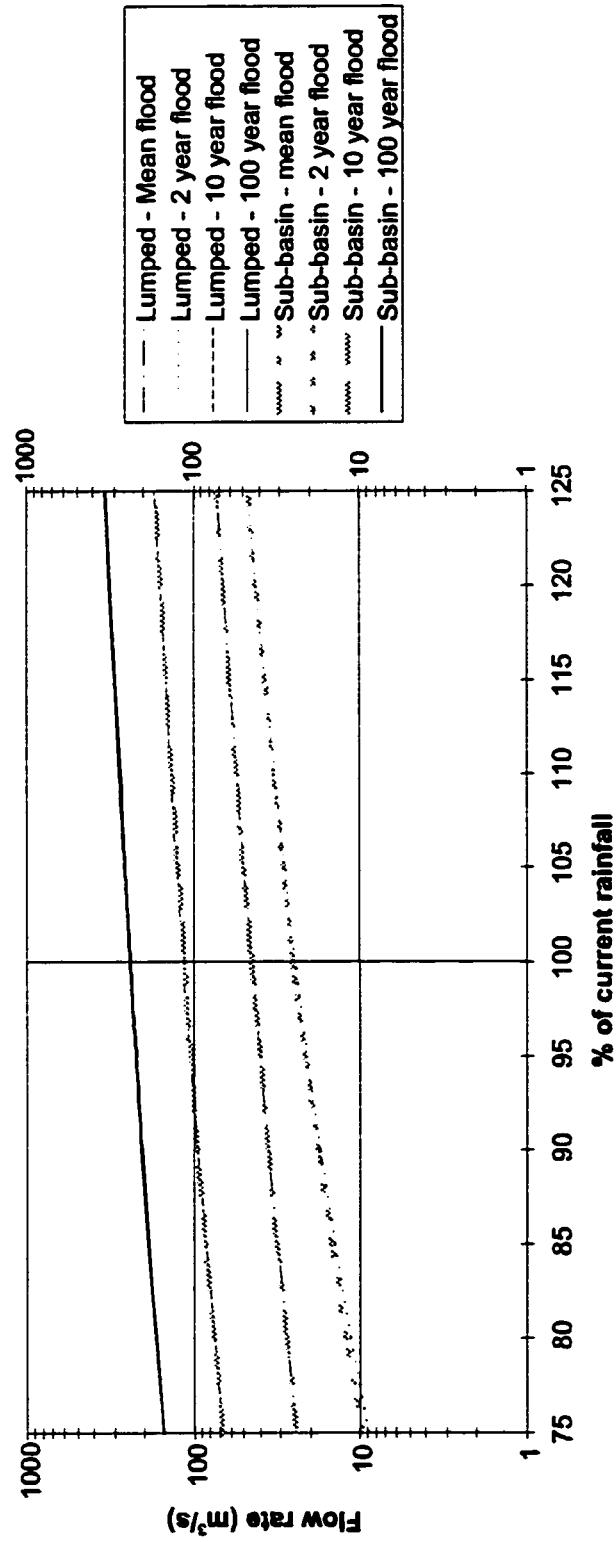


Figure 4.2 - n-year floods and rainfall

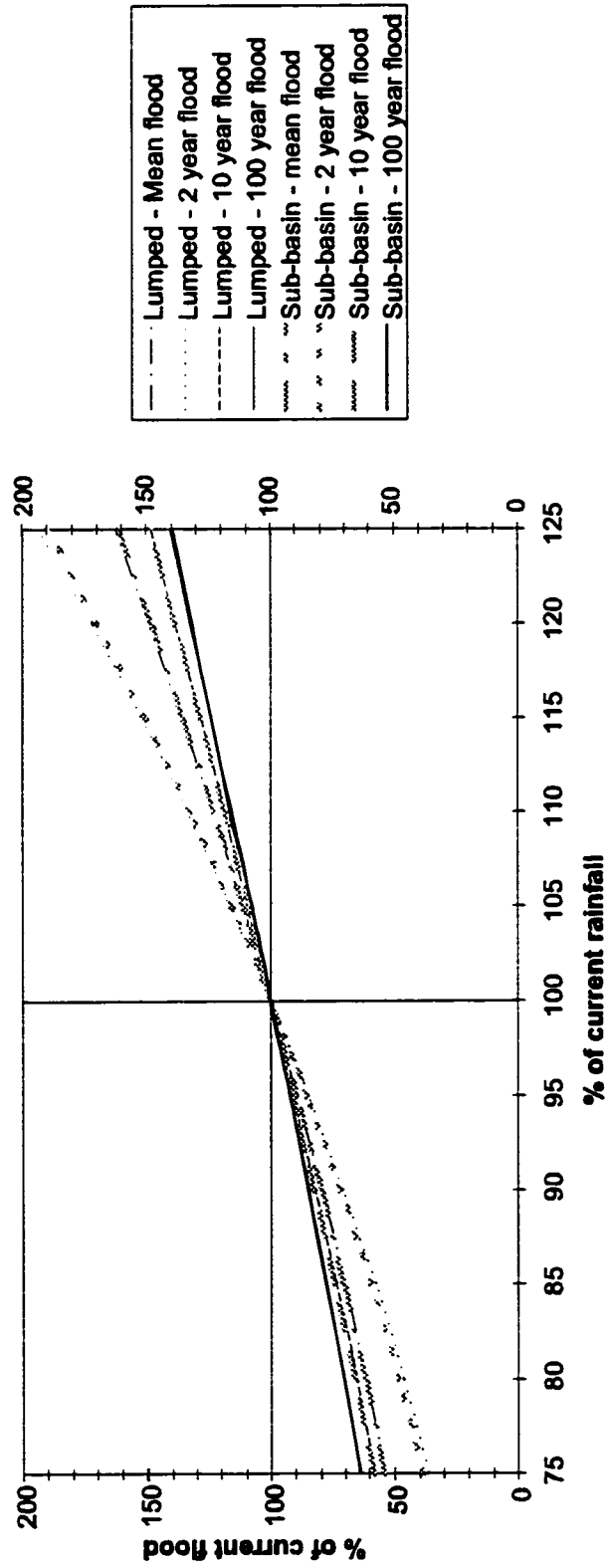
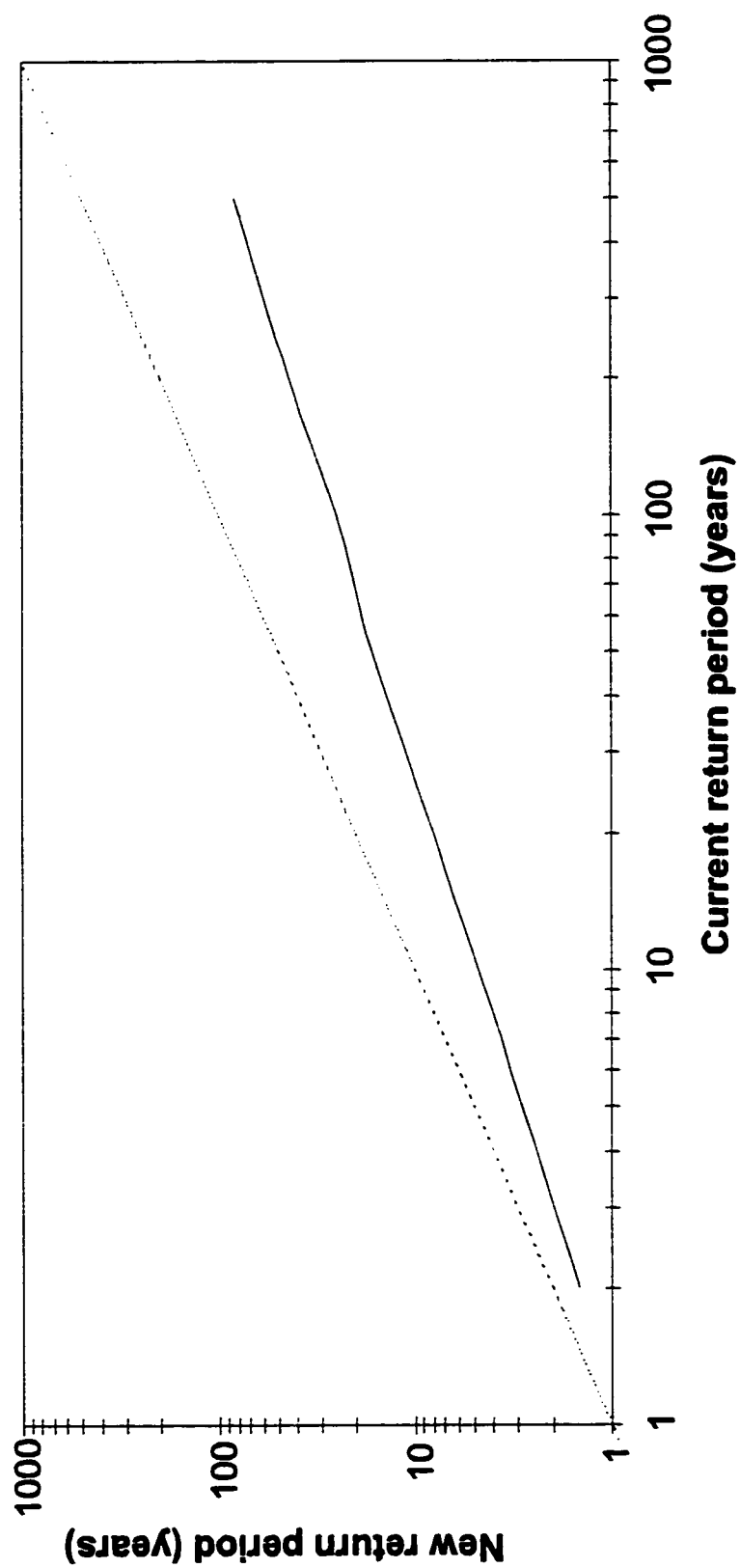


Figure 4.3 - % change in flood level

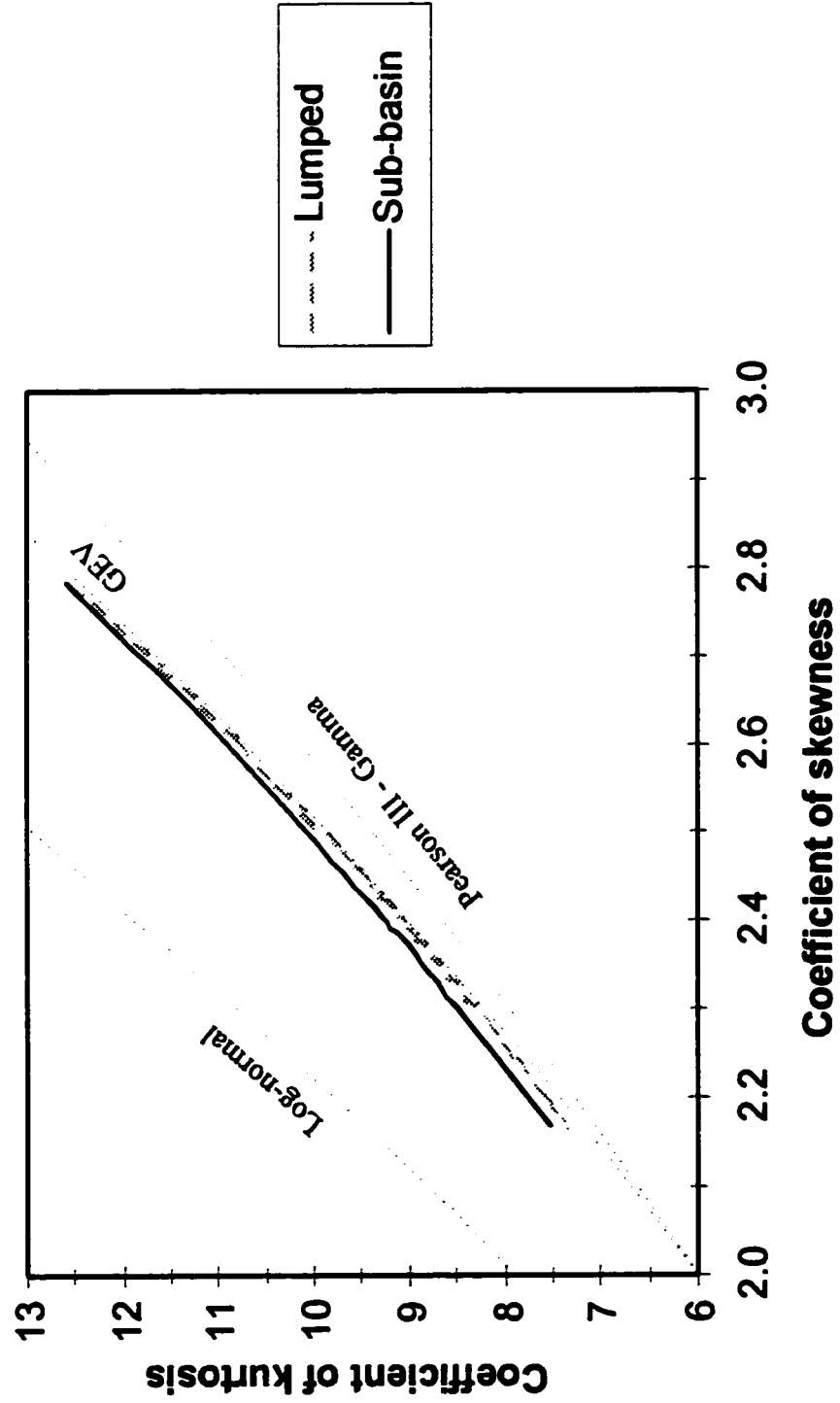


**Figure 4-4**  
**Changes in flood frequency due to a 25% increase in extreme rainfall**

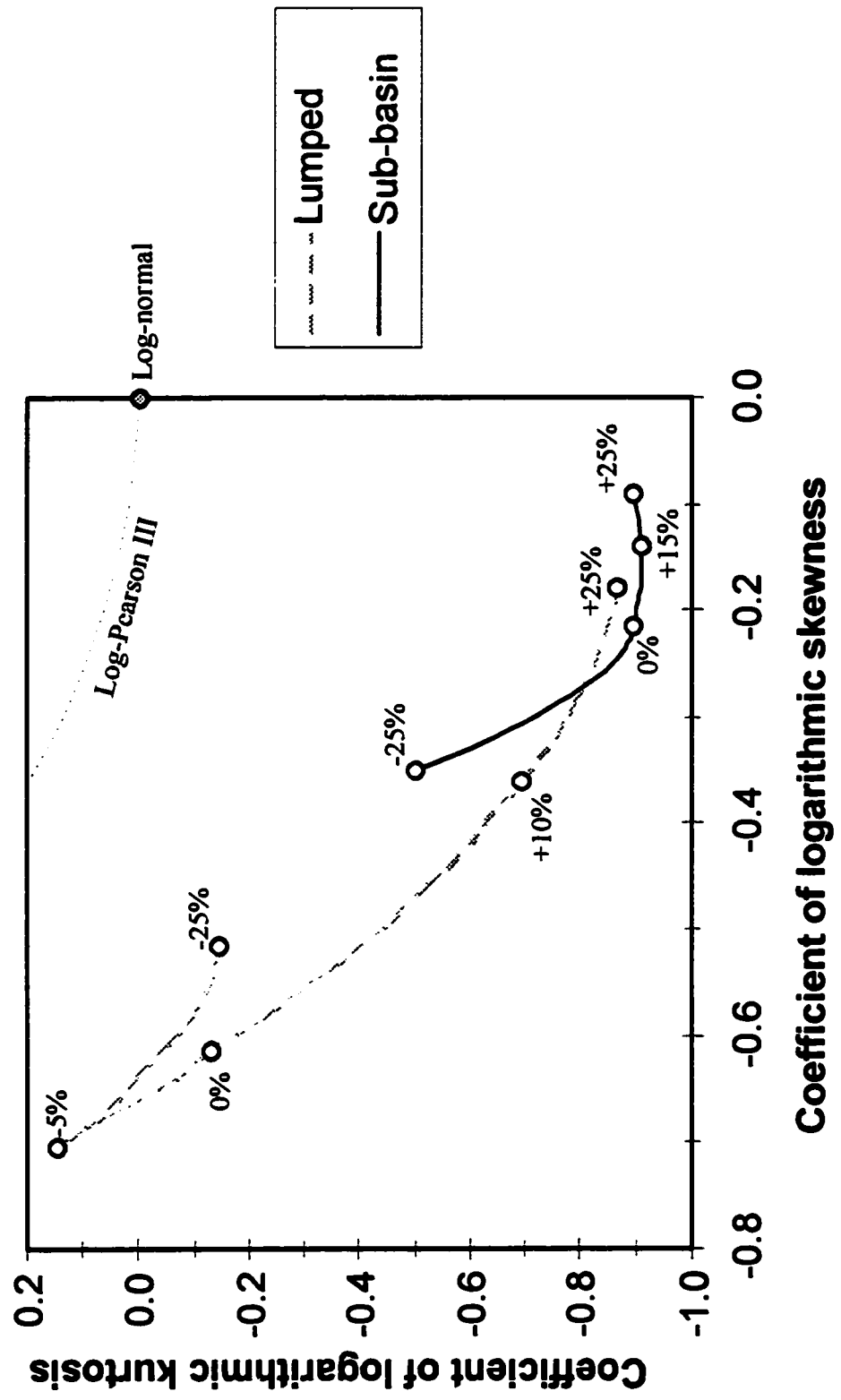
#### 4.2.2 Statistical parameters

Figure 4.5 is a plot of the coefficient of kurtosis versus the coefficient of skewness. Skewness and kurtosis are used because they are both independent of linear transformation and so they can easily be compared to theoretical relationships. From the figure it can be seen that both coefficients increase with decreasing rainfall and that both models predict almost identical curves. Figure 4.5 also includes the theoretical relationship between skewness and kurtosis for the log-normal, gamma (or Pearson type III), and generalized extreme value (or GEV) distributions as derived from equations in Patel et al. (1976) and Weisstein (1998). The model results lie just above the gamma and GEV curves and run roughly parallel to all three theoretical distributions. The close proximity of the gamma distribution and especially the EV3 distribution suggests that they could be good candidates for flood frequency analysis in this watershed and perhaps the general region. The GEV distribution is especially interesting because it is an extreme value distribution and therefore has a strong theoretical basis for being an appropriate distribution.

Figure 4.6 is similar to Figure 4.5 but in this case logarithmic skewness and kurtosis are plotted, and these curves are shown with the theoretical relationships for the log-Pearson III and log-normal distributions (Patel et al., 1976). In this study the terms ‘logarithmic skewness’ and ‘logarithmic kurtosis’ refer to the coefficients of skewness and kurtosis for the logarithm of the data set. Logarithmic statistical parameters are quite different for the two models, especially at the lower rainfall levels. This is primarily due to smaller floods. In a climate with less extreme rainfall, the maximum floods in dry years start to approach zero and so their logarithms become large negative values, especially for the lumped model. At first



**Figure 4.5 - Skewness vs Kurtosis**



**Figure 4.6 - Ln Skewness vs Ln Kurtosis rainfall**

a few very small floods will have more effect on kurtosis and skewness than they do on the standard deviation and mean, and so kurtosis increases and skewness becomes more negative. However, as rainfall continues to decrease, the ever increasing number of very small floods will increase their effects on the standard deviation and mean, and so the kurtosis and skewness start to reverse because they are functions of both the standard deviation and the mean. The sub-basin model does not show as much of this behaviour because it simulates the abstraction process more accurately than the lumped model and even a small amount of excess rainfall can easily increase the peak runoff by  $0.1 \text{ m}^3/\text{s}$ . This small difference has almost no effect on conventional statistical parameters, but it has a large effect on logarithmic ones. Because of this, the behaviour of the logarithmic parameters under reduced extreme rainfall should be treated with extreme caution for both models (especially the lumped model).

Both models show that with increasing rainfall, logarithmic skewness continues to increase fairly rapidly, but logarithmic kurtosis approaches a minimum value of around -0.9. The sub-basin model does reach a minimum kurtosis of -0.914 at +15% rainfall. In all likelihood, further increases in extreme rainfall would result in a slow increase in logarithmic kurtosis, a deceleration of the logarithmic skewness, and a rapid closing of the lumped and sub-basin curves.

### **4.3 Changes in rainfall - standard deviation**

The next series of simulations involved adjusting the rainfall standard deviations by -50% to +50% for both models, while holding the means constant.

#### **4.3.1 N-year floods**

A plot of annual flood standard deviation against percent change in extreme rainfall standard deviation can be seen in Figure 4.7. Figure 4.8 is a plot of the lumped and sub-basin model predictions for the mean, 2-year, 10-year, and 100-year floods. The two models offer almost identical predictions for all five of these parameters, especially in terms of trend. As would be expected, increasing the rainfall standard deviation increases the flood standard deviation but to a lesser extent. A 50% increase in rainfall standard deviation results in a 31% increase in flood standard deviation. Also, the mean annual (approximately 3-year) flood increases slightly but the median (2-year) flood stays constant.

Figure 4.9 is a plot of these same flood levels but they are plotted in terms of percent change from current flood levels. This time, large floods are much more sensitive than smaller floods. In the sub-basin model, a 50% increase in rainfall standard deviation results in a 35% increase in the 100-year flood, a 19% increase in the 10-year flood, a 17% increase in the mean annual flood, and less than a 2% increase in the 2-year flood.

Another way of analyzing the data is to compare how the frequency of current floods changes with the climate. Figure 4.10 is a plot of current flood frequencies versus their equivalent frequencies after a 50% increase in the standard deviation of extreme rainfall according to the sub-basin model. Under such conditions, what would now be considered



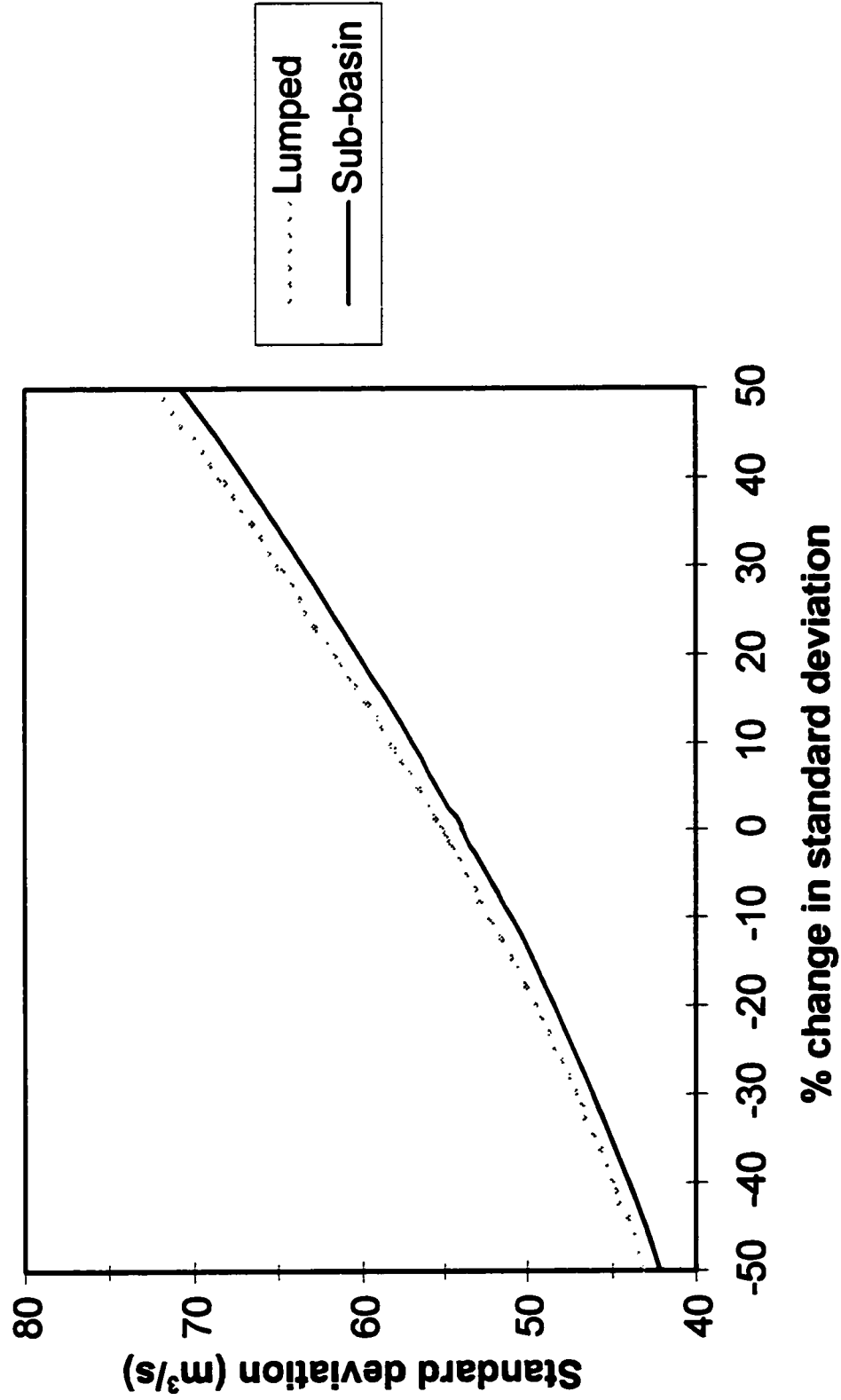


**Figure 4.7 - Flood standard deviation rainfall standard deviation**

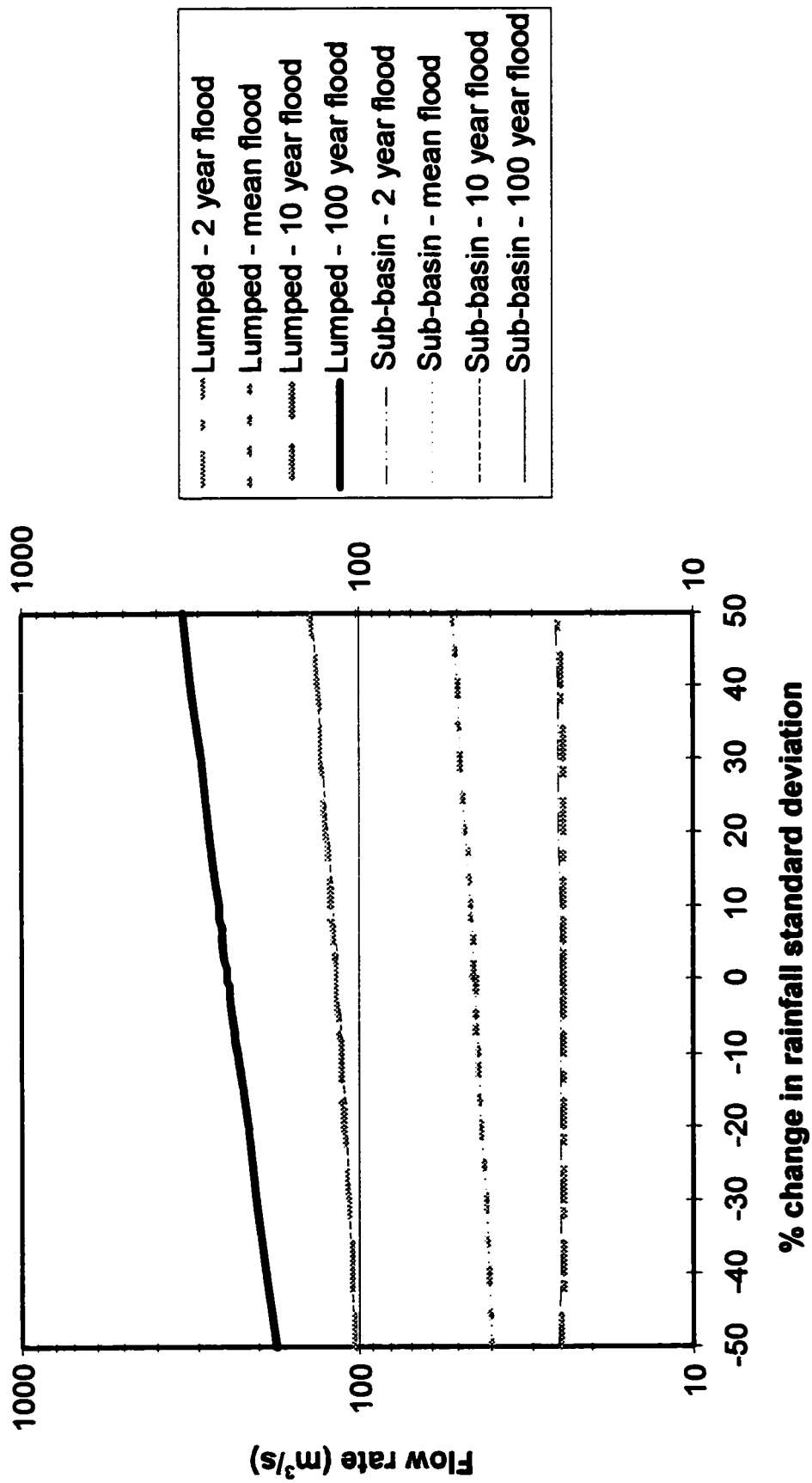


**Figure 4.8 - N-Year Floods**  
**Rainfall standard deviation**

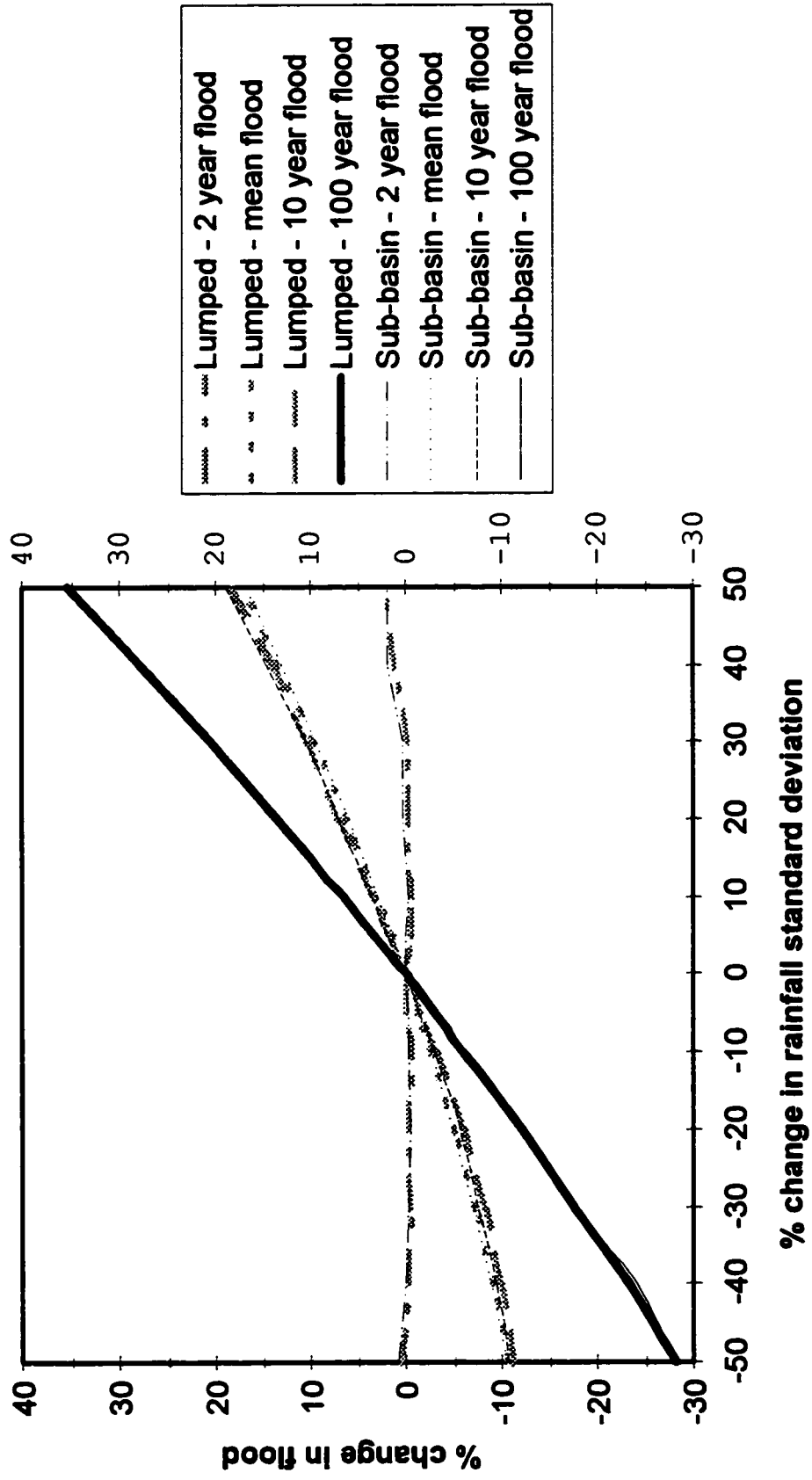


**Figure 4.9 - % change in flood level  
Rainfall standard deviation**

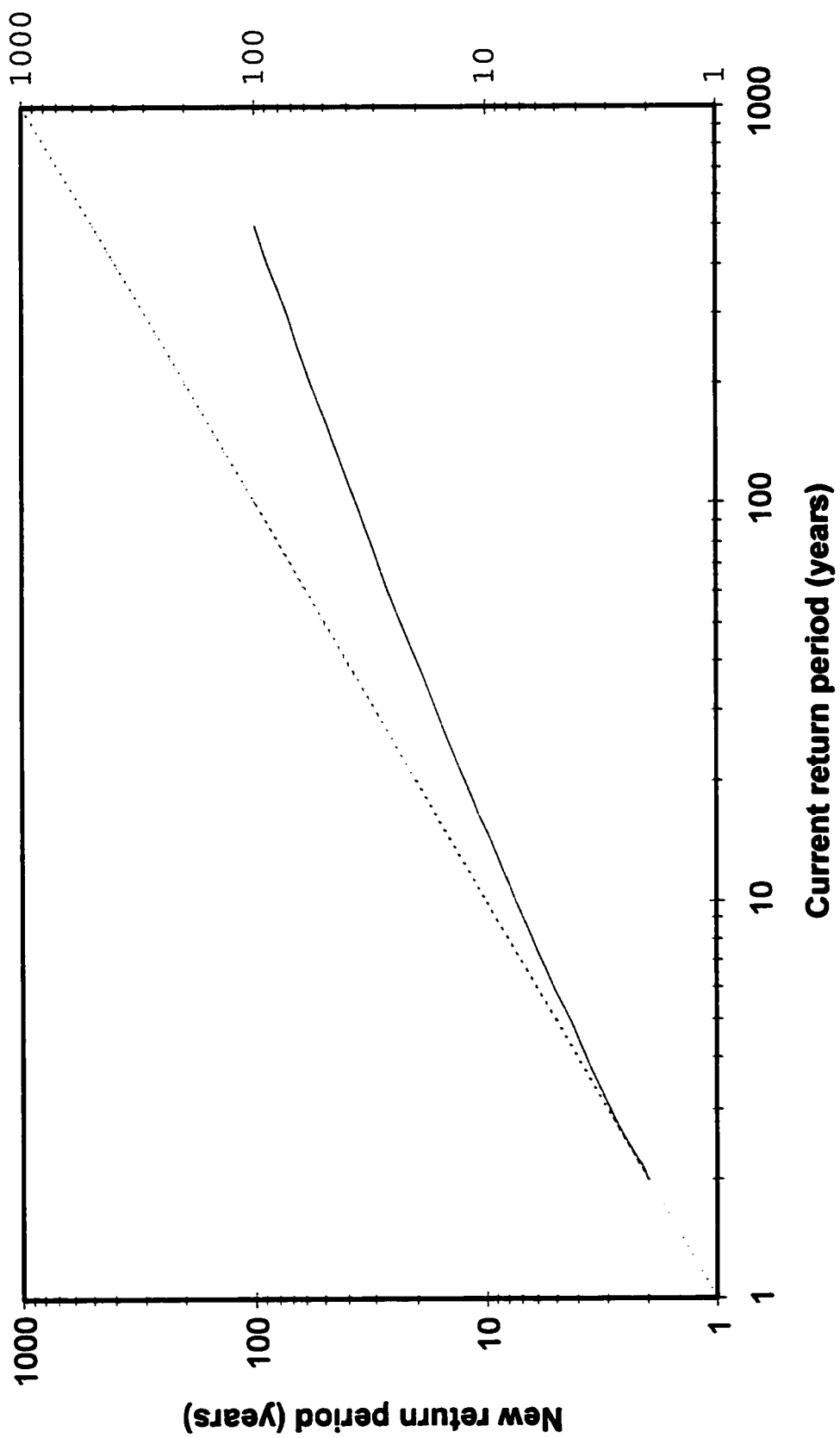


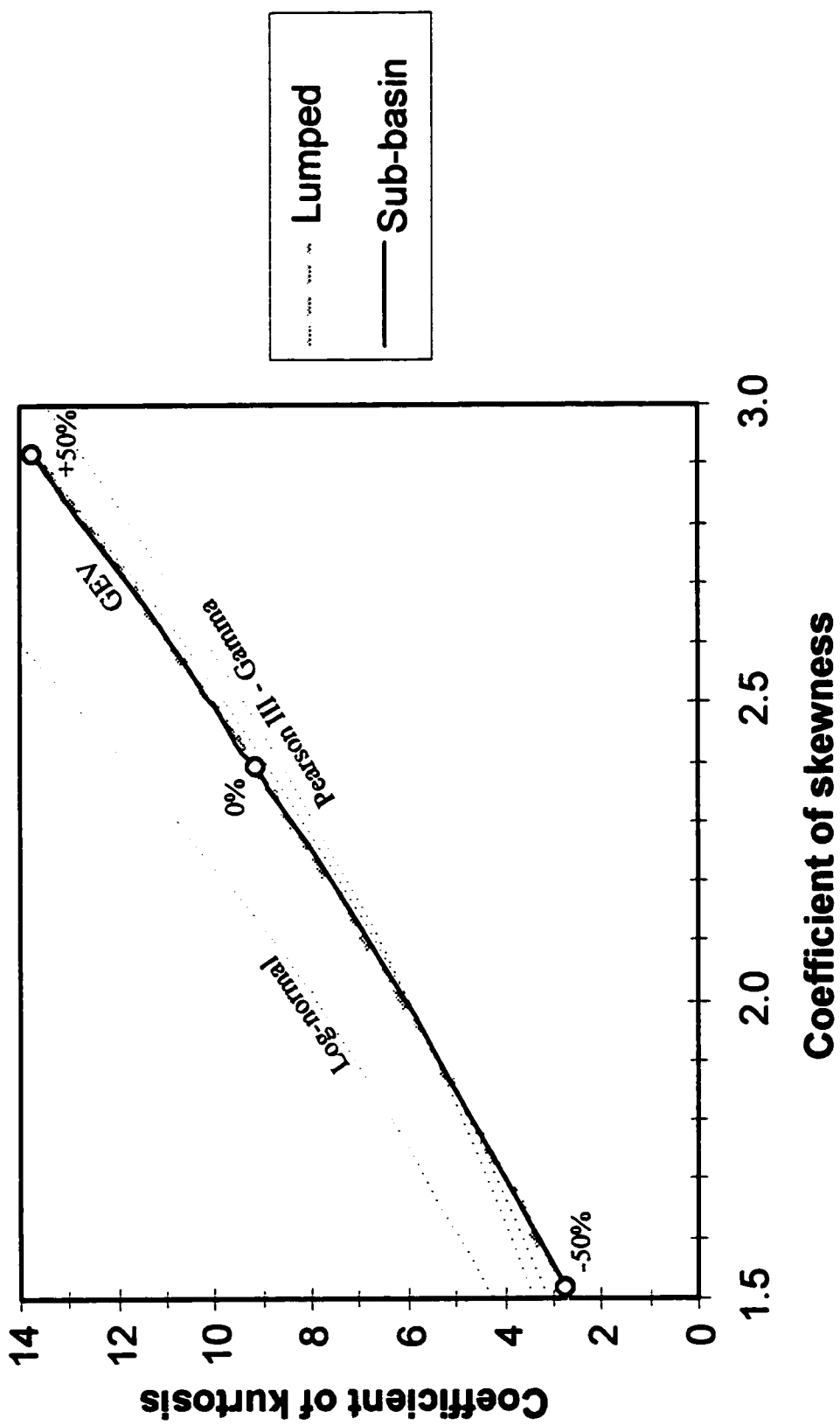
**Figure 4.10**  
**Changes in flood frequency - Rainfall standard deviation +50%**

a 200-year flood, becomes a 60-year flood. The current 50-year flood becomes a 25-year flood, and a 10-year flood becomes a 7-year flood. Floods below the 5-year level hardly change at all. This illustrates a problem with the available data. Less than 10% of the gauges used had more than 20 years of data (Environment Canada, 1985). While the data is sufficient to estimate the mean of extreme rainfall events, estimating standard deviation requires as much data as possible. This study shows that predictions of floods over the 10-year level are very sensitive to the estimated rainfall standard deviation. An updated rainfall atlas using data from the last 15 years would be very useful.

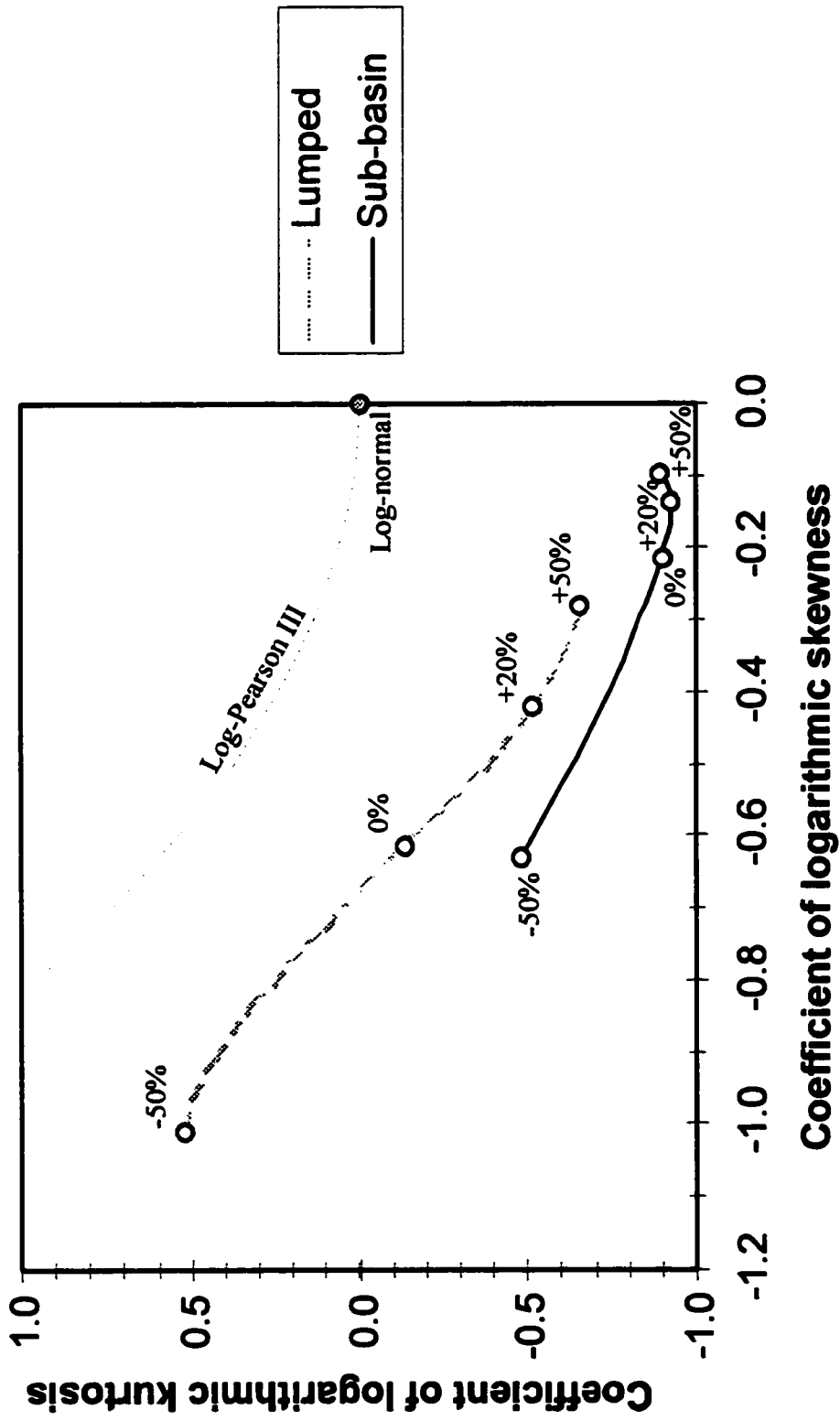
#### **4.3.2 Statistical parameters**

Figure 4.11 is a plot of the coefficient of kurtosis versus the coefficient of skewness. From the figure it can be seen that both coefficients increase with increasing standard deviation of rainfall and that both models predict almost identical curves. The figure also includes the theoretical relationship between skewness and kurtosis for the log-normal, gamma, and GEV distributions. The model results lie mostly above the gamma and EV3 curves, dropping below the GEV and gamma curves for  $C_s < 2.0$ .

Figure 4.12 is similar to Figure 4.11 but in this case logarithmic skewness and kurtosis are plotted, and these curves are shown with the theoretical relationships for the log Pearson III and log-normal distributions. Unlike with conventional statistical parameters, logarithmic statistical parameters are quite different for the two models. Both curves show the same general trend, with logarithmic kurtosis decreasing and logarithmic skewness increasing, as extreme rainfall standard deviation increases, and two curves run roughly parallel to the log



**Figure 4.11 - Skewness vs Kurtosis  
rainfall standard deviation**



**Figure 4.12 - Ln Skewness vs Ln Kurtosis  
rainfall standard deviation**

Pearson III curve. However, they are also significantly offset from each other.

#### **4.4 Rainfall climate scenarios**

To simulate the possibility of a southern rainfall climate "moving" northward, extreme rainfall statistics from three selected locations were applied to both models. The three locations are:

- 1) 49° 30' N 114° W, in Southern Alberta;
- 2) 46° N 110° W, in Montana;
- 3) 40° N 105° W, in Colorado.

All three sites are on the eastern slopes of the Rocky Mountains, and are at elevations similar to the study site. Table 4.2 contains the temperature and rainfall data for these locations taken from the "Climate atlas of North and Central America" (World Meteorological Organization, 1979) and the "Rainfall frequency atlas of the United States" (Hershfield, 1963).

Both models produced very similar results and so only the sub-basin predictions are presented here. Figure 4.13 displays the flood-frequency curves under the four climate scenarios. Although the annual mean temperature increases as the scenario site moves south, extreme rainfall can either increase or decrease. The 100-year flood decreases 12% in the Montana scenario, and increases 27% in the Southern Alberta scenario. This illustrates the fact that although temperature is an important factor in determining rainfall, it is not the only one. Figure 4.14 shows how current return periods would change if the climate changed to one of the three scenarios. Depending on the scenario, what is now a 100-year flood could



	<b>Little Red Deer River</b>		<b>Southern Alberta</b>		<b>Montana</b>		<b>Colorado</b>	
<b>Mean Annual Precipitation (mm)</b>	500		500		400		400	
<b>Mean Temperature (°C)</b>	2.5		4.5		8.0		10.0	
<b>Storm Duration (hours)</b>	<b>Mean</b>	<b>Std. Dev.</b>	<b>Mean</b>	<b>Std. Dev.</b>	<b>Mean</b>	<b>Std. Dev.</b>	<b>Mean</b>	<b>Std. Dev.</b>
	<b>(mm)</b>	<b>(mm)</b>	<b>(mm)</b>	<b>(mm)</b>	<b>(mm)</b>	<b>(mm)</b>	<b>(mm)</b>	<b>(mm)</b>
<b>6</b>	26.0	7.0	29.0	13.0	27.4	11.5	35.3	14.6
<b>12</b>	36.5	14.0	39.0	16.5	34.0	13.5	40.6	16.2
<b>24</b>	47.0	15.2	55.0	18.0	39.4	15.8	43.9	20.0
<b>48</b>	63.5	20.5	74.3	24.3	53.2	21.3	59.3	27.0
<b>72</b>	70.5	22.8	82.5	27.0	59.1	23.7	65.9	30.0

**Table 4.2**

**Climate scenario statistics**

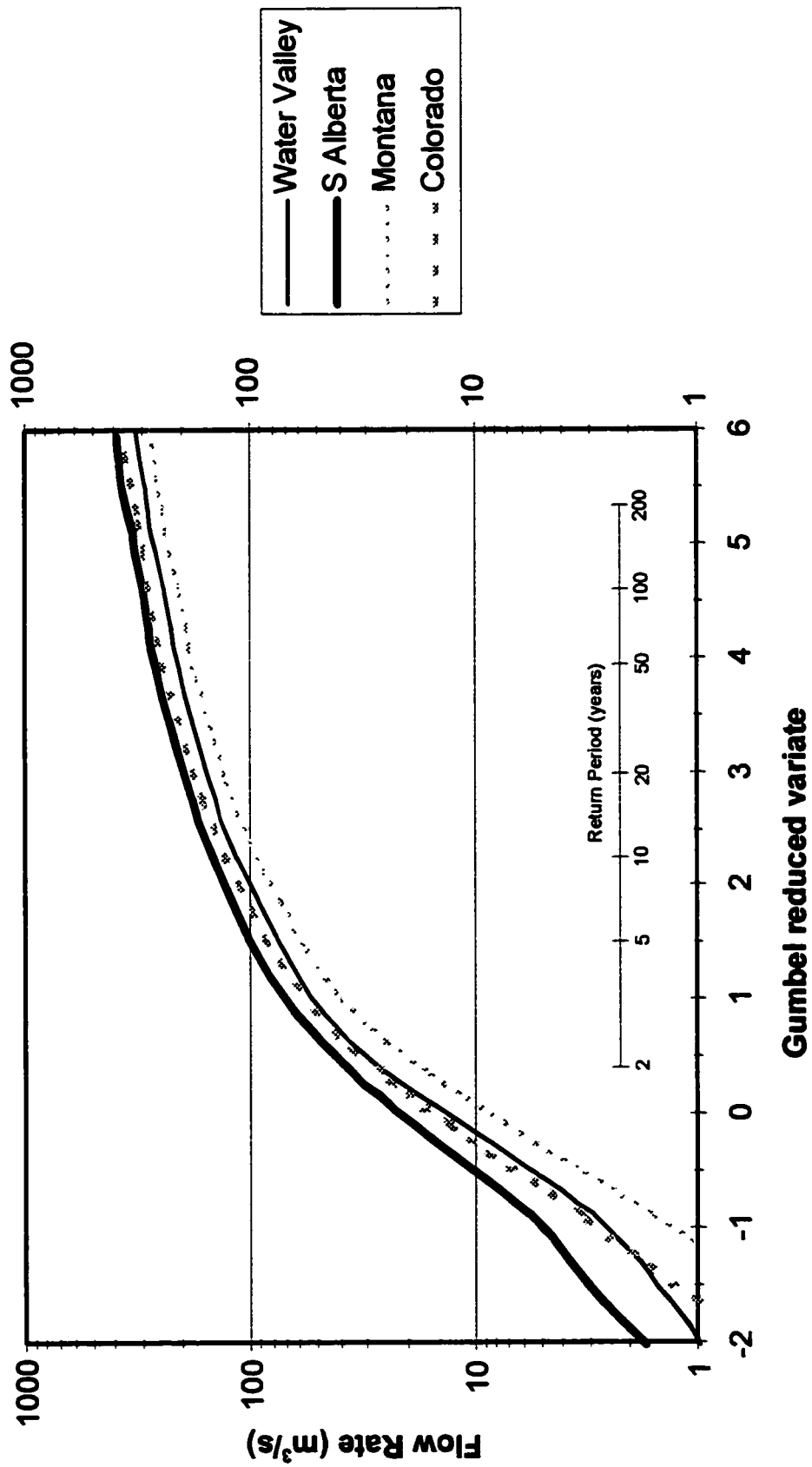


**Figure 4.13**  
**Climate change scenarios**

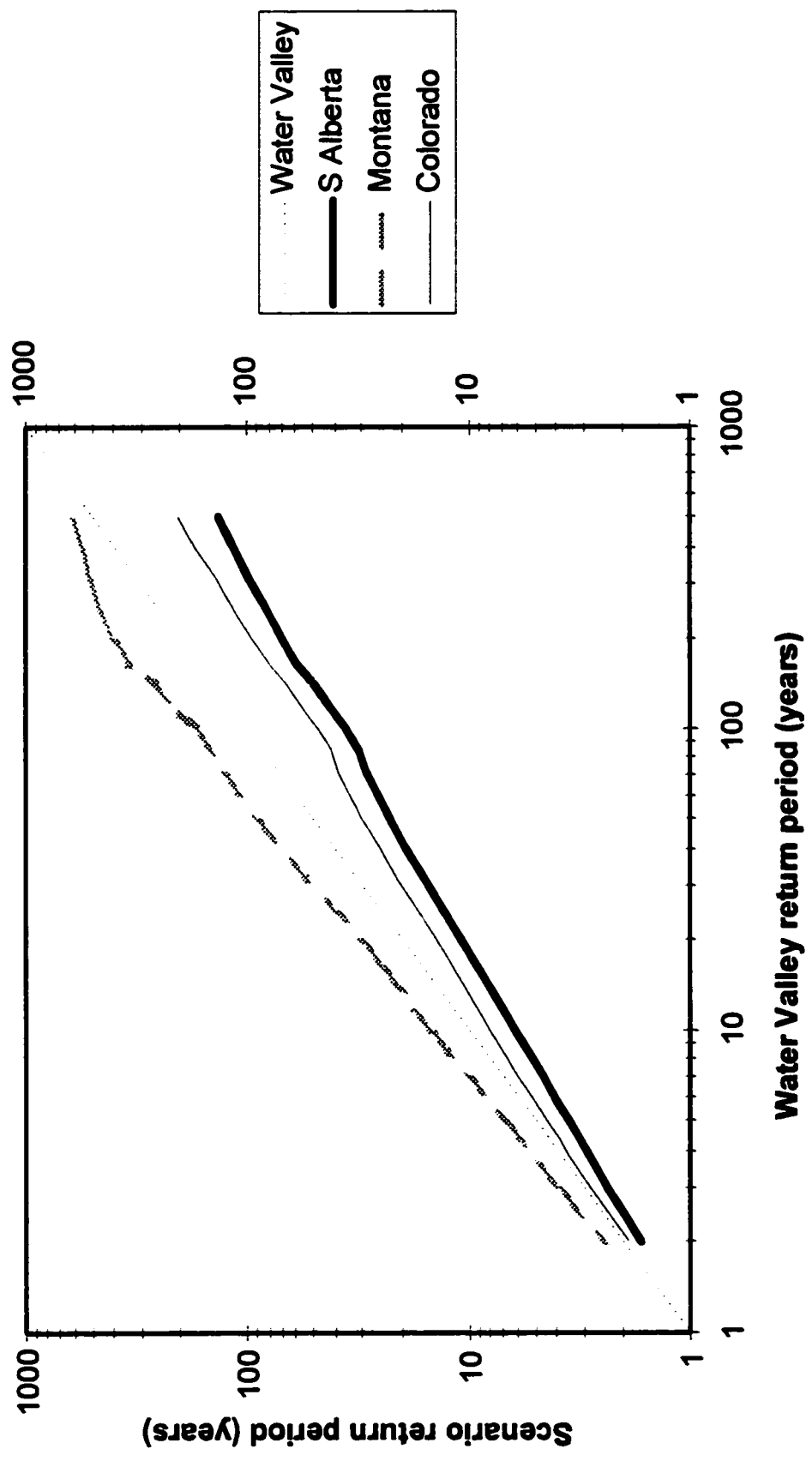


**Figure 4.14**  
**Changes in flood frequency - Climate scenarios**

become a 35-year flood, as in the Southern Alberta scenario, or a 175-year flood, as in the Montana scenario.

It should be emphasized that the scenarios selected for this study are purely hypothetical. Because rainfall is so sensitive to local geography, it is almost impossible to find locations where the only significant variable is latitude. For example, the Colorado site is much farther from the Pacific Ocean, and much nearer to the Gulf of Mexico. It is far from clear how much of the variation between scenarios is due to their local geographies, and how much is due to their temperature. However, these scenarios do represent real climates under conditions similar to those at the study site, and are included in this study to estimate the range of possible changes. The results of this study suggest that the range is very large.

#### **4.5 Urbanization**

The last series of simulations involved simulating urbanization of the watershed by changing the S.C.S. curve numbers.

##### **4.5.1 N-year floods**

Figure 4.15 is a plot of the lumped and sub-basin model predictions for the mean, 2-year, 10-year, and 100-year floods. The two models offer very similar predictions, especially for the 10-year and 100-year floods, but the sub-basin model predicts somewhat higher flow rates for the mean and 2-year floods for 5% to 80% urbanization. This is because in the sub-basin model entire sub-basins are becoming urbanized while others are remaining in their current state. This means that the sub-basin model takes into account the spatial variation in

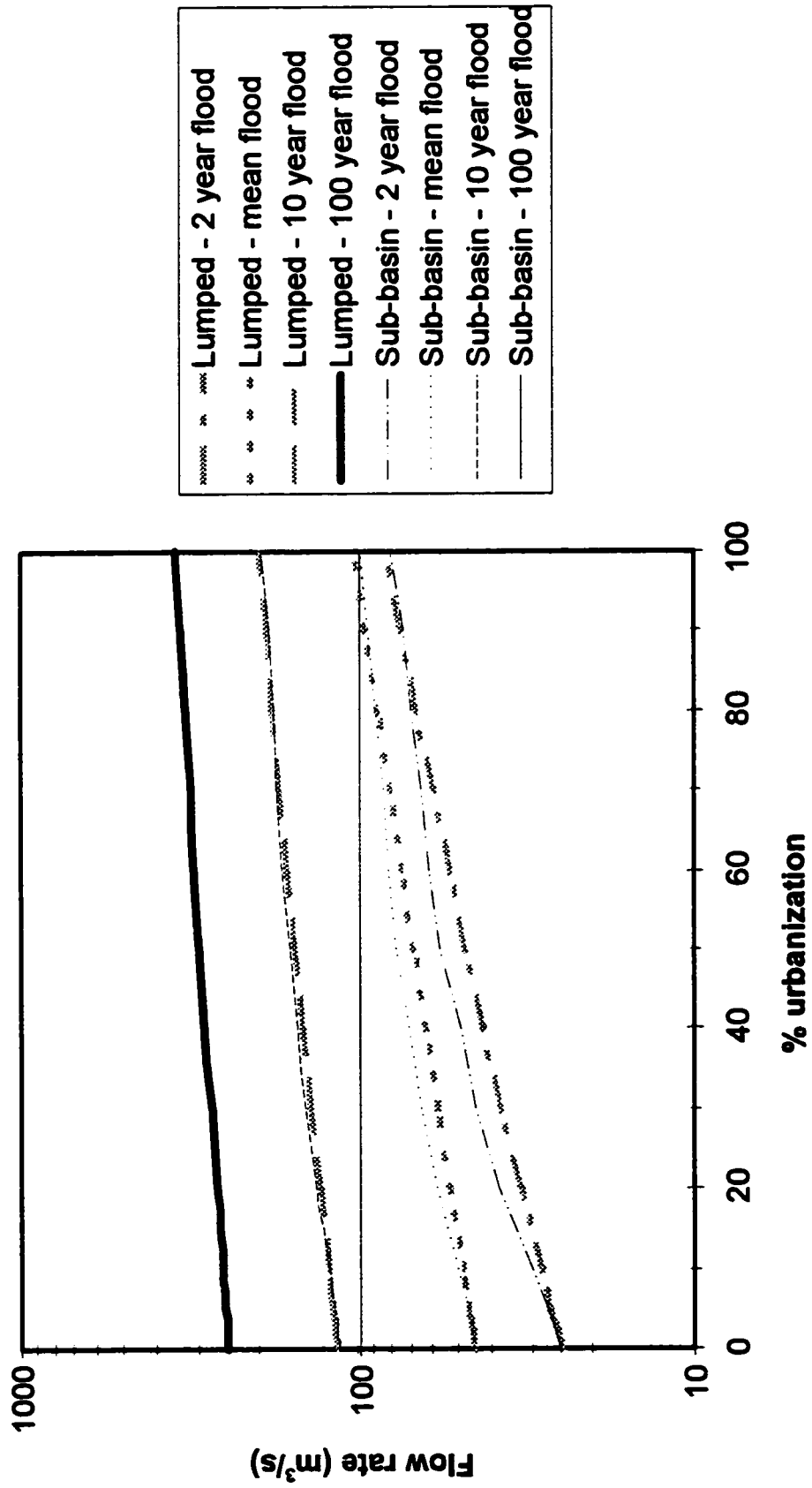
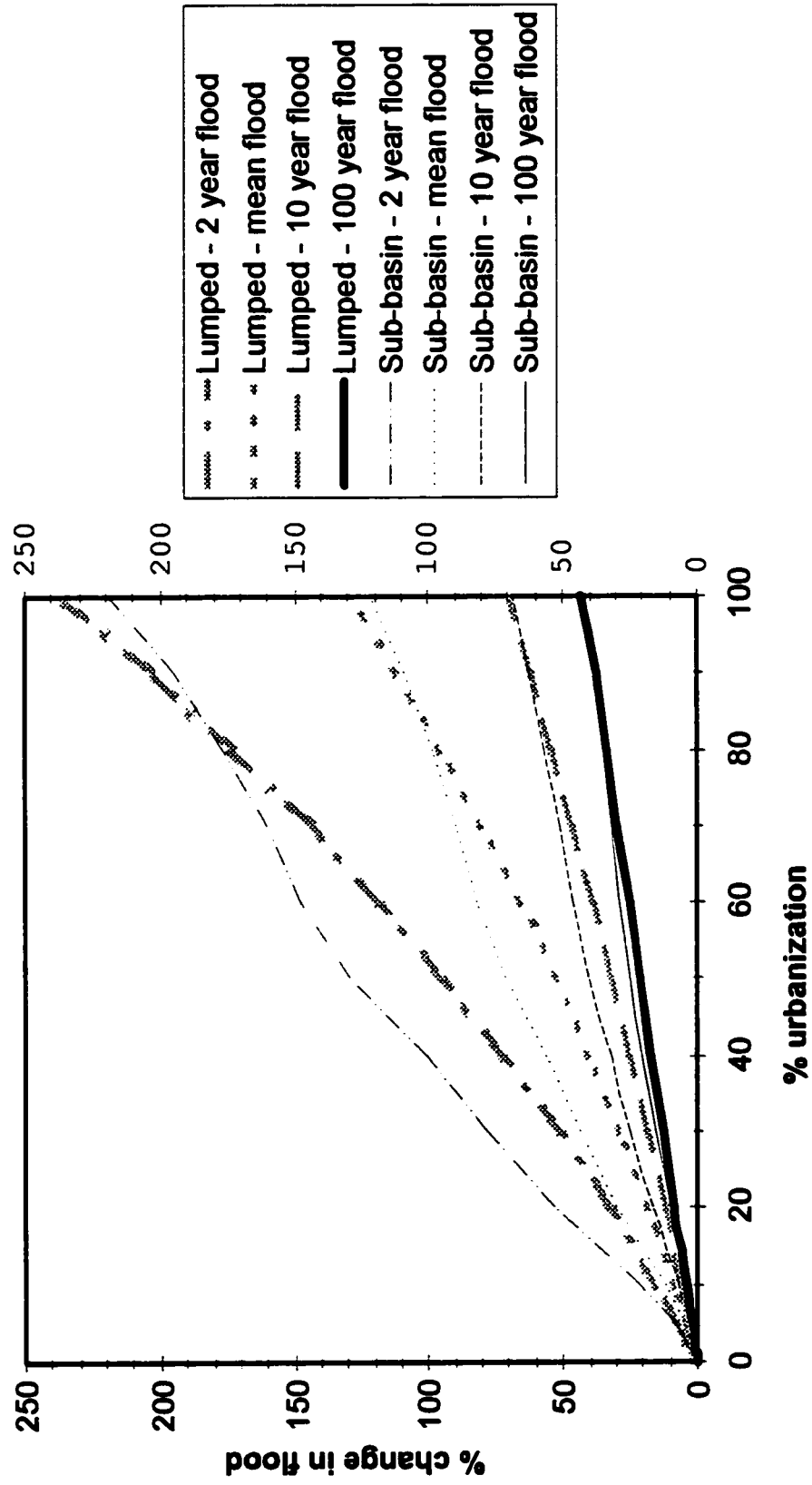


**Figure 4.15 - N-Year Floods  
Urbanization**

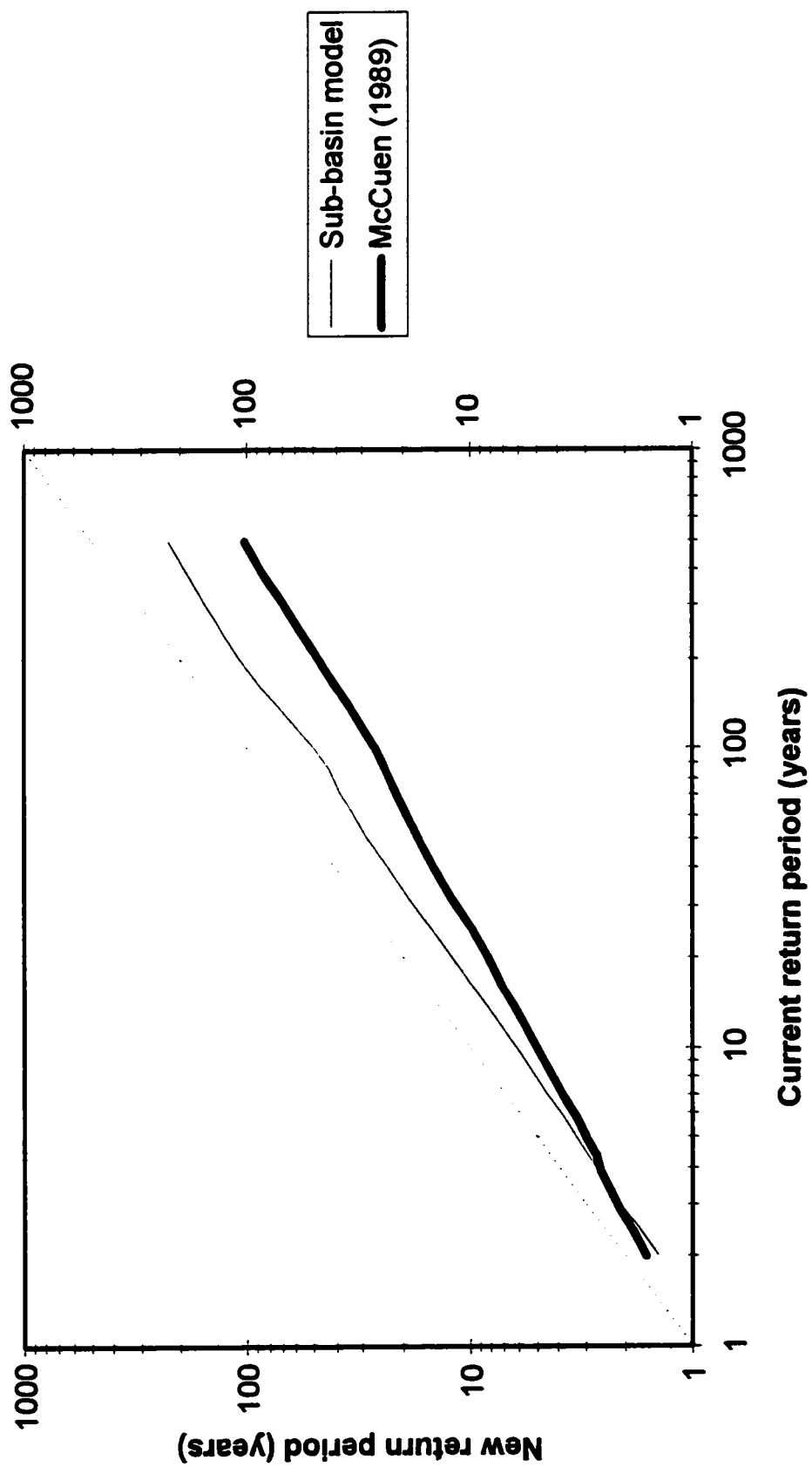
curve number which the lumped model ignores. Increasing the curve number range tends to result in increased runoff (i.e. a watershed in which half the land has a curve number of 60 and half has a curve number of 80 will experience more runoff than a watershed in which all the land has a curve number of 70). Also, the sub-basin model assumes that urbanization starts in the east and "moves" west. Since most of the low curve number land is in the east, the sub-basin model's equivalent curve number will rise faster than the lumped model's resulting in more predicted runoff.

Figure 4.16 is a plot of these same flood levels but they are plotted in terms of percent change from current flood levels. As with rainfall changes before, the smaller the flood the greater the effect of urbanization. In the sub-basin model, 30% urbanization results in a 16% increase in the 100-year flood, a 25% increase in the 10-year flood, a 43% increase in the mean annual (approximately 3-year) flood, and a 78% increase in the 2-year flood.

The data was also analyzed by comparing how the frequency of current floods changes with urbanization. Figure 4.17 is a plot of current flood frequencies against their equivalent frequencies after 30% urbanization according to the sub-basin model. Under such conditions, what would now be considered a 200-year flood, becomes a 100-year flood. The current 100-year flood becomes a 50-year flood, and a 10-year flood becomes a 6-year flood. In general, return periods are cut in half. This is roughly the same effect as a 10-15% increase in extreme rainfall would be expected to have. In fact, in general an X% increase in extreme rainfall has the same effect on 10+ year flood levels as 3X% urbanization. Also included in Figure 4.17 is a theoretical curve based on McCuen's index adjustment method (McCuen, 1989). As can be seen, McCuen's method predicts more severe floods than the



**Figure 4.16 - % change in flood level  
Urbanization**



**Figure 4.17**  
**Changes in flood frequency - 30% urbanization**



sub-basin model. This is probably because the sub-basin model does not take into account changes in the unit hydrograph during urbanization.

#### 4.5.2 Statistical parameters

Figure 4.18 is a plot of the coefficient of kurtosis versus the coefficient of skewness. From the figure it can be seen that both coefficients decrease with increasing urbanization and that both models predict almost identical curves. Figure 4.18 also includes the theoretical relationship between skewness and kurtosis for the log-normal, gamma, and GEV distributions. Again, the model results lie above the gamma and GEV curves and run roughly parallel to all three theoretical distributions.

In Figure 4.19, logarithmic skewness and kurtosis are plotted, and these curves are shown with the theoretical relationship for the log-normal distribution. Logarithmic statistical parameters are very different for the two models. The lumped model has a very smooth curve with log skewness increasing with urbanization at a decelerating rate. The curve reaches a minimum log kurtosis of -0.872 at 40% urbanization. This curve represents the general expected relationship if land use is assumed to be evenly distributed across the watershed. The sub-basin curve shows how much difference land use distribution can make. For this model, log kurtosis at first decreases and then increases, more or less smoothly, with increasing urbanization. Log skewness, however, behaves very strangely. First, as urbanization increases, log skewness rapidly increases, and then at 20% urbanization it abruptly stops and slowly decreases in an oscillating manner.

The most probable reason for this behaviour is that with urbanization, runoff from a

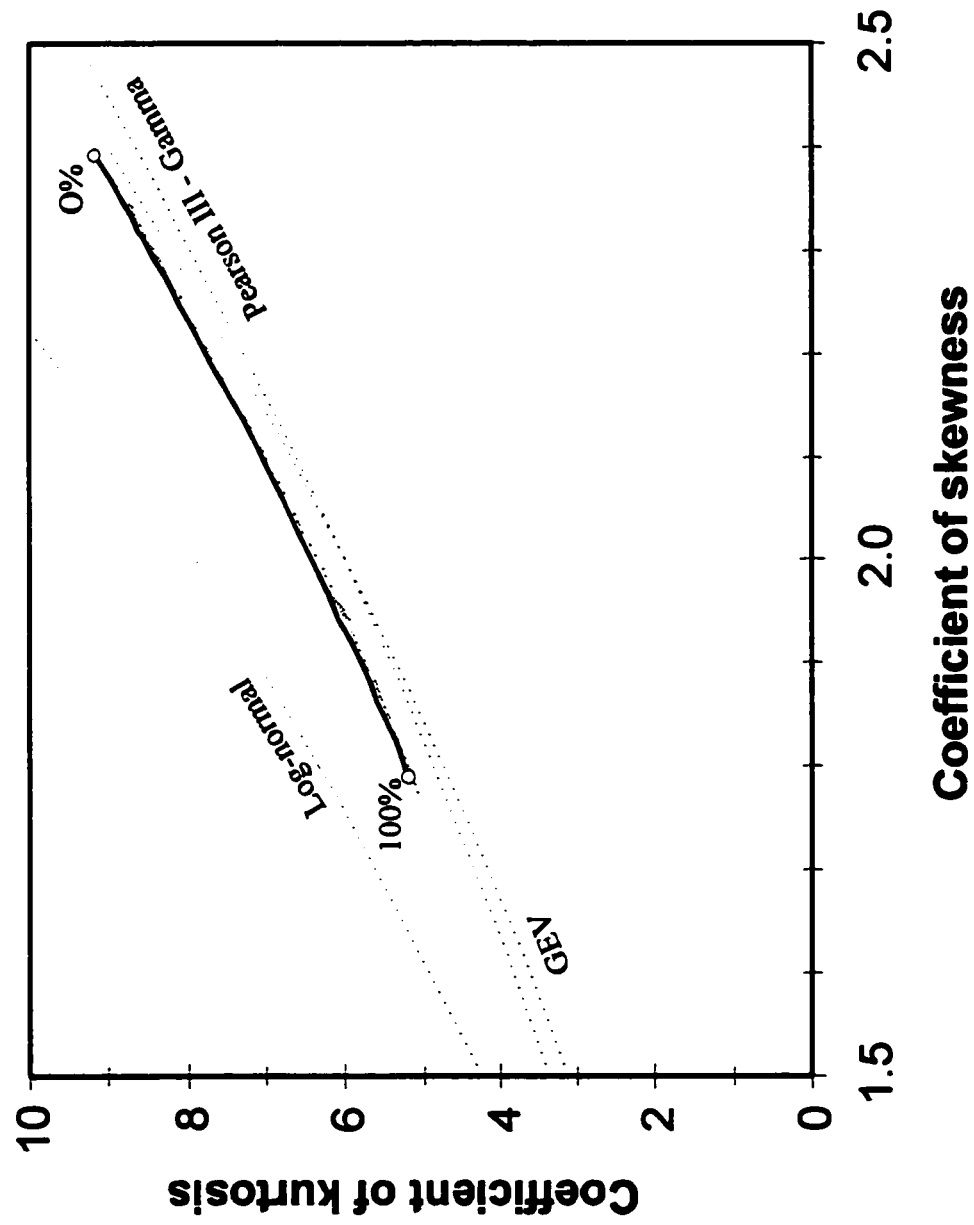


**Figure 4.18 - Skewness vs Kurtosis  
urbanization**

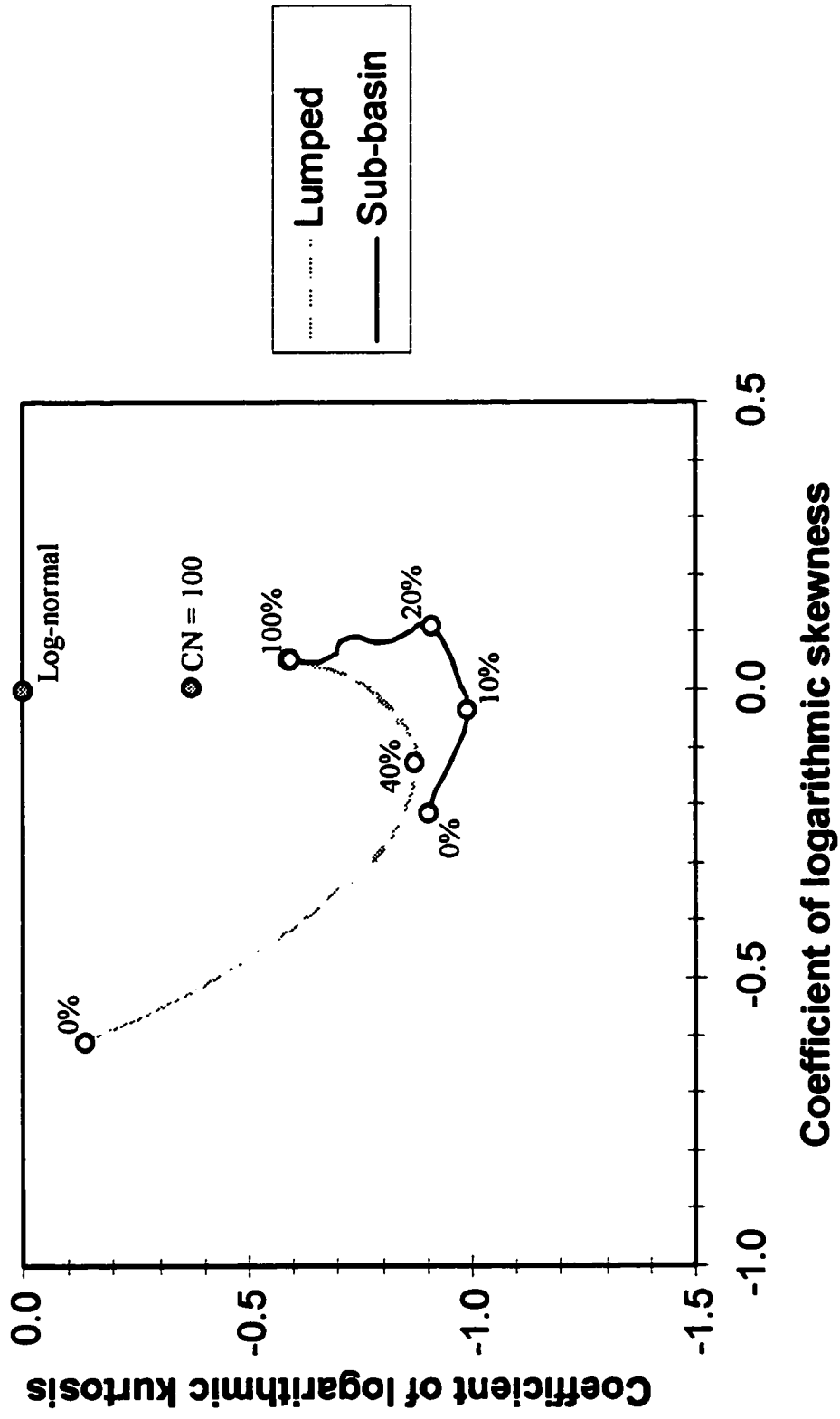


**Figure 4.19 - Ln Skewness vs Ln Kurtosis  
urbanization**

storm event exhibits two distinct peaks. The first is from the urbanized portion and the second is from the unurbanized portion. For the smallest rainfall events, the small initial increase in urbanization is enough to produce a slightly larger flood peak. As mentioned before, this change would be greatly exaggerated by taking the logarithm of the peak. Once urbanization reaches 20%, the smallest floods must now be large enough that any modest increase doesn't have much effect on their logarithms. This theory is supported by the fact that the greatest increase in log skewness occurs when urbanization increases from 5% to 10% and from 10% to 20%, when entire small sub-basins are being added instead of portions of sub-basins. Because skewness is a measure of symmetry, and this phenomenon is purely asymmetric, the log skewness is much more sensitive than the log kurtosis. While this helps explain the sudden change in direction of the sub-basin curve, it doesn't explain the oscillation behaviour, the cause of which is a mystery.

As would be expected, the two curves meet at 100% urbanization when the entire watershed is urbanized and so there is a virtually even distribution of curve numbers. Both models seem to be slowly approaching the ultimate point where the watershed curve number is 100 (see figure 4.19), when all rainfall becomes runoff.

#### **4.6 Summary of data results**

Figure 4.20 is a plot of all the skewness and kurtosis data. Because the lumped model results are so similar to the sub-basin results, only the sub-basin results are shown. The term 'general rainfall' refers to the set of simulations where both rainfall mean and standard deviation were changed. The data is very linear, and so the least-squares line of best fit was

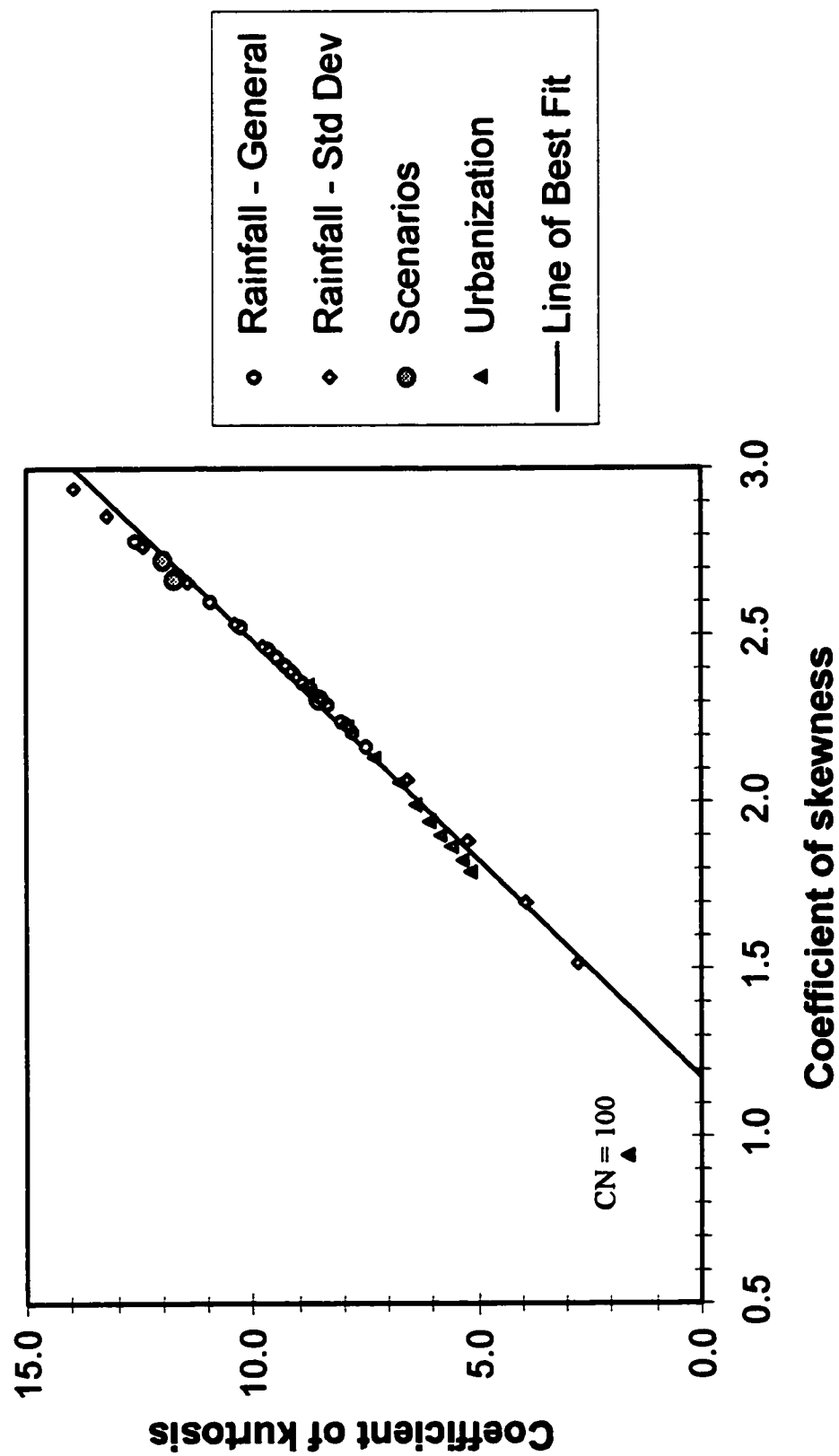


**Figure 4.20 - Summary of skewness and kurtosis results**  
**Sub-basin model**

derived using all the climate change data (i.e., the rainfall and scenario data). The equation of this line is:

$$C_k = 7.666 C_s - 9.013 \quad (4.1)$$

As can be seen, the urbanization data follows almost the same trend as the climactic change data, but as the average watershed curve number increases the urbanization data progressively diverge from the rest of the data. By the time a curve number of 100 is reached, the discrepancy is quite large. However, even at the extreme condition of 100% urbanization there is only a small difference. This suggests that Equation 4.1 reflects assumptions inherent in the mathematical models used in the study, namely the Log-Pearson III distribution of storm duration, the Gumbel distribution of extreme rainfall, the S.C.S. curve number method for determining excess rainfall, and the unit hydrograph model. But since these models are based on the geomorphology and climate of the watershed, the equation is also a characteristic of the watershed. It should be noted here that the most significant feature of Equation 4.1 is its slope. As was mentioned in Chapter 3, 10 000 simulation points were not enough to achieve consistent estimates of skewness and especially kurtosis. Because of this, a fixed set of random numbers was used for all simulations in order to eliminate this source of noise. This set was selected purely because it was the first generated, and not because it fit the data any better. Therefore, the position of the line is somewhat arbitrary, but the trend is not.

Figure 4.21 is a summary of the logarithmic skewness and kurtosis data for the sub-

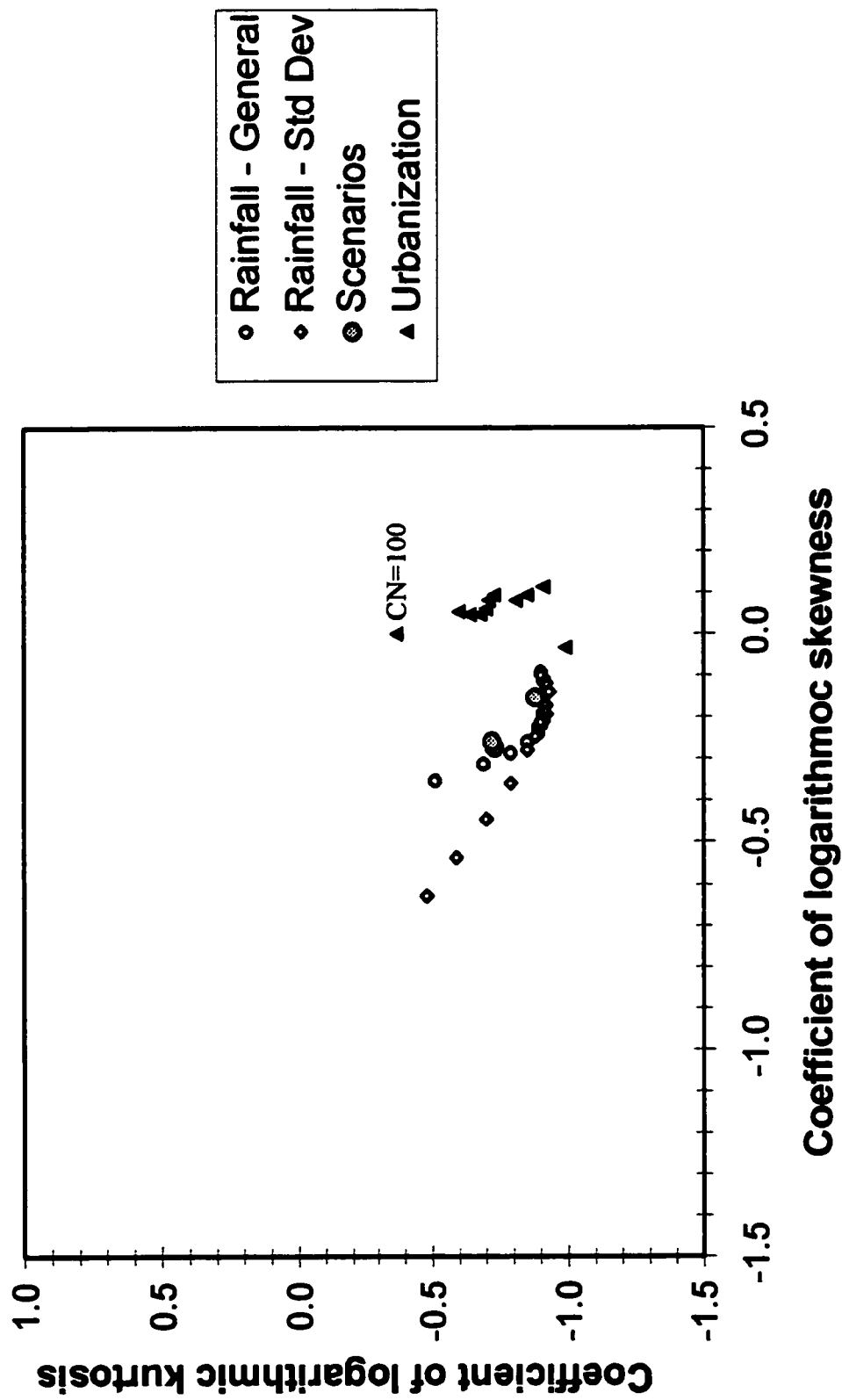


**Figure 4.21 - Summary of Ln skewness and Ln kurtosis results  
Sub-basin model**

basin model. The general rainfall change and rainfall standard deviation data follow similar trends, and overlap significantly over a large range. The isolation of the urbanization data reflects changes in the watershed geomorphology that significantly increase the smallest floods. Figure 4.22 is a summary of the logarithmic skewness and kurtosis data for the lumped model. While the location of the lumped data is different from the sub-basin data, similar trends are apparent. Once again, the general rainfall and rainfall standard deviation data overlap significantly, and the urbanization data is distinct (although not nearly as distinct as in the sub-basin model).

The most striking feature of the data is the fact that increasing rainfall standard deviation increases skewness and kurtosis, while increasing both rainfall mean and standard deviation decreases skewness and kurtosis. However, in the case of logarithmic skewness and kurtosis, increasing rainfall standard deviation has the same effect as increasing both rainfall mean and standard deviation. This is because changing the standard deviation of rainfall has a greater effect on large floods than small ones, while increasing the mean has a greater effect on small floods. For conventional statistics, the increasing standard deviation's emphasis on large floods causes the skewness and kurtosis to increase, and the increasing mean's emphasis on small floods causes them to decrease. Logarithmic skewness, however, is extremely sensitive to very small floods and a significant number of small floods are due to above average rainfall events under dry soil conditions. For such floods increasing the standard deviation can induce a significant increase in the logarithm of the runoff. Below average rainfall events under dry conditions, however, can't fall below the stream baseflow and so the logarithm of their peak flow won't decrease much. As a result, skewness increases. This



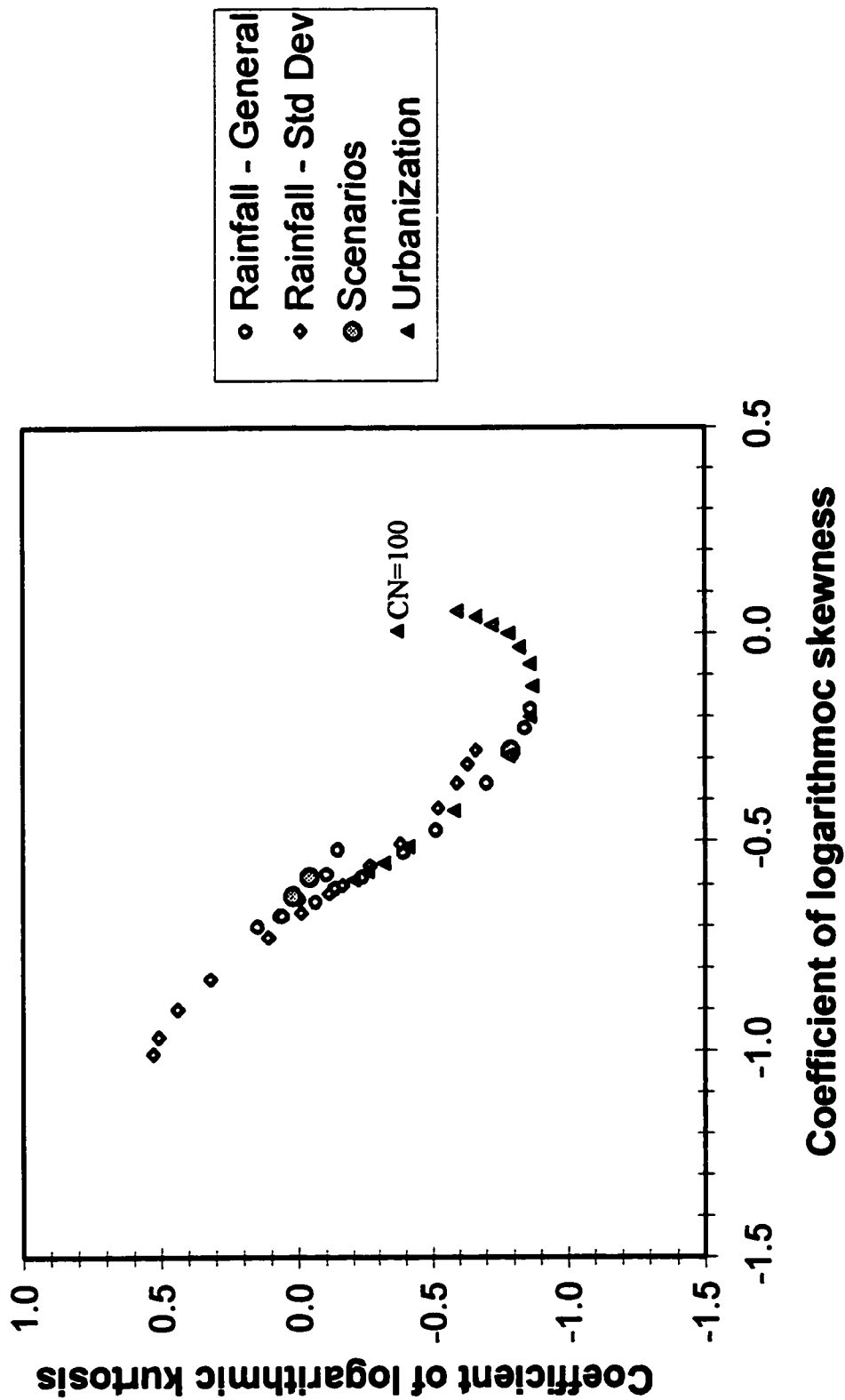


**Figure 4.22 - Summary of Ln skewness and Ln kurtosis results**  
**Lumped model**

sensitivity to near zero floods could have been avoided by assigning an arbitrary minimum peak flow rate of about  $1 \text{ m}^3/\text{s}$  for the logarithmic analysis. Since this is a study of flood frequency, and not drought frequency, the analysis should emphasize tools that are sensitive to medium to large floods. Because of this, the majority of the conclusions will be drawn from the analysis of conventional statistics.

## **CHAPTER 5**

### **CONCLUSIONS AND RECOMMENDATIONS**

#### **5.1 Conclusions**

The rainfall-runoff process for the Little Red Deer River near Water Valley watershed was simulated using two models: one which treated the watershed as a single system (the lumped model), and one which treated the watershed as the sum of 12 sub-systems (the sub-basin model). Current environmental conditions defined by land use, soil, and extreme rainfall maps were varied to determine how flood frequencies change when environmental conditions change.

A comparison of the model predictions under current conditions with observed data shows that the models simulate flood frequencies well, especially for return periods under 5 years. For return periods over 20 years, the models seem to predict larger than observed floods by up to 50%. However, chi-square tests show that this discrepancy is well within a tolerable range given the relatively short historical record.

Both models found that in terms of amplitude, small to average sized annual floods are far more sensitive to changes in rainfall than large annual floods. This result can best be explained by the use of the S.C.S. curve number method for converting total rainfall to excess rainfall since excess rainfall is more sensitive to changes in total rainfall when total rainfall is smaller. However, in terms of return period, the frequency of large floods is very sensitive to changes in rainfall. In the case of increased rainfall, the much increased average to slightly

above average floods approach levels that are currently only seen once every 100 years. This means that projects that are designed in terms of service life expectancy might fail much earlier than expected because of floods only marginally larger than they were designed for. In the case where only rainfall standard deviation was changed, large floods were found to be much more sensitive than average floods. The frequency of large floods was also found to increase drastically. Because it has a greater effect on average sized annual floods, a change in the mean of extreme rainfall would be relatively easy to detect from observed data after 10 years. If only the standard deviation of extreme rainfall were to change however, it could take as much as 100 years to detect because only floods with a return period of over 10 years would be significantly effected.

In order to gain a grasp of what the potential range of climate change was, three additional scenarios were simulated where the rainfalls of southern climates were applied to the study watershed. The results showed that the range of changes in rainfall used in this study produce results similar to current conditions in the warmer south. These scenarios don't suggest how the climate will change in the study region, but they do show that the current range of spatial climate variability is similar to the range of climate changes used in this study, and therefore climate changes on the order of  $\pm 25\%$  in extreme rainfall are reasonable.

In the case of urbanization, once again average sized floods are more sensitive to environmental change than large floods. The effect of urbanization on flood frequencies was found to be very similar to that of increased rainfall. The most notable result was the much greater discrepancy between the predictions of the lumped and sub-basin models. In the other

sets of simulations, all significant discrepancies were constrained to the smallest floods. Such floods are symptoms of drought, and since it is unreasonable to study drought by analyzing extreme rainfall events, these floods are not of interest to this study. Urbanization invalidates the lumped model's assumption that soil and land use in the watershed are uniform. This assumption causes the lumped model to under predict runoff. The sub-basin model simulates urbanization far better because it includes some of the watershed's variable land use and soil conditions, and this is the primary reason why it simulates the watershed better. However, the sub-basin model assumes that conditions are uniform throughout each sub-basin. The predictions of both models would be improved by considering the range of land use and soil conditions rather than just the average. The model used to simulate the effect of urbanization did not consider the effect urbanization would have on the shape of the unit hydrograph. Studies have shown that increasing urbanization tends to increase the peak of the unit hydrograph and shorten its lag time. These changes, especially the increased peak, would have a significant effect on flood levels. Future studies into the effect of urbanization on flood frequency should include this effect.

The relationship between the coefficient of skewness and the coefficient of kurtosis was found to be very close to linear for almost all the simulations conducted in this study. The reason for this relationship is not clear and could be reason for further study. This relationship was found to be very similar to that of the Pearson III (or gamma) distribution and the generalized extreme value distribution. This suggests that these distributions may hold promise for future flood-frequency analysis in the study watershed and others. The fact that the GEV is an extreme value distribution gives it a solid mathematical reason to consider

it for future study.

Conclusions based on the results of logarithmic statistical analysis are severely limited by the influence of the smallest simulated floods. The inclusion of a minimum annual flood would have greatly assisted logarithmic analysis.

The results of this study are not meant to serve as a prediction of exactly how flood levels will actually change with climate change. Perhaps the greatest factor limiting this study was the lack of consideration of the effects of climate change on vegetation and antecedent moisture conditions. In this study these factors were assumed to remain the same as they are today, and this does not seem reasonable to the author. The results should be looked at as the effects of extreme rainfall change alone, with all other parameters held constant. While this perspective may be limited, it does serve as a starting point for future research.

## **5.2 Recommendations**

Based on the results of this study, the following recommendations are made for future study:

1. The S.C.S. curve number method used in this study should be modified to include the distribution of curve numbers in a watershed, rather than just the arithmetic average.
2. The rainfall data for extreme rainfall frequency used in this study was published 13 years ago. An extreme rainfall map of Southern Alberta should be made using all available data.
3. In this study, watershed response to rainfall was simulated by a number of models. The effect each element of these models, and others not used in this study, have on

the skewness-kurtosis relationship of annual floods should be studied.

4. Most of the watershed parameters used in this study were assumed to be constant for all antecedent moisture and storm conditions. In reality, these parameters should change as conditions change. Techniques such as stochastic modeling should be used to simulate parameter variability.
5. When a watershed urbanizes, its geomorphology changes drastically. The effect of urbanization on the shape of the unit hydrograph should be included in the model to take this into account.
6. Almost nothing is known about how extreme rainfall events change as annual mean precipitation changes. Studies should be carried out to determine a relationship between annual precipitation and extreme rainfall events.
7. The applicability of the generalized extreme value distribution for rainfall frequency analysis as an improvement on the Gumbel distribution should be studied.
8. The fact that 10 000 simulations per run was not sufficient for a consistent estimation of the higher order statistical parameters such as kurtosis suggests that longer simulations should be run.
9. Alternatively, because 10 000 simulations was not sufficient to estimate kurtosis, it should be considered whether methods other than the Monte Carlo approach should be used when trying to estimate kurtosis
10. The effects of climate change on vegetation and antecedent moisture conditions should be studied.

11. This study focused on the Little Red Deer near Water Valley watershed. The computer models used in this study should be applied to other watersheds in the region to see how results compare.
12. The potential of paleological data to supply a several thousand year historical flood record suggests that such a study should be carried out in Alberta. This knowledge could supply a much better understanding of the potential size of flooding, as well as how flooding patterns change in Alberta with the climate.



## REFERENCES

- Abramowitz, M. and Stegun, I. A., (1965), "Handbook of mathematical functions", Dover, New York, USA.
- Ajward, M. H., (1996), "A spatially distributed unit hydrograph model using a geographic information system", Ph.D. Dissertation, Department of Civil Engineering, University of Calgary, Calgary, Alberta, Canada.
- Alberta Energy and Natural Resources, (1975), "Composite Forest Cover Series", Edmonton, Alberta, Canada.
- Alberta Energy and Natural Resources, (1978), "Ecological Land Classification and Evaluation," Edmonton, Alberta Canada.
- Aston, A. R., (1984), "The effect of doubling CO<sub>2</sub> on streamflow: A simulation", Journal of Hydrology, Vol. 27, p. 273.
- Boorman, D. B. and Sefton, C. E. M., (1997), "Recognising the uncertainty in the quantification of the effects of climate change on hydrological response", Climatic Change, Vol. 35, pp. 415-434.
- Canadian National Soil Survey Committee, (1974), "The system of soil classification for Canada", Canada Department of Agriculture, Publication 1455, Ottawa, Ontario, Canada.
- Chang, C., (1992), "A physically-based flood prediction model aided by a geographic information system", Ph.D. Dissertation, Department of Civil Engineering, University of Calgary, Calgary, Alberta, Canada.
- Chow, V. T., Maidment, D. R. and Mays, L. W., (1988), "Applied Hydrology", McGraw-Hill, New York, USA.
- Dvorak, V., Hladny, J. and Kasperek, L., (1997), "Climate change hydrology and water resources impact and adaption for selected river basins in the Czech Republic", Climatic Change, Vol. 36, pp. 93-107.
- Environment Canada, (1985), "Rainfall Frequency Atlas of Canada", Canadian Climate Program, Canadian Government Publishing Centre, Ottawa, Ontario, Canada.
- Environment Canada, (1995), "HYDAT CD-ROM Version 4.94 - Surface water and sediment data", EarthInfo Inc., Boulder, Colorado, USA..

- Espey, W. H., Winslow, D. E. and Morgan, C. W., (1969), "Urban effects on the Unit Hydrograph", in Moore, W. L. and Morgan, C. W., eds., *Effects of Watershed Changes on Streamflow*, University of Texas Press, Austin, Texas, USA., pp. 215-228.
- Fisheries and Environment Canada, (1978), "Hydrological Atlas of Canada", Printing and Publishing Supply Services Canada, Ottawa, Ontario, Canada.
- Fisher, R. A. and Tippett, L. H. C., (1928), "Limiting forms of the frequency distribution of the largest or smallest member of a sample", *Proc. Cambridge Phil. Soc.*, Vol 24, pp. 180-191.
- Flaschka, I. M., Stockton, C. W. and Boggess, W. R., (1987), "Climatic variation and surface water resources in the Great Basin region", *Water Resources Bulletin*, Vol. 23, pp. 47-57.
- Frederick, K. D. and Major, D. C., (1997), "Climate change and water resources", *Climatic Change*, Vol. 37, pp. 7-23.
- Gleick, P. H., (1986), "Methods of evaluating the regional impacts of global climatic changes", *Journal of Hydrology*, Vol. 88, pp. 99-116.
- Gleick, P. H., (1987), "Regional hydrologic consequences of increases in atmospheric CO<sub>2</sub> and other trace gases", *Climatic Change*, Vol. 10, pp. 137-161.
- Hershfield, D. M., (1963), "Rainfall frequency atlas of the United States: for durations from 30 minutes to 24 hours and return periods from 1 to 100 years", Department of Commerce, Weather Bureau, Washington, D.C., USA.
- Huff, F. A., (1967), "Time distribution of rainfall in heavy storms", *Water Resources Research*, Vol. 3, pp. 1007-1019.
- Intergovernmental Panel on Climate Change, (1990), "Climate change the IPCC scientific assessment", World Meteorological Organization, Cambridge University Press, Cambridge, U.K.
- Jenkinson, A. F., (1955), "The frequency distribution of the annual maximum (or minimum) values of meteorological elements", *Quart. Jour. Met. Soc.*, Vol. 81, pp. 158-171.
- Kacholia, K. and Reck, R. A., (1997), "Comparison of global climate change simulations for 2 x CO<sub>2</sub>-induced warming", *Climatic Change*, Vol. 35, pp. 53-69.

- Karl, T. R. and Riebsame, W. E., (1989), "The impact of decadal fluctuations in mean precipitation and temperature on runoff: A sensitivity study over the United States", *Climatic Change*, Vol. 15, pp. 423-227.
- Karl, T. R., Knight, R. W. and Plummer, N., (1995), "Trends in high-frequency climate variability in the twentieth century", *Nature*, Vol. 377, pp. 217-20.
- Knox, J. C. and Kundzewicz, Z. W., (1997), "Extreme hydrological events, palaeo-information and climate change", *Hydrological Sciences Journal*, Vol. 42(5), pp. 765-779.
- Knox, J. C., (1990), "Hydrologic and geomorphic implications of climate change", Institute for Water Resources, US Army Corps of Engineers, Fort Belvoir, Virginia, USA.
- Knox, J. C., (1993), "Large increases in flood magnitude in response to modest changes in climate", *Nature*, Vol. 361, pp. 430-432.
- Langbein, W. B., (1949), "Annual runoff in the United States", U.S. Geological Survey Circular, U.S. Department of the Interior, Washington, USA.
- Lazaro, T. R., (1979), "Urban hydrology - a multidisciplinary perspective", Ann Arbor Science Publishers Inc., Ann Arbor, Michigan, USA.
- Leopold, L. B., (1968), "Hydrology for urban land planning - a guidebook on the hydrologic effects of urban land use", US Geological Survey, Circular 554.
- Loukas, A. and Quick, M. C., (1996), "Effect of climate change on hydrologic regime of two climatically different watersheds", *ASCE Journal of Hydrologic Engineering*, Vol. 1, pp. 77-87.
- McCabe, G. J. and Wollock, D. M., (1992), "Effect of climate change and climatic variability on the Thornthwaite moisture index in the Delaware river basin", *Climatic Change*, Vol. 20, pp. 143-153.
- McCuen, R. H., (1989), "Hydrologic Analysis and Design", Prentice Hall, Englewood Cliffs, New Jersey, USA.
- McCuen, R. H. and Thomas, W. O., (1991), "Flood frequency analysis techniques for urbanizing watersheds", in Jennings, M. E., ed., *Symposium proceedings on urban hydrology*, American Water Resources Association, Bethesda, Maryland, USA.

- Microsoft, (1995), "Microsoft Excel for Windows 95", Version 7, Microsoft Corp., Redmond, Washington, USA.
- Nash, L. L. and Gleick, P. H., (1991), "Sensitivity of the Colorado Basin to climate changes", *Journal of Hydrology*, Vol. 125, pp. 221-241.
- National Research Council, (1982), "Carbon dioxide and climate: A second assessment", National Academy of Sciences Press, Washington, USA, p. 72.
- Nemec, J. and Schaake, J. C., (1982), "Sensitivity of water resources systems to climatic variation", *Hydrological Sciences Journal*, Vol. 17, pp. 327-343.
- Patel, J. K., Kapadia, C. H. and Owen, D. B., (1976), "Handbook of Statistical Distributions", Marcel Dekker, Inc., New York, USA.
- Pilon, P. J., Condie, R. and Harvey, K. D., (1985), "Consolidated Frequency Analysis Package, CFA, User Manual for Version 1-DEC PRO Series", Water Resources Branch, Inland Water Directorate, Environment Canada, Ottawa, Ontario, Canada.
- Pomeroy, S. J., (1987), "Runoff predictions at ungauged sites from rainfall statistics using a geographic information system", M.Sc. Thesis, Department of Civil Engineering, University of Calgary, Calgary, Alberta, Canada.
- PowerBASIC, (1996), "FirstBasic Compiler for DOS, Version 1.00", PowerBasic Inc., Carmel, California, USA.
- Rao, A. R. and Al-Wagdany, A., (1995), "Effects of climatic change in Wabash river basin", *ASCE Journal of Irrigation and Drainage Engineering*, Vol. 121, pp. 207-215.
- Reck, R. R., (1981), "Introduction to the proceedings of the workshop on the responsible interpretation of atmospheric models and related data", General Motors Research Publication GMR-3800, Warren, Michigan, USA, p. 22.
- Schaake, J. C., (1990), "From climate to flow", in Waggoner, P. E., ed., *Climate change and U.S. water resources*, John Wiley and Sons, New York, pp. 177-206.
- Schneider, S. H., Gleick, P. H. and Mearns, L. O., (1990), "Prospects for climate change", in Waggoner, P. E., ed., *Climate change and U.S. water resources*, John Wiley and Sons, New York, pp. 177-206.

- Sherman, I. K., (1932), "Streamflow from rainfall by unit-graph method", Engineering News-Record, Vol. 108, pp. 501-505.
- Skiles, J. W. and Hanson, J. D., (1994), "Responses of arid and semiarid watersheds to increasing carbon dioxide and climate change as shown by simulation studies", Climatic Change, Vol. 26, p. 377.
- Soil Conservation Service, (1972), "National Engineering Handbook", United States Department of Agriculture, United States Government, Washington, USA.
- United States Army Corps of Engineers, (1987), "HEC-1 Flood Hydrograph Package", United States Government, Washington, USA.
- Weisstein, E. W., (1998), "The CRC encyclopedia of mathematics", currently yet to be published.
- Whetton, P. H., Fowler, A. M., Haylock, M. R. and Pittock, A. B., (1993), "Implications of climate change due to the enhanced greenhouse effect on floods and droughts in Australia", Climatic Change, Vol. 25, pp. 289-317.
- World Meteorological Organization, (1979), "Climatic atlas of North and Central America", UNESCO, Geneva, Switzerland.
- Zar, J., (1984), "Biostatistical Analysis", Prentice-Hall, Eaglewood Cliffs, New Jersey, USA.

## **APPENDIX A**

### **Summary of results**

% of current rainfall	Return period (years)													
	1.0005	1.005	1.1	1.5	2	3	5	10	20	50	100	200	500	1000
75	0.00	0.03	0.60	3.63	8.88	22.56	41.31	67.25	92.96	129.69	154.43	180.10	213.34	279.43
80	0.00	0.04	0.67	4.42	11.32	26.67	47.38	75.85	104.41	145.21	172.25	200.96	235.64	307.81
85	0.00	0.06	0.76	5.29	14.07	31.25	53.91	85.74	117.44	161.35	190.31	224.39	258.41	336.52
90	0.01	0.06	0.93	6.65	17.29	36.31	61.00	95.64	129.71	177.46	208.31	245.95	281.47	365.50
95	0.01	0.10	1.17	8.39	20.72	41.66	68.46	105.90	143.03	193.52	226.03	267.23	304.77	394.73
97	0.02	0.13	1.38	9.20	22.17	43.82	71.76	110.03	148.29	200.08	233.65	275.82	314.15	406.48
99	0.02	0.17	1.64	10.08	23.69	46.05	74.95	114.39	153.63	206.89	240.82	284.44	323.56	418.27
100	0.04	0.22	1.77	10.56	24.47	47.25	76.34	116.53	156.32	210.17	244.42	288.69	328.33	424.17
101	0.07	0.27	1.90	11.01	25.27	48.46	78.16	118.75	158.93	213.93	248.03	292.64	333.24	430.08
103	0.16	0.40	2.23	11.94	26.87	50.84	81.60	122.97	164.52	220.74	255.53	300.55	343.10	442.29
105	0.31	0.57	2.58	12.93	28.46	53.18	84.97	127.29	169.98	227.30	262.88	308.49	353.00	456.34
110	0.85	1.18	3.64	15.54	32.68	59.40	93.36	138.20	184.64	243.99	284.68	328.42	377.91	491.78
115	1.66	2.06	4.90	18.59	37.21	65.96	101.72	149.43	198.30	261.95	303.82	348.46	403.03	521.95
120	2.53	3.12	6.36	21.98	42.15	72.69	110.70	161.29	212.40	279.55	324.46	372.05	428.35	552.16
125	3.34	4.29	7.99	25.54	47.35	79.57	119.90	173.10	226.94	297.31	344.49	398.44	457.49	582.05

**Table A.1**  
**N-year floods - rainfall - Lumped model**  
(all flow rates in m<sup>3</sup>/s)

% of current rainfall	Return period (years)														
	1.0005	1.005	1.1	1.5	2	3	5	10	20	50	100	200	500	1000	
75	0.02	0.11	0.87	4.26	9.60	22.88	41.19	66.51	91.45	128.24	152.98	178.55	211.62	275.79	
80	0.08	0.19	1.07	5.10	12.02	26.97	47.26	75.47	103.14	143.06	169.60	198.31	233.92	303.61	
85	0.17	0.32	1.36	6.13	14.81	31.71	53.59	84.71	115.14	159.51	187.14	217.87	256.24	331.74	
90	0.37	0.55	1.78	7.55	17.94	36.50	60.65	94.49	127.77	175.11	204.50	240.39	278.72	360.34	
95	0.64	0.86	2.28	9.38	21.28	41.68	68.00	104.49	140.51	191.38	222.16	261.76	302.03	389.27	
97	0.78	1.02	2.53	10.23	22.69	43.94	70.96	108.40	145.95	197.81	229.58	270.40	311.43	400.91	
99	0.92	1.20	2.79	11.05	24.21	46.14	74.23	112.49	151.03	204.16	237.03	279.08	320.88	412.57	
100	0.98	1.30	2.94	11.47	24.96	47.20	75.77	114.54	153.74	207.64	240.77	283.40	325.70	418.69	
101	1.06	1.40	3.10	11.91	25.73	48.24	77.32	116.53	156.51	211.43	244.48	287.26	330.57	425.53	
103	1.21	1.61	3.43	12.88	27.24	50.57	80.40	120.73	161.59	217.33	251.71	295.01	340.11	439.27	
105	1.42	1.86	3.82	13.88	28.90	52.84	83.82	125.04	167.40	224.91	258.98	302.77	349.56	453.07	
110	1.99	2.56	4.91	16.56	32.99	59.26	91.97	135.75	180.63	241.57	278.45	324.56	373.48	487.79	
115	2.74	3.41	6.15	19.53	37.56	65.40	100.64	146.90	194.69	258.34	298.89	346.64	399.60	520.72	
120	3.37	4.31	7.65	22.78	42.46	72.00	109.18	158.47	208.44	276.22	317.88	368.92	424.65	550.41	
125	4.10	5.22	9.34	26.32	47.34	78.85	118.37	170.28	222.75	293.16	337.29	391.59	449.86	580.13	

**Table A.2**  
**N-year floods - rainfall - Sub-basin model**  
 (all flow rates in m<sup>3</sup>/s)



% of current std dev	Return period (years)														
	1.0005	1.005	1.1	1.5	2	3	5	10	20	50	100	200	500	1000	
50	0.00	0.06	0.85	11.79	24.60	45.16	74.40	103.43	126.37	156.04	175.52	192.17	228.94	262.80	
60	0.01	0.07	0.96	11.32	24.41	45.82	74.32	104.89	132.02	164.41	187.65	210.55	249.63	296.20	
70	0.01	0.09	1.08	11.01	24.33	46.10	74.61	106.69	136.60	175.51	201.69	224.98	266.86	327.74	
80	0.02	0.13	1.25	10.84	24.41	46.64	74.73	109.44	141.69	186.36	214.47	241.67	287.16	360.30	
90	0.02	0.16	1.52	10.67	24.35	46.81	75.19	112.77	149.11	199.25	230.06	265.15	307.64	392.11	
95	0.02	0.18	1.67	10.58	24.47	47.18	75.69	114.59	152.51	204.11	237.11	278.32	317.94	408.11	
99	0.03	0.21	1.75	10.55	24.46	47.21	76.46	115.89	155.60	209.19	243.22	287.11	326.21	420.95	
100	0.04	0.22	1.77	10.56	24.47	47.25	76.34	116.53	156.32	210.17	244.42	288.69	328.33	424.17	
101	0.04	0.22	1.79	10.53	24.48	47.35	76.82	116.93	157.15	211.56	246.07	289.46	330.85	427.39	
105	0.06	0.26	1.89	10.44	24.35	47.38	77.36	118.55	160.17	215.51	252.68	292.55	340.99	442.94	
110	0.10	0.29	1.98	10.37	24.32	47.58	77.92	120.38	164.48	222.89	260.43	303.10	353.73	465.42	
120	0.13	0.36	2.13	10.48	24.37	47.76	79.47	124.74	173.01	236.08	277.65	322.20	379.38	506.27	
130	0.14	0.45	2.23	10.68	24.42	48.20	82.18	128.47	181.04	250.48	294.53	343.87	410.77	541.20	
140	0.14	0.49	2.34	10.62	24.71	48.61	84.37	132.73	190.22	263.94	312.27	363.90	445.66	576.36	
150	0.14	0.51	2.41	10.68	25.01	49.32	86.81	138.34	200.25	277.92	330.64	386.58	470.15	612.73	

**Table A.3**  
**N-year floods - rainfall standard deviation - Lumped model**  
 (all flow rates in m<sup>3</sup>/s)

% of current std dev	Return period (years)														
	1.0005	1.005	1.1	1.5	2	3	5	10	20	50	100	200	500	1000	
50	0.20	0.43	1.72	12.55	25.13	45.09	73.49	102.08	124.88	153.74	173.08	190.46	225.25	260.53	
60	0.32	0.60	1.98	12.27	24.98	45.79	73.43	103.79	130.38	162.19	183.12	208.12	244.94	293.61	
70	0.46	0.76	2.27	11.90	24.90	45.96	73.29	105.80	134.17	172.67	198.41	221.95	261.94	324.16	
80	0.67	0.95	2.55	11.70	24.82	46.47	73.89	108.09	140.47	183.99	211.74	241.21	282.37	355.19	
90	0.84	1.14	2.81	11.57	24.88	46.72	74.54	111.19	146.85	196.85	226.17	260.52	303.03	386.68	
95	0.92	1.22	2.87	11.57	24.90	47.16	75.00	112.97	150.16	201.75	233.11	270.42	314.14	402.52	
99	0.98	1.27	2.92	11.50	24.97	47.24	75.74	114.18	152.95	206.59	239.24	280.83	323.31	415.23	
100	0.98	1.30	2.94	11.47	24.96	47.20	75.77	114.54	153.74	207.64	240.77	283.40	325.70	418.69	
101	0.99	1.32	2.95	11.43	24.97	47.14	75.92	114.95	154.51	209.02	242.20	284.15	328.06	422.92	
105	1.03	1.36	2.99	11.36	24.96	47.34	76.39	116.58	157.53	212.69	247.91	291.56	337.14	439.91	
110	1.07	1.42	3.04	11.50	24.89	47.54	77.14	118.66	161.77	218.88	257.29	298.90	350.83	464.47	
120	1.03	1.44	3.13	11.52	25.03	47.76	78.67	122.74	170.28	231.60	271.80	317.28	376.21	504.57	
130	1.01	1.43	3.20	11.68	25.05	48.23	81.11	126.65	177.83	245.10	291.54	336.90	407.72	540.73	
140	0.94	1.39	3.25	11.70	25.41	48.43	83.46	131.35	187.13	258.88	307.55	353.77	431.30	577.09	
150	0.90	1.35	3.20	11.80	25.43	49.45	85.96	136.25	197.13	272.71	324.64	379.70	460.54	613.62	

**Table A.4**  
**N-year floods - rainfall standard deviation - Sub-basin model**  
(all flow rates in m<sup>3</sup>/s)

	Return period (years) - Lumped model													
	1.0005	1.005	1.1	1.5	2	3	5	10	20	50	100	200	500	1000
S Ab	1.19	1.70	4.47	17.81	35.38	65.01	101.80	150.81	203.24	269.27	311.93	359.19	418.98	536.42
Mont	0.01	0.06	0.91	6.20	15.94	34.27	60.11	95.69	132.31	183.39	216.65	252.11	299.96	391.58
Colo	0.03	0.22	2.24	12.00	26.38	50.42	84.66	131.84	180.11	245.96	292.33	332.93	406.05	529.61
	Return period (years) - Sub-basin model													
S Ab	1.71	2.62	5.72	18.71	35.79	64.57	100.21	148.33	198.23	264.62	304.95	353.71	416.09	533.84
Mont	0.18	0.38	1.62	7.12	16.63	34.38	59.75	94.31	130.30	180.56	211.52	248.22	294.85	389.74
Colo	0.60	1.01	3.34	13.03	26.94	50.37	83.45	129.60	177.37	243.12	286.70	321.81	399.72	527.88

**Table A.5**  
**N-year floods - climate scenarios**  
(all flow rates in m<sup>3</sup>/s)

% urban	Return period (years)														
	1.0005	1.005	1.1	1.5	2	3	5	10	20	50	100	200	500	1000	
1	0.05	0.25	1.85	10.80	24.87	47.74	77.12	117.20	157.06	211.21	245.32	289.52	329.42	425.28	
2	0.08	0.28	1.94	11.05	25.24	48.26	77.76	117.95	157.77	212.38	246.21	290.35	330.51	426.38	
3	0.11	0.33	2.04	11.27	25.60	48.73	78.43	118.62	158.63	213.24	247.49	291.18	331.60	427.49	
5	0.17	0.42	2.24	11.76	26.38	49.75	79.68	119.93	160.25	214.84	249.00	292.84	333.79	430.24	
10	0.44	0.72	2.80	13.08	28.29	52.18	82.78	123.29	164.44	218.95	253.74	296.96	339.26	439.17	
20	1.32	1.72	4.27	16.11	32.41	57.50	89.02	130.41	172.53	227.66	264.62	305.14	350.19	453.54	
30	2.52	3.11	6.09	19.69	37.05	63.06	95.35	138.01	180.43	236.55	275.18	314.73	361.16	466.72	
40	3.64	4.64	8.32	23.63	42.12	68.98	102.03	146.04	189.03	246.20	286.34	327.01	377.00	474.42	
50	4.85	6.23	11.21	28.12	47.73	75.22	109.60	154.14	198.18	255.41	296.73	336.45	387.45	484.05	
60	6.38	8.04	14.51	33.21	53.40	82.23	117.47	162.05	207.94	263.98	306.66	345.75	402.53	493.95	
70	8.32	10.23	18.46	38.78	59.71	89.27	126.10	170.80	217.65	275.21	317.29	359.44	419.95	503.93	
80	10.61	12.56	23.08	44.82	66.79	96.78	134.65	180.05	227.07	285.63	326.90	371.55	434.23	513.95	
90	13.27	15.46	28.26	51.67	74.29	104.66	143.20	188.87	237.09	297.29	336.95	385.23	443.54	523.81	
100	16.35	18.79	33.81	59.34	82.56	113.54	151.96	198.54	247.20	308.78	349.81	396.70	451.97	533.52	
CN=100	90.01	117.60	166.97	224.94	266.14	312.33	356.45	407.10	455.44	517.38	560.01	605.52	668.48	732.38	

**Table A.6**  
**N-year floods - urbanization - Lumped model**  
 (all flow rates in m<sup>3</sup>/s)

% urban	Return period (years)													
	1.0005	1.005	1.1	1.5	2	3	5	10	20	50	100	200	500	1000
5	1.35	1.76	3.64	13.00	27.12	49.80	79.02	118.19	158.01	212.14	245.68	287.61	331.21	427.96
10	2.81	3.44	5.57	15.69	30.23	53.56	82.87	122.43	162.82	217.22	250.44	291.96	336.58	437.48
20	5.41	6.39	10.70	22.51	38.15	62.42	92.85	133.25	174.55	229.58	264.08	306.08	352.22	457.50
30	6.53	7.74	13.28	27.44	44.44	69.62	101.66	143.23	185.11	239.95	278.22	318.95	365.96	470.22
40	7.63	9.13	15.97	32.09	49.99	76.49	109.55	151.28	195.44	249.69	289.21	329.93	382.13	481.39
50	9.82	11.49	20.29	38.19	57.16	84.36	118.36	161.19	204.99	260.62	300.86	340.87	395.64	492.32
60	10.90	12.66	22.56	41.78	61.76	89.61	124.98	168.13	212.72	270.34	310.72	350.75	403.92	501.40
70	11.36	13.16	23.74	44.13	65.02	93.46	129.57	173.57	219.01	277.30	317.84	359.13	412.45	509.63
80	12.21	14.12	25.66	47.38	68.92	98.14	134.80	179.72	226.08	284.37	324.84	367.28	424.65	518.01
90	13.63	15.65	28.65	51.60	73.69	103.60	140.91	186.17	233.16	292.40	334.02	376.40	437.20	526.24
100	15.75	17.93	32.59	56.99	79.58	109.95	147.80	193.30	241.54	300.13	341.84	386.88	445.72	534.46
CN=100	87.77	116.25	162.83	220.33	261.23	306.06	349.10	398.69	447.07	505.51	550.50	590.49	658.10	721.22

**Table A.7**  
**N-year floods - urbanization - Sub-basin model**  
(all flow rates in m<sup>3</sup>/s)

% of current rainfall	mean (m <sup>3</sup> /s)	standard deviation (m <sup>3</sup> /s)	skewness	kurtosis	In mean	In standard deviation	In skewness	In kurtosis
75	23.896	34.432	2.785	12.542	2.014	1.813	-0.516	-0.145
80	27.479	38.434	2.683	11.596	2.180	1.814	-0.575	-0.104
85	31.370	42.530	2.591	10.784	2.355	1.793	-0.635	-0.003
90	35.566	46.697	2.509	10.089	2.538	1.748	-0.679	0.071
95	40.066	50.918	2.436	9.496	2.728	1.678	-0.705	0.146
97	41.950	52.618	2.409	9.283	2.807	1.638	-0.678	0.060
99	43.882	54.322	2.384	9.084	2.886	1.592	-0.641	-0.065
100	44.867	55.175	2.371	8.989	2.927	1.567	-0.613	-0.138
101	45.863	56.029	2.359	8.898	2.967	1.541	-0.582	-0.233
103	47.891	57.740	2.337	8.724	3.047	1.489	-0.522	-0.387
105	49.965	59.453	2.315	8.560	3.124	1.439	-0.468	-0.504
110	55.347	63.745	2.265	8.191	3.305	1.332	-0.360	-0.695
115	60.998	68.048	2.221	7.870	3.468	1.244	-0.281	-0.793
120	66.903	72.358	2.182	7.588	3.615	1.172	-0.223	-0.841
125	73.051	76.674	2.146	7.340	3.750	1.111	-0.178	-0.859

**Table A.8**  
**Statistics - rainfall - Lumped model**

% of current rainfall	mean (m <sup>3</sup> /s)	standard deviation (m <sup>3</sup> /s)	skewness	kurtosis	In mean	In standard deviation	In skewness	In kurtosis
75	24.094	33.803	2.782	12.582	2.161	1.633	-0.351	-0.503
80	27.674	37.685	2.687	11.685	2.349	1.583	-0.309	-0.682
85	31.554	41.655	2.601	10.915	2.538	1.523	-0.281	-0.783
90	35.731	45.695	2.524	10.252	2.724	1.459	-0.255	-0.849
95	40.197	49.791	2.455	9.679	2.902	1.393	-0.235	-0.884
97	42.063	51.441	2.429	9.473	2.971	1.367	-0.227	-0.891
99	43.974	53.098	2.405	9.279	3.039	1.341	-0.219	-0.897
100	44.946	53.928	2.393	9.186	3.072	1.328	-0.215	-0.899
101	45.930	54.760	2.382	9.096	3.105	1.316	-0.211	-0.900
103	47.929	56.426	2.359	8.923	3.170	1.290	-0.202	-0.903
105	49.971	58.097	2.338	8.760	3.234	1.265	-0.193	-0.906
110	55.264	62.286	2.289	8.390	3.386	1.205	-0.166	-0.912
115	60.813	66.489	2.245	8.066	3.528	1.148	-0.139	-0.914
120	66.607	70.704	2.205	7.781	3.660	1.097	-0.113	-0.908
125	72.634	74.927	2.169	7.528	3.784	1.052	-0.091	-0.896

**Table A.9**  
**Statistics - rainfall - Sub-basin**

% of current rainfall std dev	mean (m <sup>3</sup> /s)	standard deviation (m <sup>3</sup> /s)	skewness	kurtosis	ln mean	ln standard deviation	ln skewness	ln kurtosis
50	40.084	43.069	1.507	2.719	2.759	1.781	-1.011	0.523
60	40.804	44.951	1.683	3.870	2.795	1.732	-0.967	0.508
70	41.642	47.130	1.866	5.135	2.831	1.685	-0.905	0.434
80	42.598	49.578	2.045	6.447	2.864	1.641	-0.829	0.320
90	43.673	52.269	2.215	7.746	2.896	1.602	-0.727	0.105
95	44.255	53.697	2.295	8.377	2.912	1.584	-0.668	-0.016
99	44.742	54.876	2.356	8.868	2.924	1.570	-0.624	-0.115
100	44.867	55.175	2.371	8.989	2.927	1.567	-0.613	-0.138
101	44.993	55.477	2.386	9.110	2.930	1.564	-0.601	-0.164
105	45.508	56.702	2.444	9.582	2.942	1.551	-0.555	-0.268
110	46.180	58.274	2.512	10.151	2.956	1.537	-0.503	-0.374
120	47.609	61.544	2.637	11.211	2.984	1.518	-0.419	-0.513
130	49.150	64.968	2.746	12.161	3.009	1.507	-0.356	-0.590
140	50.797	68.531	2.841	13.002	3.032	1.503	-0.311	-0.631
150	52.547	72.222	2.922	13.735	3.053	1.505	-0.278	-0.657

**Table A.10**  
**Statistics - rainfall standard deviation - Lumped model**



% of current rainfall std dev	mean (m <sup>3</sup> /s)	standard deviation (m <sup>3</sup> /s)	skewness	kurtosis	In mean	In standard deviation	In skewness	In kurtosis
50	40.170	42.087	1.519	2.792	2.942	1.459	-0.629	-0.480
60	40.901	43.916	1.698	3.965	2.976	1.414	-0.536	-0.590
70	41.745	46.041	1.883	5.256	3.006	1.378	-0.442	-0.693
80	42.700	48.437	2.065	6.595	3.031	1.352	-0.354	-0.782
90	43.767	51.074	2.236	7.920	3.053	1.336	-0.277	-0.852
95	44.343	52.476	2.316	8.562	3.063	1.331	-0.244	-0.878
99	44.824	53.634	2.378	9.063	3.071	1.329	-0.221	-0.895
100	44.946	53.928	2.393	9.186	3.072	1.328	-0.215	-0.899
101	45.071	54.225	2.408	9.309	3.074	1.328	-0.210	-0.902
105	45.578	55.429	2.466	9.788	3.081	1.328	-0.190	-0.913
110	46.237	56.975	2.534	10.365	3.089	1.328	-0.169	-0.923
120	47.636	60.192	2.659	11.436	3.104	1.334	-0.137	-0.928
130	49.142	63.562	2.767	12.394	3.118	1.344	-0.116	-0.921
140	50.751	67.069	2.861	13.239	3.132	1.358	-0.104	-0.908
150	52.459	70.702	2.941	13.976	3.145	1.374	-0.097	-0.895

**Table A.11**  
**Statistics - rainfall standard deviation - Sub-basin model**

Lumped model									
	mean (m <sup>3</sup> /s)	standard deviation (m <sup>3</sup> /s)	skewness	kurtosis	ln mean	ln standard deviation	ln skewness	ln kurtosis	
<b>S Ab</b>	60.741	69.780	2.286	8.323	3.427	1.283	-0.279	-0.787	
<b>Mont</b>	35.214	48.178	2.704	11.778	2.499	1.754	-0.629	0.021	
<b>Colo</b>	50.437	64.269	2.638	11.459	3.047	1.546	-0.607	-0.006	
Sub-basin model									
<b>S Ab</b>	60.575	68.219	2.308	8.517	3.489	1.188	-0.152	-0.879	
<b>Mont</b>	35.323	47.099	2.721	12.003	2.670	1.497	-0.274	-0.725	
<b>Colo</b>	50.319	62.739	2.664	11.758	3.164	1.351	-0.258	-0.721	

**Table A.12**  
**Statistics - climate scenarios**

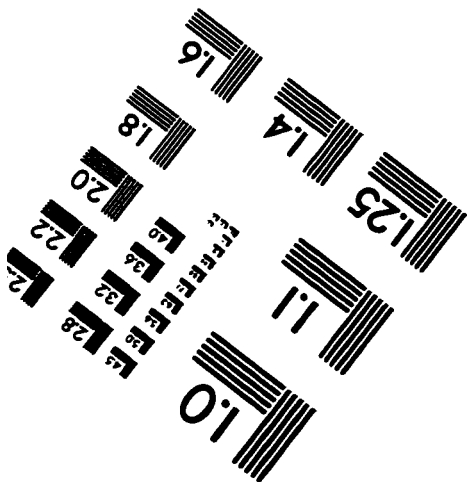
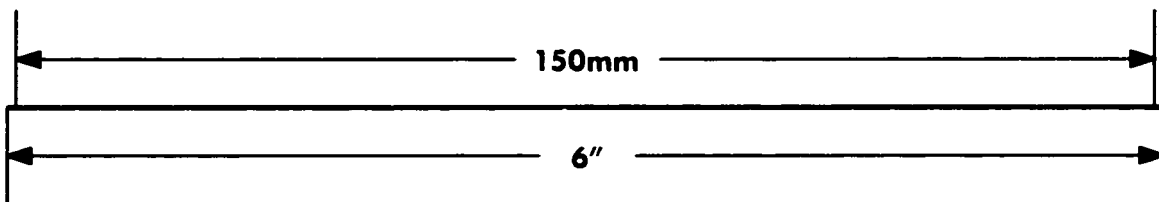
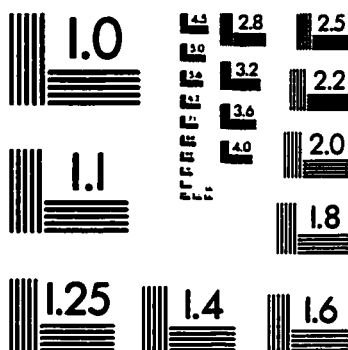
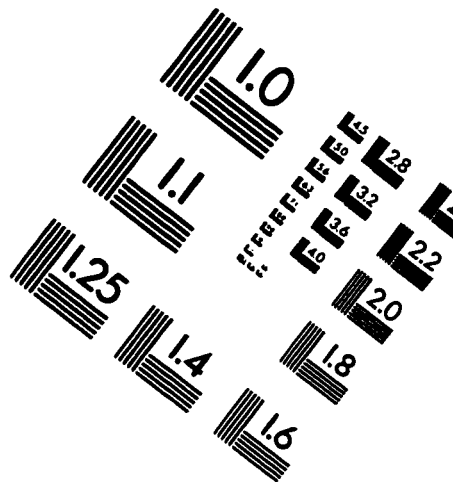
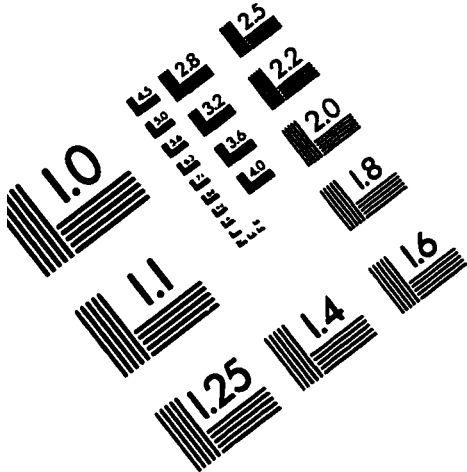
% urbanization	mean (m <sup>3</sup> /s)	standard deviation (m <sup>3</sup> /s)	skewness	kurtosis	In mean	In standard deviation	In skewness	In kurtosis
1	45.247	55.386	2.363	8.922	2.948	1.549	-0.593	-0.200
2	45.630	55.597	2.354	8.856	2.969	1.531	-0.572	-0.258
3	46.018	55.807	2.345	8.790	2.990	1.513	-0.552	-0.311
5	46.802	56.225	2.329	8.662	3.033	1.477	-0.513	-0.404
10	48.826	57.261	2.288	8.356	3.136	1.392	-0.425	-0.581
20	53.144	59.285	2.213	7.801	3.327	1.249	-0.290	-0.776
30	57.834	61.245	2.143	7.312	3.500	1.132	-0.195	-0.855
40	62.915	63.136	2.080	6.879	3.658	1.036	-0.126	-0.872
50	68.407	64.956	2.021	6.493	3.804	0.954	-0.073	-0.856
60	74.334	66.700	1.967	6.150	3.940	0.883	-0.032	-0.821
70	80.722	68.366	1.915	5.842	4.067	0.820	-0.001	-0.773
80	87.603	69.950	1.867	5.563	4.188	0.764	0.023	-0.716
90	95.015	71.450	1.820	5.309	4.303	0.714	0.040	-0.654
100	103.000	72.866	1.774	5.077	4.414	0.668	0.052	-0.588
CN = 100	280.102	96.417	0.940	1.614	5.578	0.338	0.008	-0.364

**Table A.13**  
**Statistics - urbanization - Lumped model**

% urbanization	mean (m <sup>3</sup> /s)	standard deviation (m <sup>3</sup> /s)	skewness	kurtosis	In mean	In standard deviation	In skewness	In kurtosis
5	47.184	55.002	2.346	8.821	3.175	1.264	-0.184	-0.911
10	50.309	55.758	2.311	8.556	3.346	1.122	-0.033	-0.987
20	58.266	57.777	2.229	7.946	3.641	0.933	0.113	-0.906
30	64.486	60.192	2.135	7.287	3.789	0.879	0.095	-0.851
40	70.204	62.236	2.060	6.790	3.910	0.835	0.082	-0.803
50	77.227	63.982	1.994	6.388	4.050	0.774	0.094	-0.731
60	81.820	65.648	1.944	6.070	4.125	0.752	0.082	-0.705
70	85.125	67.233	1.903	5.815	4.171	0.745	0.063	-0.696
80	89.179	68.759	1.863	5.577	4.229	0.729	0.051	-0.675
90	93.993	70.134	1.826	5.367	4.298	0.706	0.048	-0.640
100	99.783	71.349	1.790	5.184	4.378	0.675	0.052	-0.592
CN = 100	274.521	94.761	0.939	1.629	5.558	0.339	0.004	-0.369

**Table A.14**  
**Statistics - urbanization - Sub-basin model**

# IMAGE EVALUATION TEST TARGET (QA-3)



APPLIED IMAGE, Inc  
1653 East Main Street  
Rochester, NY 14609 USA  
Phone: 716/482-0300  
Fax: 716/288-5989

© 1993, Applied Image, Inc., All Rights Reserved

